The Oligo-Miocene deepwater system of the Levant Basin

Michael Gardosh, Yehezkel Druckman,
Binyamin Buchbinder, Rani Calvo

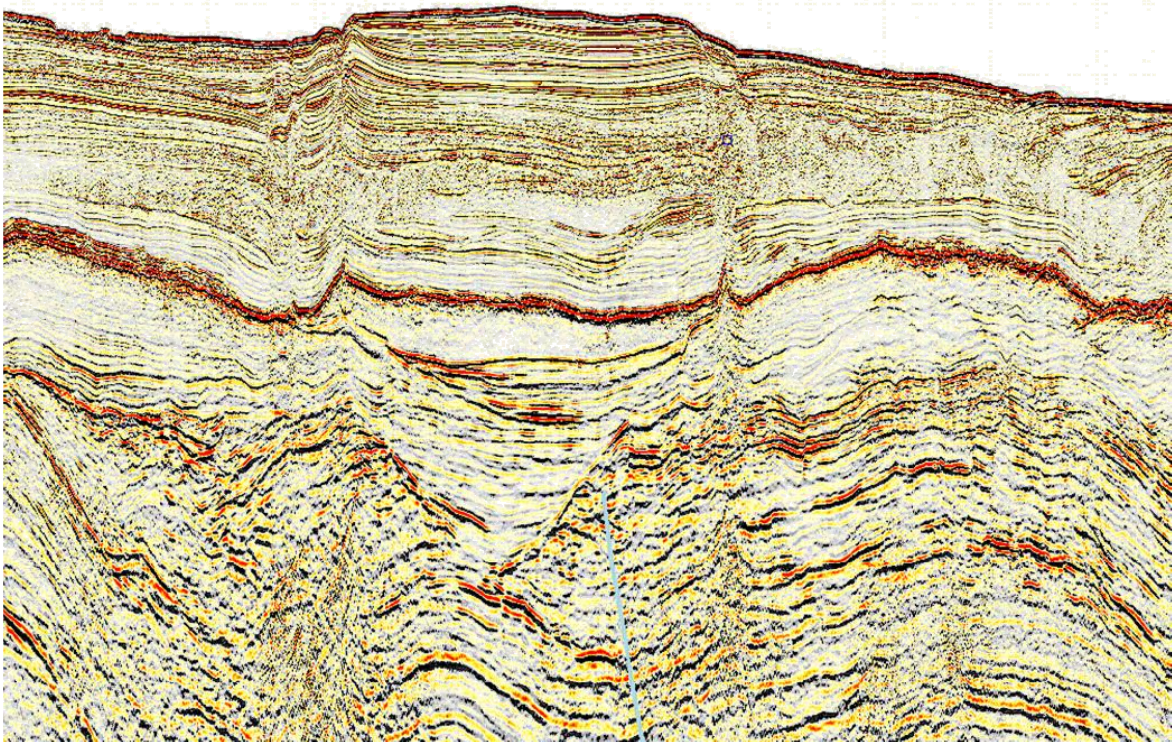

Prepared for the Petroleum Commissioner,
The Ministry of National Infrastructures

GSI/33/2008 **GII 446/426/08**

December 2008

The Oligo-Miocene deepwater system of the Levant Basin

Michael Gardosh[1], Yehezkel Druckman[2], Binyamin Buchbinder[2], Rani Calvo[2]

[1] - Geophysical Institute of Israel, P.O.B. 182, Lod 71100, Israel, **miki@gii.co.il**
[2] - Geological Survey of Israel, 30 Malkhe Israel St., Jerusalem 95501, Israel, **ydruckman@gsi.gov.il, b.buchbinder@gsi.gov.il, rani.calvo@gsi.gov.il**

Prepared for the Petroleum Commissioner,
The Ministry of National Infrastructures

GSI/33/2008 **GII 446/426/08**

December 2008

Table of content Page

List of Tables Page

List of Figures Page

Abstract

A study of the Oligo-Miocene section utilizing modern seismic data and well logs, revealed an extensive, siliciclastic deep-water, system in the Levant Basin and margin. The sedimentary succession reaches a few hundred meters onshore, and ~ 5,600 m in the deep basin. The latter consists of 3,500 m of clastics, overlain by up to 2,100 m of evaporates.

Four regional unconformity surfaces were detected in the seismic records within the Oligo-Miocene succession: (1) Early Oligocene; (2) Middle Miocene; (3) Late Miocene (upper Tortonian); and (4) latest Miocene (post-evaporites) time. The Early Oligocene, Late Miocene (upper Tortonian) and latest Miocene (post-evaporites) surfaces reveal a series of stacked submarine canyons on the Levant slope. Some of the canyons are deeply incised. Other canyons, less incisive, are located along structural lows. The Middle Miocene surface does not coincide with canyon incision. It rather reflects the Serravallian crisis characterized by deteriorated climatic conditions (cooling) and by local lowstand conditions and hardground. The canyons acted as conduits for transporting products of gravity flows from the shelf into the basin.

The Early Oligocene incision carved the two major canyons on the continental slope: the Afiq and Ashdod canyons. These two, together with their tributaries, are the main conduits trough which most, if not all, the sediment load was funneled down to the deep basin. These two canyons were filled to their rims by Oligocene sediments. Later in Late Tortonian times they were reactivated, deeply incised and partially refilled by Late Tortonian carbonates and clastics to be later buried by the massive Messinian evaporates overlapping their rims.

Unlike the Early Oligocene and Late Tortonian incision events, which took place under a continental slope setting, the latest Miocene (post-evaporites) incision took place subaerially following a 800 m drawdown of the sea level by the end of the upper evaporite deposition, leading to fluvial and lacustrine clastic deposition on the exposed continental slope.

Transport of sands from their provenance in the East and Southeast was probably more effective and widespread during the lower Oligocene and most of the Miocene, whereas, during the upper Miocene through the Pliocene, basinward transport was more restricted, because of increased subsidence in the Dead Sea Rift, which became a major trap for sediments from the East, and the uplift of the mountainous backbone of Israel.

Oligo-Miocene sands were deposited under two settings: (1) as channel fill within the canyons, in a confined, intra-slope setting, or (2) as sheets and lobes in an unconfined setting at the lower slope and basin floor. Channel-fill sands were penetrated by several wells and interpreted from seismic data. Basin floor sands were not yet tested by drilling and their existence is only inferred based on the seismic data. Both occurrences are considered as attractive, potential hydrocarbons traps. The Oligo-Miocene deep-water system of the Levant Basin overlies Mesozoic source rocks and is overlain by the Messinian evaporite seal. This combination strongly suggests a significant potential for major hydrocarbon discoveries in the Levant Basin.

1. Introduction

1.1 Exploration history

The Levant Basin occupies the Eastern Mediterranean Sea (Fig. 1). Its southern part, offshore Egypt hosts the prolific Nile Delta hydrocarbon province where extensive exploration and production activity is taking place. The increase in demand and rising price of oil in recent years has promoted a growing interest in the less known and under-explored, central and northern parts of the basin, offshore Israel, Lebanon and Cyprus.

Petroleum exploration in the Levant Basin offshore Israel has a long history and so far has yielded modest success. The first stage of exploration started in the 1960's and continued through the late 1990's. Most of the 16 wells that were drilled during this time targeted Mesozoic reservoirs in Syrian Arc type structures. Significant light oil accumulations were found in the Mango-1 borehole ($41\text{-}50^0$ API gravity oil that flowed at a rate of about 10,000 Bbl/day) and in the Yam-2 and Yam Yafo-1 boreholes ($44\text{-}47^0$ API gravity oil that flowed in a rate of 500-800 Bbl/day); however, no commercial production was established.

The second and more successful stage of exploration started in 1999-2000. Several large gas fields were discovered at a shallow depth in Pliocene deep-water turbidite sands west of the towns of Ashqelon and Gaza (Fig. 1). The reserves in these fields (Noa, Mari B, Nir and Gaza Marine) are estimated at about 3 TCF. Gas is presently produced from the Mari B field and is piped onshore to various Israeli consumers. The discovery of gas in Pliocene reservoirs established the status of the Levant Basin as a hydrocarbon province. It also focused attention to the significant potential of the Tertiary, deep-water section offshore Israel.

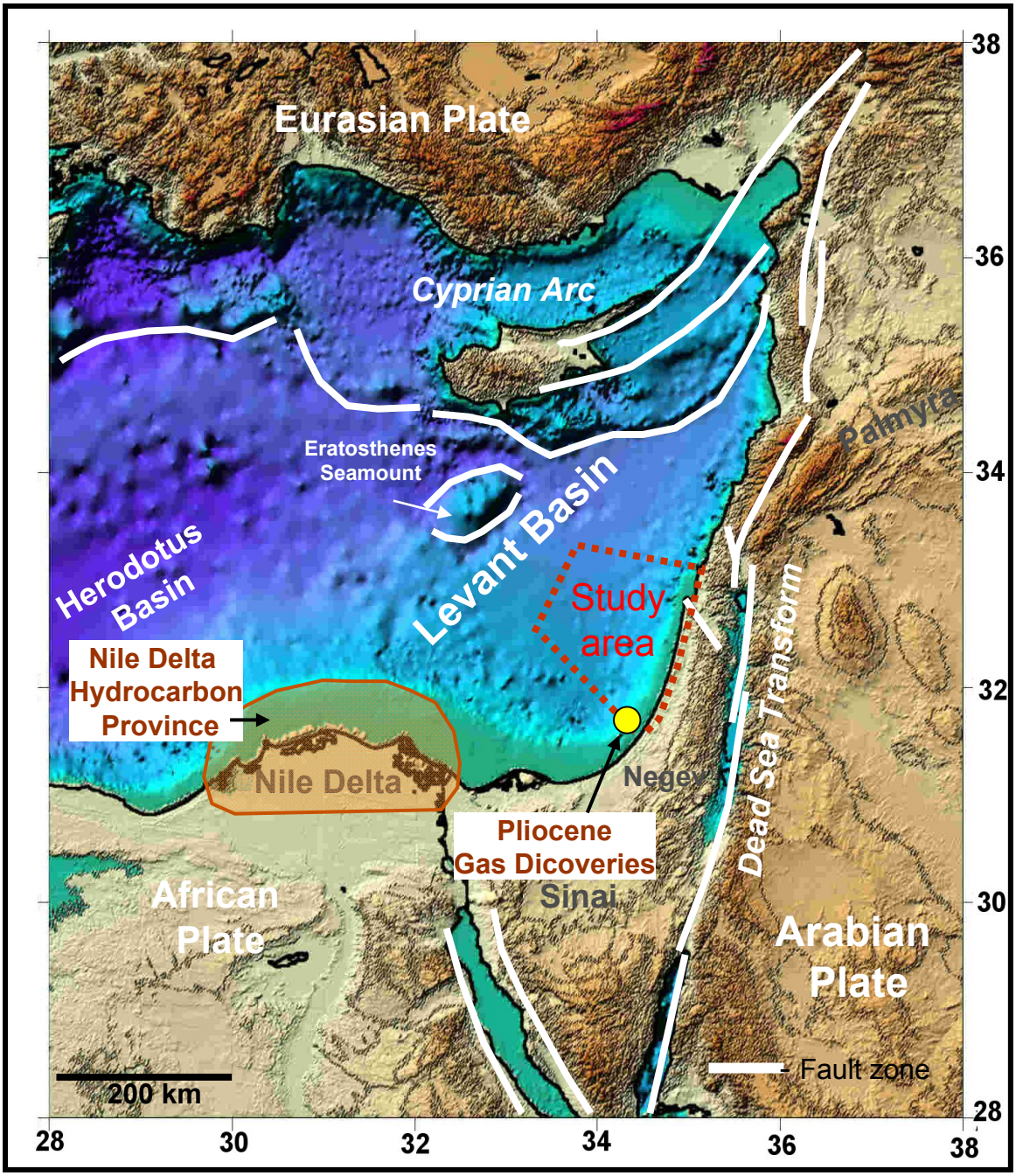

Figure 1: Regional setting of the study area and the location of Pliocene gas discoveries offshore Israel.

The discoveries of the early 2000's promoted the acquisition of geophysical data throughout the entire Eastern Mediterranean area. The new geophysical data sets include about 12,000 km of regional 2D seismic reflection lines and several 3D seismic cubes, as well as new gravity and magnetic surveys.

Following the successful drilling, the petroleum commissioner in the Israeli Ministry of Infrastructure initiated a regional analysis of the Levant Basin and margin. The first phase of this study that was completed in 2006 was aimed at reconstructing the overall basin's stratigraphy, structure and tectonic history (Gardosh et al., 2006; Gardosh et al., 2008). One of the main results of this study was the finding of an extensive submarine canyon system in the Oligo-Miocene section offshore Israel. The stratigraphic position of these canyons is below the Messinian evaporite seal and above potential Mesozoic source rocks. They are therefore considered as a prime target for exploration.

The purpose of this report is to analyze the Oligo-Miocene depositional system in the Levant Basin and surrounding area. We hope that the results presented herein will encourage and support further exploration activity of the prolific, yet under-explored, Levant Basin.

1.2 Geologic setting

The Levant Basin and surrounding area were shaped by three distinct tectonic phases:

(a) Rifting phase
(b) Post-rift, passive margin phase
(c) Convergence phase

Rifting in the Levant region is related to the breakup of the Gondwana plate and the formation of the Neotethys Ocean system (Freund et al., 1975; Garfunkel and Derin, 1984; Garfunkel, 1998; Gardosh and Druckman, 2006). Four extensional pulses were postulated: (1) in the latest Paleozoic; (2) in Middle Triassic (3) in Late Triassic; and (4) in Early Jurassic. These pulses are reflected in normal faulting with throw reaching several kilometers, in magmatic activity and in the formation of NE-SW oriented graben and horst systems. Four basement structures associated with the Early Mesozoic extension are found in the deep parts of Levant Basin (from east to west): the Yam, Jonah, Leviathan, and the Eratosthenes highs (Gardosh et al., 2006; Gardosh et al., 2008). The main structures inland are the Gevim, Ga'ash and Ma'anit highs and the northern Sinai, Judea and Asher grabens. The rifting in the Levant area reached an early magmatic stage. Although magmatic

intrusion and stretching of the crust took place, no indications for sea-floor spreading and emplacement of new oceanic crust are found (Gardosh and Druckman, 2006).

The post-rift phase is associated with cooling and subsidence that was probably more intense within the basin than on the eastern margin. The Late Jurassic to Middle Cretaceous section records a gradual formation of a passive-margin profile and the subsequent development of a deep-marine basin bordered by a shallow-marine shelf (Bein and Gvirtzman, 1977; Garfunkel, 1998). The passive-margin stage is characterized by recurring cycles of marine transgression and regression associated with relative sea-level changes (Flexer et al., 1986; Gardosh, 2002). These are reflected by marine onlaps, unconformity surfaces, stacking of carbonate platforms, on the basin's margin, and mass transported deposition in the basin.

The convergence phase is related to the closure of the Neotethyan Ocean system and the northward motion of the Afro-Arabian plate towards Eurasia (Robertson, 1998). In the Levant region this motion is manifested by large-scale contractional deformation of the Syrian Arc fold belt (Krenkel, 1924; Picard, 1959). Syrian Arc type folds are found throughout the Levant region, in an area extending from the Western Desert of Egypt, through Israel to Lebanon and Syria. Based on surface studies, Walley (2001) suggested two main folding phases: Late Cretaceous and Early Tertiary. The subsurface study of the Levant Basin confirmed this suggestion (Gardosh and Druckman, 2006; Gardosh et al., 2006; Bar et al., 2008; Gardosh et al., 2008). The Late Cretaceous Syrian Arc phase I is characterized by inversion of the Early Mesozoic normal faults and the development of asymmetric, high-amplitude folds found mostly near the eastern Levant margin and further inland. The Early Tertiary Syrian Arc phase II is characterized by the formation of low-amplitude folds throughout the basin, uplifting and tilting of marginal blocks at the eastern part of the basin and further inland. The contractional activity resulted with the formation of a wide elevated fold belt in the eastern part of Levant basin, extending 50-70 km west of the present-day coastline (Gardosh and Druckman, 2006; Gardosh et al., 2006; Gardosh et al., 2008).

Tertiary tectonic activity and sea-level falls caused intense erosion and accumulation of several kilometers thick basin-fill (Gardosh et al., 2006; Gardosh et al., 2008). Fluvial systems flowed on the exposed shelf from elevated areas in the east, while submarine turbidity currents incised the upper slope and transported siliciclastic sediments further into the basin (Druckman et al., 1995). The Oligo-Miocene and Pliocene drainage system includes several main submarine canyons and numerous secondary conduits (Gardosh et al., 2006; Gardosh et al., 2008). Two of the canyons in

the southeastern part of the basin, e.g. Afiq and Ashdod, are incised several hundred meters on the continental slope. Other canyons were less erosive and their flow pattern was for the most part dictated by pre-existing synclines. The Tertiary drainage system was shut-off temporarily during the Messinian salinity event and was turned-on again during post-evaporite, latest Miocene to Early Pliocene lowstands. A subsequent Plio-Pleistocene transgression was followed by the accumulation of a thick, siliciclastics prograding wedge along the Levant continental slope.

2. Data sets

2.1 Well and outcrop data

The well data used in this study is based on 44 wells located in the basin or on its eastern margin (Fig. 2). Stratigraphic subdivisions of these wells were, for the most part, taken from the lithostratigraphic database of oil and gas wells drilled in Israel (Table 1) compiled by Fleischer and Varshavsky (2002). Biostratigraphic data, from part of the wells, were reexamined and their stratigraphy was updated in the framework of this project (Siman-Tov, 2008a,b). Velocity data and time-converted wire-line logs were used for correlation of stratigraphic tops with the seismic data (Table 1). The lithostratigraphy and biostratigraphy of selected wells were thoroughly reviewed and were used to construct four detailed stratigraphic cross-sections extending from the coastal area to the eastern part of the basin (Fig. 2). Additional well and outcrop data from the Levant margin were analyzed and were integrated into a stratigraphic table and the marine onlap curve of the Tertiary succession (Fig. 3).

Table 1: Summary of well data used in the present study. The depth of chronostratigraphic and lithostratigraphic tops in the wells is in meters below MSL. These depth values were used for calibration the seismic data with depth maps. Abbreviations of lithostratigraphic units are: TY - Talme Yafe Formation, Mt Sc - Mount Scopus Group, Av - Avedat Group, BG - Bet Guvrin Formation, AshCl - Ashdod Clastics, Mav - Mavqiim Formation.

Chronostrat. Boundary		**Base Up. Cretaceous**	**Base Oligocene**	**Early Mid. Miocene ?**	**Base Messinian**	**Base Pliocene**
Seismic horizon		**Green**	**Red**	**Cyan**	**Purple**	**Violet**
Well names:	**Well Abbrv.**					
Andromeda-1	AND1				2149/Ziqim	2127/Mav
Ashdod-1	ASH1	2208/TY	2208	1785/BG	1710/Pattish	1690/Mav
Asher Yam-1	ASYM1	479/Yagur	479	479	479	479
Ashqelon-2	ASHQ2	2234/TY	2040/Av	1303/BG	1120/Ziqim	1063/Mav
Ashqelon-3	ASHQ3	2098/TY	1955/Av	1245/BG	1009/Ziqim	961/Mav
Atlit-1 Deep	ATLT1	45/Negba	45	45	45	45
Bat Yam-1	BYAM1	2432/TY	2197/Av	2087/BG	1479/AshCl	1479/NPVulc
Bravo-1	BRV1	2939Daliyya	2197/Av	1627/BG	1380/Ziqim	1350/Mav

Chronostrat. Boundary		Base Up. Cretaceous	Base Oligocene	Early Mid. Miocene ?	Base Messinian	Base Pliocene
Seismic horizon		**Green**	**Red**	**Cyan**	**Purple**	**Violet**
Well names:	**Well Abbrv.**					
Caesarea-2	CSR2	512/Bina	437/MtSc	437	437	437
Caesarea-3	CSR3	304/Bina	184/MtSc	184	184	184
Canusa-9	CAN9		885/Av	730/BG	393/Ziqim	360/Mav
Canusa-10	CAN10		192/Av	132/BG	132	132
Delta-1	DLT1	1416/Negba	1133/Av	1062/BG	1062	1062
Echo-1	ECO1			1972/BG	1972	1807/Mav
Foxtrot-1	FXT1	247/Negba	247	247	247	247
Gaash-2	GSH2	772/Daliyya	772	772	772	772
Gad-1	GAD1			2445/BG	1926	1848/Mav
Gaza-1	GAZ1	1657/TY	1631/Av	1367/BG	1367	1255/Mav
Hannah-1	HAN1	3963/ Gevar'am	3963	2914/BG	2786/Ziqim	1921/Mav
Hadera-1	HAD1		788/Av	583/BG	436/Ziqim	436
Hof Ashdod-1	HASD1	2583/TY	2220/Av	1901/BG	1859/Pattish	1739/Mav
Item-1	ITM1	1007/Daliyya	777/Av	727/BG	687/Ziqim	687
Kfar HaYarok-1	KYRK1	1297/Negba	1297	1297	1135/Volc.	1056/Mav
Jaffa-1	JAF1	2315/TY	2015Av	1472/BG?	1235/Ziqim	1212/Mav
Joshua-2	JOSH1		2502/Av	2305/AshCl	2230/Pattish	2077/Mav
Mari-3	MARI3				2021/Ziqim	1924/Mav
Menashe T3	MENT3		260/Av	112	112	112
Nahal Oz-1	NOZ1	1823/TY	1823	1741	1306/Ziqim	1115
Netanya-1	NAT1	1223/Bina	1053/MtSc	1053	1053	1053
Netanya-2	NAT2	1335/Negba	1335	1190	1041/Patish	938/Mav
Nir-1	NIR1				2053/Afridar	2004/Mav
Nissanit-1	NIS1	1642/TY	1602/Av	1035/BG	919/Ziqim	919
Noa-1	NOA1					1960/Mav
Noa South-1	NOA1S					1936/Mav
Nordan-4	NORD4			1320/BG	1134/Ziqim	1055/Mav
Or-1	OR1					1973/Mav
Or South-1	OR1S					1984/Mav
QishonYam-1	QISHY1	_____	_____	_____	1550	1200/Mav
Romi-1	ROM1					1428/Mav
Shiqma-1	SHQ1		1968/Av	1395	1360	1165/Mav
Yam-2	YAM2	2717/Negba	2123/Av	2095/Lakhish	2095	1772/Mav
Yam West-1	YAMW1	2848/TY	2395/Av	2216/BG	1731/Ziqim	1657/Mav
Yam West-2	YAMW2	2495/ Gevar'am	2438/Av	2028/BG	1714/Ziqim	1663/Mav
Yam Yafo-1	YAMY1	2380/Daliyya	1774/Av	1694/BG	1557/Ziqim	1524/Mav

= Wells used for depth to time correlation

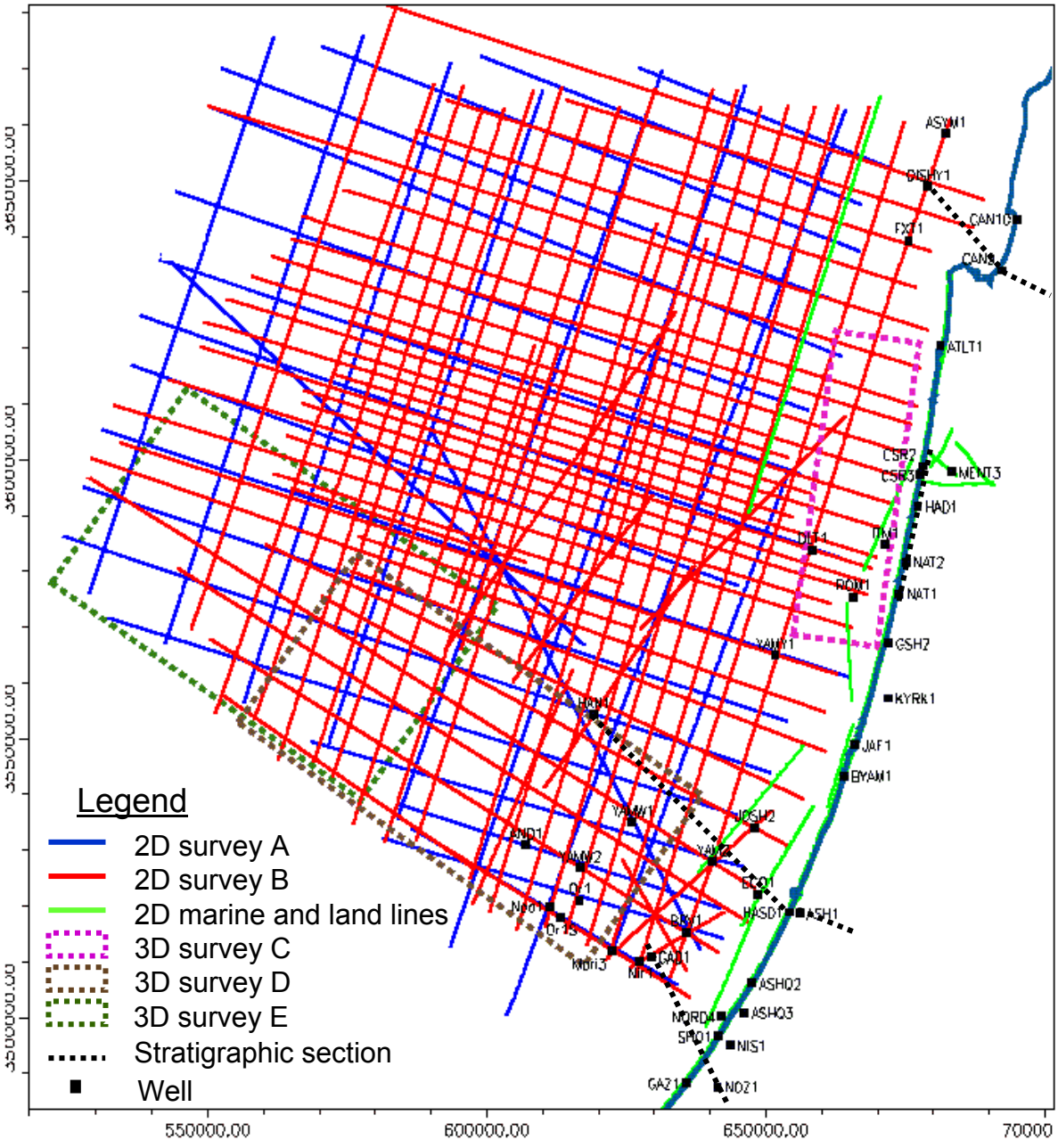

Figure 2: Location map of seismic lines, wells and stratigraphic sections (WGS 1984, UTM 36N projection).

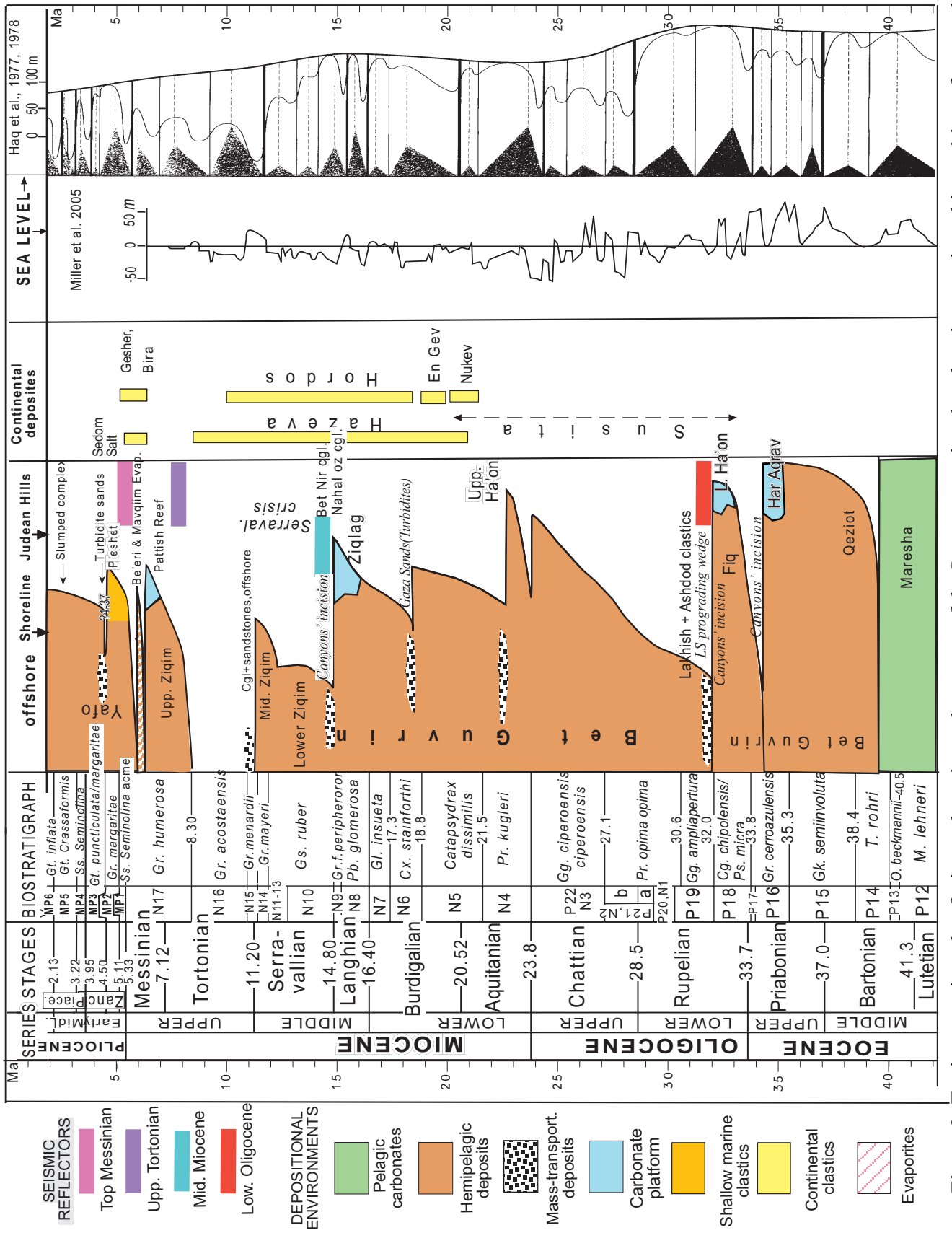

Figure 3: Tertiary stratigraphy, facies and marine onlap curve of the Levant margin, also showing stratigraphic position of mapped seismic reflectors.

2.2 Seismic data

The seismic interpretation of the Levant Basin is based on two large 2D reflection surveys that were acquired in 2001 (A and B in Fig. 2). Several additional 2D reflection lines from the eastern part of the basin and the coastal area onshore were integrated into the seismic data set (Fig. 2). These include 4 marine lines from the marine 94 series (310, 313, 330, 333); 2 marine lines from the marine 91 (214, 232); marine line BG-99-20, three on land vibroseis lines (DS-3597, MI-3597 and MI-3772), that extend along the entire coastline of Israel, and five on land vibroseis lines form the Caesarea area (DS-587, 588, 662, LP-2139, 2239). In most of the seismic lines the existing time migrated stacked versions were used for interpretation. Reprocessing was performed in the framework of this project on the marine line BG-99-20 and on the five vibroseis lines from the Caesarea area. The entire interpreted 2D dataset includes about 12,000 km.

Time migrated cubes of three 3D marine surveys were interpreted and integrated into the seismic data: Survey C- offshore the Caesarea-Netanya area and Surveys D and E, offshore the Ashdod-Ashqelon area (Fig. 2).

3. Tertiary stratigraphy

3.1 General

A major change in depositional style took place in the Levant region during the Late Eocene. Deposition of carbonates ceased and was replaced by siliciclastic deposition. This change reflects a major change in depositional settings, most likely due to tectonic activity on both regional and local scale. The basinward transport of the siliciclastic erosion products was associated with extensive erosion and incision on the Levant slope, followed by the accumulation of several kilometers thick Tertiary fill (Gardosh et al., 2006; Gardosh et al., 2008) in the Levant Basin. The Oligocene to Pliocene section was termed the Saqiye Group (Gvirtzman, 1970). It is characterize by marine onlaps forming cycles of different scales, separated by numerous unconformities which are partly associated with relative sea level changes (Fig. 3).

Four major seismic events were identified in the Oligo-Miocene succession and subsequently were presented in contour maps: (a) lower Oligocene (b) Middle Miocene (c) Late Tortonian (d) latest Messinian (Fig. 3). These events represent regional unconformities (Fig. 3). The lower Oligocene, the Late Tortonian and the latest Messinian events coincide with three major canyon incisions events, while the Middle Miocene seismic event apparently reflects the Serravallian crisis (units N10-13, Fig. 4) characterized by deteriorated climatic conditions (cooling) and by local lowstand

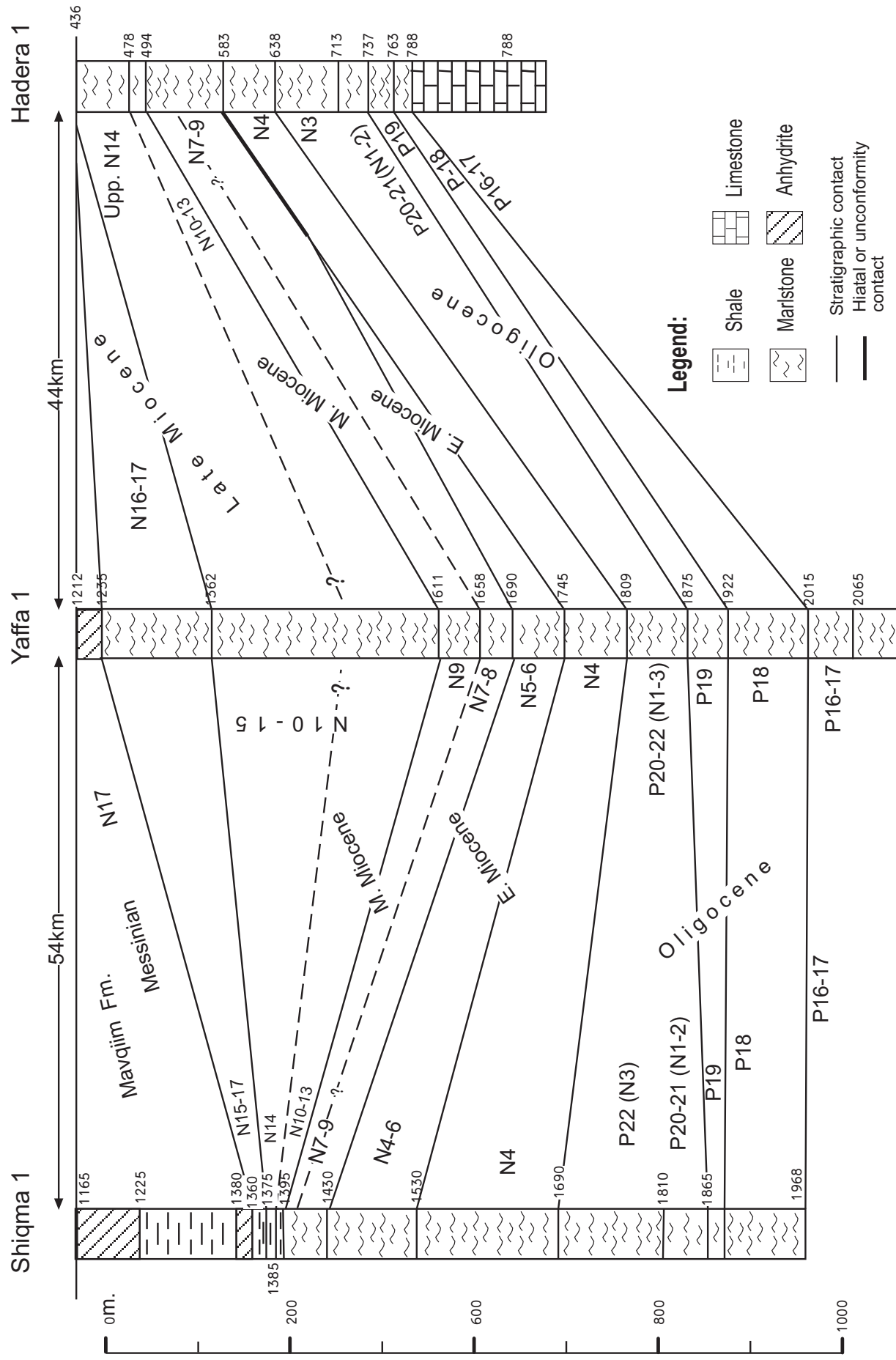

Figure 4: Regional stratigraphic cross section showing Oligo-Miocene stratigraphic units in the Levant margin. This section represents the most complete Oligo-Miocene succession in the area. Note the condensation of the Seravallian section (N0-N14) in both the Shiqma and Hadera wells. Datum: base Pliocene.

conditions, and possibly sediment starvation (Siman-Tov, 1984; Martinotti, 1990; Buchbinder et al., 1993; Esteban, et al., 1996; Gardosh et al., 2008). The Late Tortonian seismic event correlates with the erosive plane upon which the Pattish reef and the Messinian evaporites were deposited.

The Saqiye Group includes shallow to deep marine units found today at the Coastal Plain and offshore area of Israel. At the time of deposition of the marine Saqiye sediments, continental deposits accumulated further inland (Fig. 3). The Oligo-Miocene continental units in southern and northern Israel, such as the Hazeva Group and Hordos Formation are poorly dated; therefore their correlations with the marine units of the Saqiye Group is not well established and is only schematically shown in Figure 3. The following chapters will focus on the Tertiary marine units of the Levant margin.

This submarine canyon and channel system evolved during the Early Oligocene and persisted till the Pliocene when it was finally buried under the Nilotic sediments.

3.2 Eocene

Facies patterns of the lower and Middle Eocene are predominantly pelagic. Although seemingly they contain shallower neritic interludes of nummolitic carbonates, the mixture with pelagic elements indicates a mass transport origin in a deeper basinal setting (Buchbinder et al., 1988), beginning in latest Early Eocene times (Benjamini, 1993).

In proximal areas of the northern Negev an unconformity was found between the Middle Eocene chalks of the Maresha Formation and the hemi-pelagic marls of the Qezi'ot Formation (upper Eocene, Fig. 3). Benjamini (1979, 1984) indicated that the maximum hiatus between the two formations spans the P10 to P14 biostratigraphic zones. The Qezi'ot and the Bet Guvrin formations (its equivalent in the Coastal Plain and the Shefela areas, Fig. 3) are included in the Saqiye Group (Gvirtzman, 1970). The latter signify the "Upper Clastic Division" of Ball and Ball (1953). Occasional mass transported conglomerates are found especially in distal areas. In the Shefela area, the Bet Guvrin Formation is of the upper Eocene *semiinvoluta* Zone (P15). The latest Eocene (P16) zone is missing. Siman-Tov (1991) reported on the rare occurrence of the latest Eocene *T. cerroazulensis* zone in Ofaqim and in Tel-Nagila. In other upper Eocene locations this zone was truncated by the following major unconformity in Early Oligocene. The Har-Aqrav limestone (Fig. 3), which overlies the Qezi'ot Formation in the western Negev (Benjamini, 1980), apparently

represents the highstand progradation phase of the Late Eocene cycle. Markedly, the hemi-pelagic facies of the Late Eocene is primarily uniform, both inland and far offshore.

Unlike other locations, the Eocene succession in the synclinorial area of the Golan Heights show an uninterrupted Early to Late Eocene biostratigraphic succession from P9 to P15 (Michelson and Lipson-Benitah, 1986). Therefore, the upper Eocene (P15) chalk of the Golan Heights was regarded by Michelson and Lipson-Benitah (1986) as the Maresha Formation (Fig. 3).

3.3 Lower Oligocene to lower Miocene succession

3.3.1 Lower Oligocene erosion phase

A major unconformity is found between the Late Eocene and Early Oligocene depositional cycles (Fig. 3). It could have been related to eustatic sea-level fall at 34 m.y. (shown by Haq et al., 1988 and Miller et al., 2005). Local uplift movements associated with Syrian Arc contraction or with doming of the Arabian Shield prior to the rifting of the Red Sea (Garfunkel, 1988) further intensified the erosional processes. A regional unconformity surface (peneplain) developed in the Negev and the Judea Mountains (Picard, 1951; Garfunkel and Horowitz, 1966). Zilberman (1992, 1993) named this unconformity “the upper erosion surface” and pointed out that it postdates upper Eocene deposits and predates Miocene continental deposits of the Hazeva Group. The presence of this erosion surface in the Judean hills indicates that the anticlinorial backbone of the country had already been emerged at that time. (Bar et al., 2006).

Buchbinder et al. (2005) related the first incision of canyons in the Levant margin to the Early/Late Oligocene boundary (Fig. 3). Druckman et al. (1995) associated it with P19 - *ampliapertura* Zone (Fig. 3). The main incision in the Ashdod-1 borehole (see Figure 7 in Buchbinder et al., 2005) may have been occurred at the bottom of the "Lower Sands" ("Ashdod clastics" in Fig. 3), i.e., either between P19/P20, or within the P20, P21 zones (Fig. 3). Alternatively, it may be placed at the base of the lower Oligocene (P18) conglomerates. In the Hanna-1 borehole, which is located at the distal part of the Ashdod Canyon, the base of the canyon fill was dated as P19 (Micro-Strat, 2003). The diversified ages of the entrenchment of the Ashdod Canyon are obviously the result of the poor biostratigraphic resolution, because of intense contamination and redeposition in the cutting samples. Nevertheless, for the sake of convenience and simplicity in the interpretation of the seismic data, the initial phase of the canyon's incision was placed at the P19 biozone (Fig. 3, see chapter 4).

3.3.2 Lower Oligocene sediments

Patchy outcrops of lowermost Oligocene sediments (zone P18 in Fig. 3) are scarce and are sparsely spread from the Golan to the Northern Negev. They are more common in wells along the Mediterranean coastal plain and offshore areas, where they are included in the lower part of the Bet Guvrin Formation (Fig. 3). These sediments invariably consist of deep-water pelagic marly chalks, and their aerial distribution largely follows the distribution of the upper Eocene deposits, except for their absence in the Southern Negev (Buchbinder et al., 2005). These units thus indicate that most of Israel, except the southern and central Negev, was covered by sea in earliest Oligocene times.

3.3.3 Upper Rupelian- lower Chattian transported clastics lowstand and carbonate wedge

Sediments of P19-P21 zones (*ampliapertura* to *opima opima*, Fig. 3) have a limited inland distribution. However, sediments of the *opima opima* zone penetrate more inland to the Lower Shefela region (Lakhish Formation), characterizing of slumped blocks, debris flows and occasional sandy calcareous turbidites (Lakhish area). These mass transported sediments are covered by a few meters of *in situ* large-foraminiferal limestone representing a lowstand prograding wedge (Buchbinder et al., 2005). More than 300 m of sand and conglomerates of this phase were penetrated in the Ashdod wells in the Coastal Plain (Fig. 3).

3.3.4 Upper Oligocene (P22) - lower Miocene (N4) cycles

These cycles represent the last major Oligocene transgressions (Fig. 3). They are separated by an erosional unconformity of moderate magnitude. The onlap of the Early Miocene cycle; i.e. the upper Ha'on Member (Susita Formation), reached the Golan area across the Rift Valley (Fig. 3, Buchbinder et al., 2005). However, their hemi-pelagic sediments were largely eroded from the hilly backbone of the country. The facies is ubiquitously pelagic or hemi-pelagic (Bet Guvrin type), except in the most proximal outcrops in the Golan Heights.

3.3.5 The Burdigalian lowstand (N5-N7)

Sediments of this interval are limited to the Coastal Plain and offshore area. Canyon incision was renewed and mass transported deposits occasionally accumulated, as exemplified by the Gaza sands (Fig. 3; Martinotti, 1973).

3.3.6 Lowermost Middle Miocene cycle (Ziqlag Formation)

This cycle is unique in the sense that it shows a development of a carbonate platform in times of dominant fine siliciclastic deposition (Ziqlag Formation, Fig. 3) unconformably abutting the

western flank of the Judean anticline (Buchbinder and Zilberman, 1997; Buchbinder et al., 1993). However, its life span was short (ca. 1.5 m.y.). The high sea level at that time facilitated the development of the carbonate platform by curbing siliciclastic supply, while hemi-pelagic deposition of the Bet Guvrin facies, persisted in the basin (Fig. 3). However, a thick (250 m) succession of conglomerate, consisting of limestone, chalk and chert pebbles apparently derived from Cretaceous to Tertiary formations, was found in the Nahal Oz-1 borehole in the Afiq Canyon (Druckman et al., 1995).

3.4 The Middle Miocene Serravallian crisis

The Ziqlag episode terminated abruptly when the sea level dropped and erosion and canyon incision resumed, leaving behind their products: conglomerates and overbank deposits (Bet Nir conglomerate, Buchbinder et al., 1986). This happened despite the relatively high global sea level. Apparently, a climatic, ecological and salinity crisis occurred in the Mediterranean during Serravallian times, and as a result, the Mediterranean sea-level curve departed from that of the global sea level (see Martinotti, 1990; Buchbinder et al., 1993; Esteban et al., 1996). Small onlap episodes of limited landward penetration are indicated by the middle Ziqim (N14 zone) "mini" cycle (Fig. 3).

3.4.1 Upper Miocene (Tortonian) (N16-N17) Messinian cycle

Although of limited inland penetration, sediments of this cycle are relatively common in outcrops (Buchbinder and Zilberman, 1997) and especially in wells in the Coastal Plain and offshore. The cycle is marked by the accumulation of basinal hemi-pelagic marly sedimentation, capped by coral (mostly *Porites*) and algal reefs of the Pattish Formation in proximal plarform position (Fig. 3). However, in the offshore extension of the Afiq Canyon, hemi-pelagic muds are found, interbedded with mass transported sands, conglomerates of chert pebbles. The forced regression of this cycle is represented by the lower part of the Mavqiim anhydrites.

3.5 The uppermost Miocene (Messinian) evaporites

The Messinian evaporites are found throughout the Mediterranean region (Hsu et al., 1973a; Hsu et al., 1973b; Neev et al., 1976; Ryan, 1978). The deposition of Mavqiim evaporites (Fig. 3), which are composed mainly of halite and some anhydrite, followed a major sea-level drop associated with the closure and desiccation of the Mediterranean Sea (Hsu et al., 1973a; Hsu et al., 1973b; Hsu et al., 1978; Gvirtzman and Buchbinder, 1978). The area of evaporite accumulation extended throughout the Levant basin to about 20-40 km west of the present-day coastline (Gardosh and

Druckman, 2006; Bertoni and Cartwright, 2007). The Messinian evaporites most likely filled a pre-existing topographic depression (Tibor et al., 1992) and were not associated with significant, tectonic movements. However, during short highstand onlap episodes, the brine covered the slope and penetrated through deep canyons further inland. Remnants of the Messinian evaporites in the form of a few tens of meters of thick halite and anhydrite beds were encountered in various wells in the coastal areas of Israel (Druckman et al., 1995; Cohen, 1988).

3.6 Plio-Pleistocene cycle

The abrupt sea-level rise in the Early Pliocene terminated the evaporite deposition and resulted in the deposition of hemi-pelagic clays and marls of the Plio-Pleistocene Yafo Formation (Fig. 3) reaching over 1,000 m in thickness (Neev et al., 1976). Sedimentation during the lowermost Pliocene succession was highly condensed. After deposition of a few tens of meters of hemi-pelagic marl in a period of ca. 1 m.y., a significant sea-level drop occurred, estimated to correspond with the 4.37 m.y. sequence boundary of Hardenbol et al. (1998) (correlated with Haq et al., 1988, 4.2 m.y. sequence boundary). This lowstand resulted in the deposition of gas-bearing sands of turbidite origin in a basin floor or lower slope setting (Fig. 3) (Druckman, 2001; Oats, 2001). Hemi-pelagic deposition was resumed during the following highstand and the rate of sedimentation gradually increased, eventually resulting in a progradational topset-clinoform pattern along the entire Levant margin offshore Israel.

4. Seismic interpretation

4.1 Seismic horizons in the Levant Basin fill

The seismic reflection data of the Phanerozoic section in the Levant Basin comprises a package 5 to 6 seconds thick near the Israeli coast and reaches up to 10 seconds (15-17 km) in the far offshore. Gardosh et al. (2006, 2008) subdivided the basin-fill into eight distinct seismic units that are separated by seven seismic horizons (Table 2). Each of these horizons is interpreted as an unconformity surface that bounds a regional, basin-scale depositional sequence. All the interpreted surfaces mark significant changes in seismic character within the basin-fill. Some are recognized by truncation and onlapping or downlapping reflections. The interpreted seismic markers extend throughout the entire basin; therefore they are not correlated to individual seismic reflections but rather to the tops (or bottoms) of separable seismic packages. Well control on the seismic interpretation is possible only in the relatively shallow, eastern part of the basin. In this area the horizons show good fit to the tops of lithostratigraphic units identified in the wells (Table 1).

Table 2: Correlation of interpreted seismic horizons to lithostratigraphic units of the Levant Basin. See also the Tertiary stratigrpahy in Figure 3.

Seismic Horizon	Lithostratigraphic Boundary	Estimated Age
Violet	Top Mavqiim/Afiq (M horizon)	Latest Messinian (latest Miocene)
Purple	Top middle Ziqim/Pattish, or base anhydrites (N horizon)	Late Tortonian (Late Miocene)
Cyan	Top Bet Guvrin/ Ziqlag	Langhian (early Middle Miocene)
Red	Top Avedat	Late Eocene to Early Oligocene
Green	Top Talme Yafe/ Yagur / Negba / Daliyya	Albian to Turonian

4.2 Identification of Tertiary unconformities in the seismic data

4.2.1 Elevated, eastern margin of the basin

Three Tertiary unconformities that were identified by Gardosh et al. (2006, 2008) in the Levant Basin are marked on the seismic profiles by the red, cyan and purple horizons (Figs. 5-12). The three surfaces correspond respectively to major stratigraphic boundaries of (a) base Oligocene (b) lower Middle Miocene and (c) base Messinian anhydrite (Table 2). All three surfaces are characterized on the seismic data by incision, truncation and onlapping of seismic events. These phenomena are clearly recognized in the eastern, elevated part of the basin in an area extending from the present-day coastline to some 50-70 km westward.

An excellent example for Tertiary incision is observed in a seismic profile near the Hanaha-1 borehole (Fig. 5). A conspicuous truncation surface, marked by the red horizon, is found at the center of the profile at about 3.6 sec TWT. The surface shows 800 m deep gorge cut into a mildly folded package of parallel reflections. At the bottom of this gorge, the Hanaha-1 borehole penetrated the lower Cretaceous Gevar'am Formation, whereas the overlying canyon-fill is correlated by biostratigraphic data to the lower Oligocene Bet Guvrin Formation (Fig. 5) (Micro-Strat, 2003). This truncation surface is therefore correlated to the lowermost Oligocene regional unconformity at the base of the Saqiye Group.

A second, shallower incision surface, marked by the cyan horizon, is found in the seismic profile at about 2.8 sec TWT (Fig. 5). The surface is characterized by truncation, forming a wide, 100-200 m deep canyon. In the Hanaha-1 borehole, the strata below the canyon floor (at 2,862 m below MSL) were dated as lowermost Middle Miocene (top of Bet Guvrin Formation) whereas the canyon fill is of Middle Miocene, possibly Serravallian age (Micro-Strat, 2003). This truncation surface is therefore correlated to a regional unconformity of early Middle Miocene age.

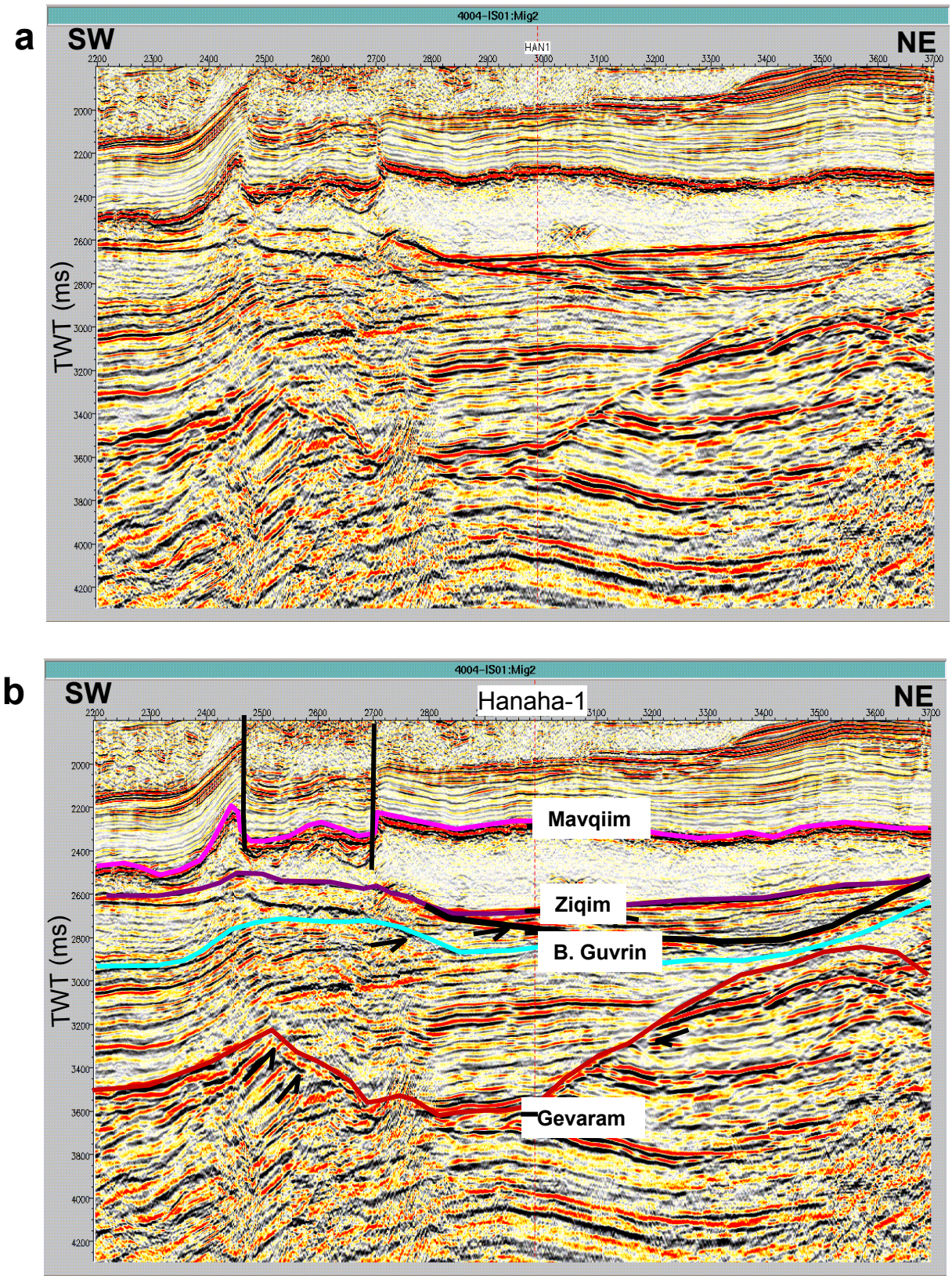

Figure 5: Time migrated 2D seismic profile across the western part of the Ashdod Canyon (a) uninterpreted, (b) interpreted. See location in Figures 13 to 15.

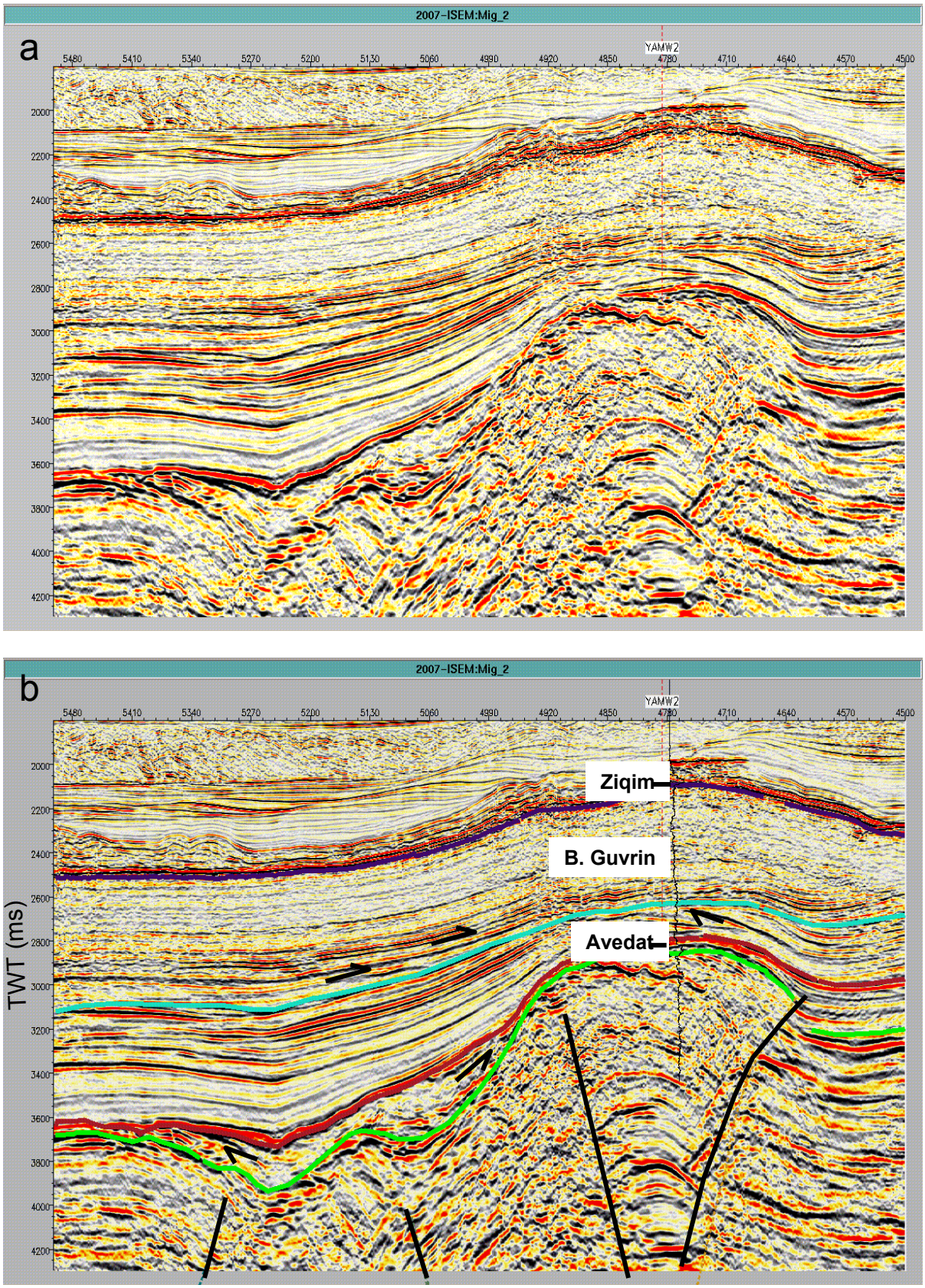

Figure 6: Time migrated 2D seismic profile across the Yam West-2 structure (a) uninterpreted, (b) interpreted. See location in Figures 13 to 15.

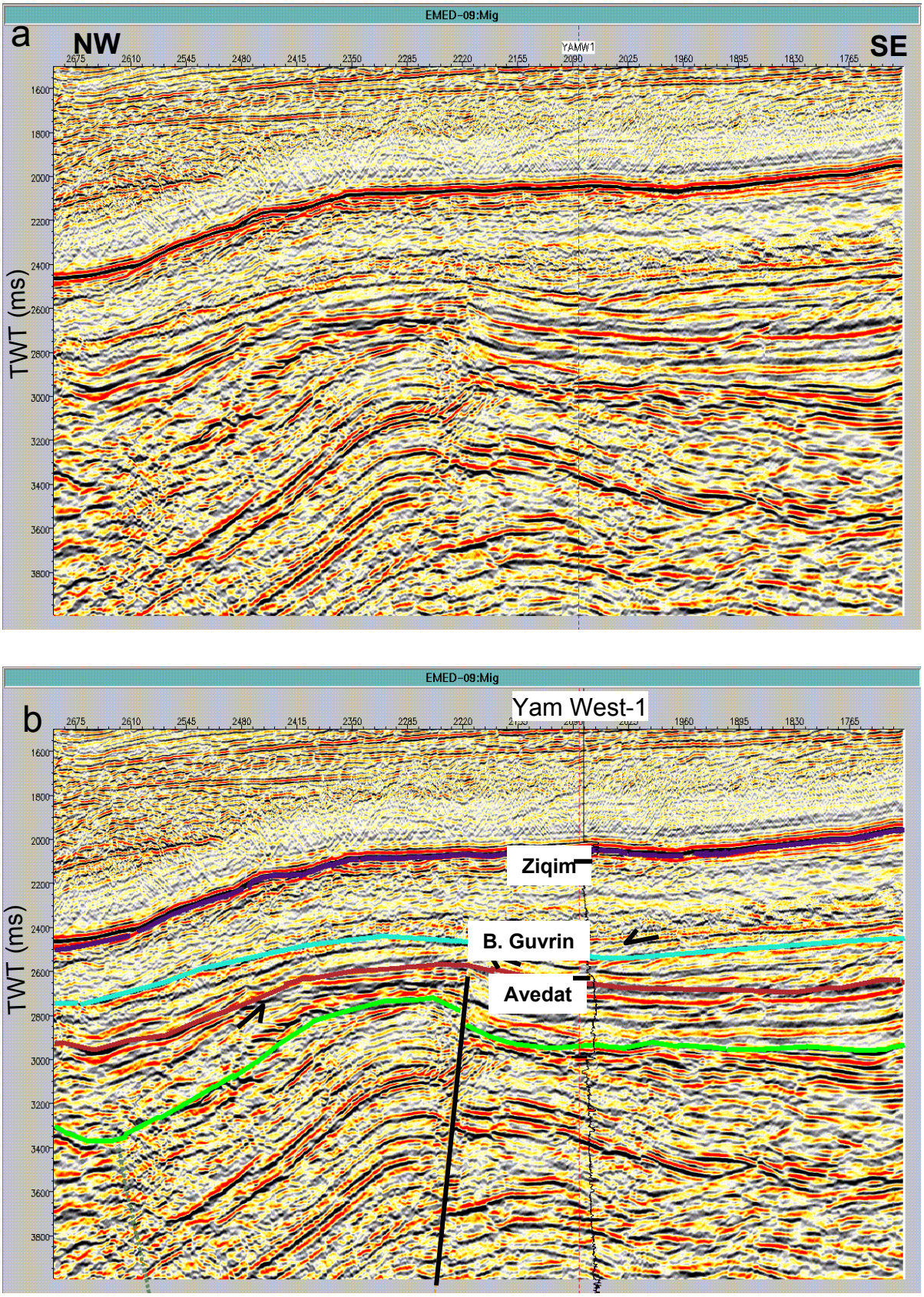

Figure 7: Time migrated 2D seismic profile across the Yam West-1 structure (a) uninterpreted, (b) interpreted. See location in Figures 13 to 15.

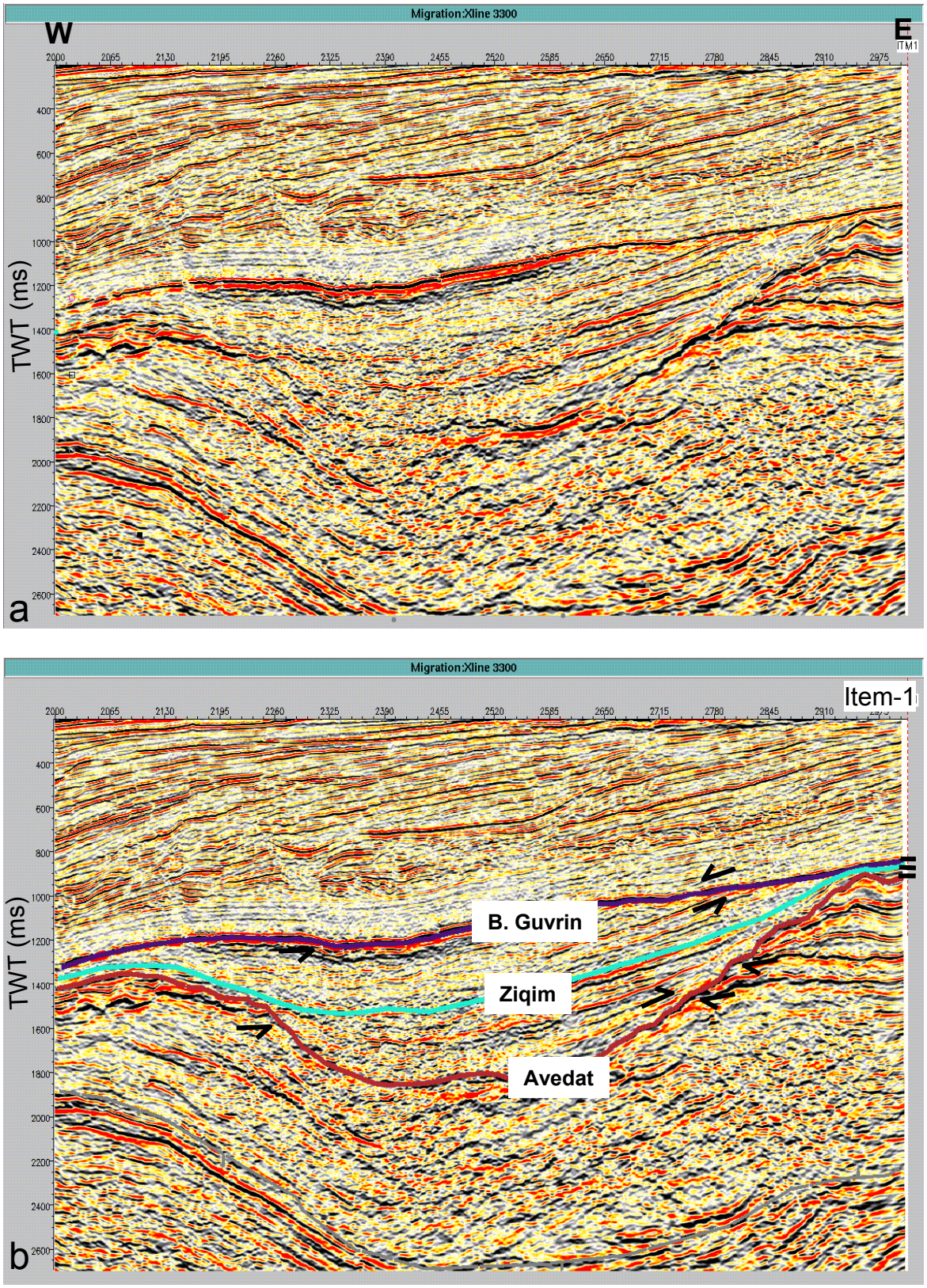

Figure 8: Time migrated 2D seismic profile across the Hadera Canyon (a) uninterpreted, (b) interpreted. See location in Figures 13 to 15.

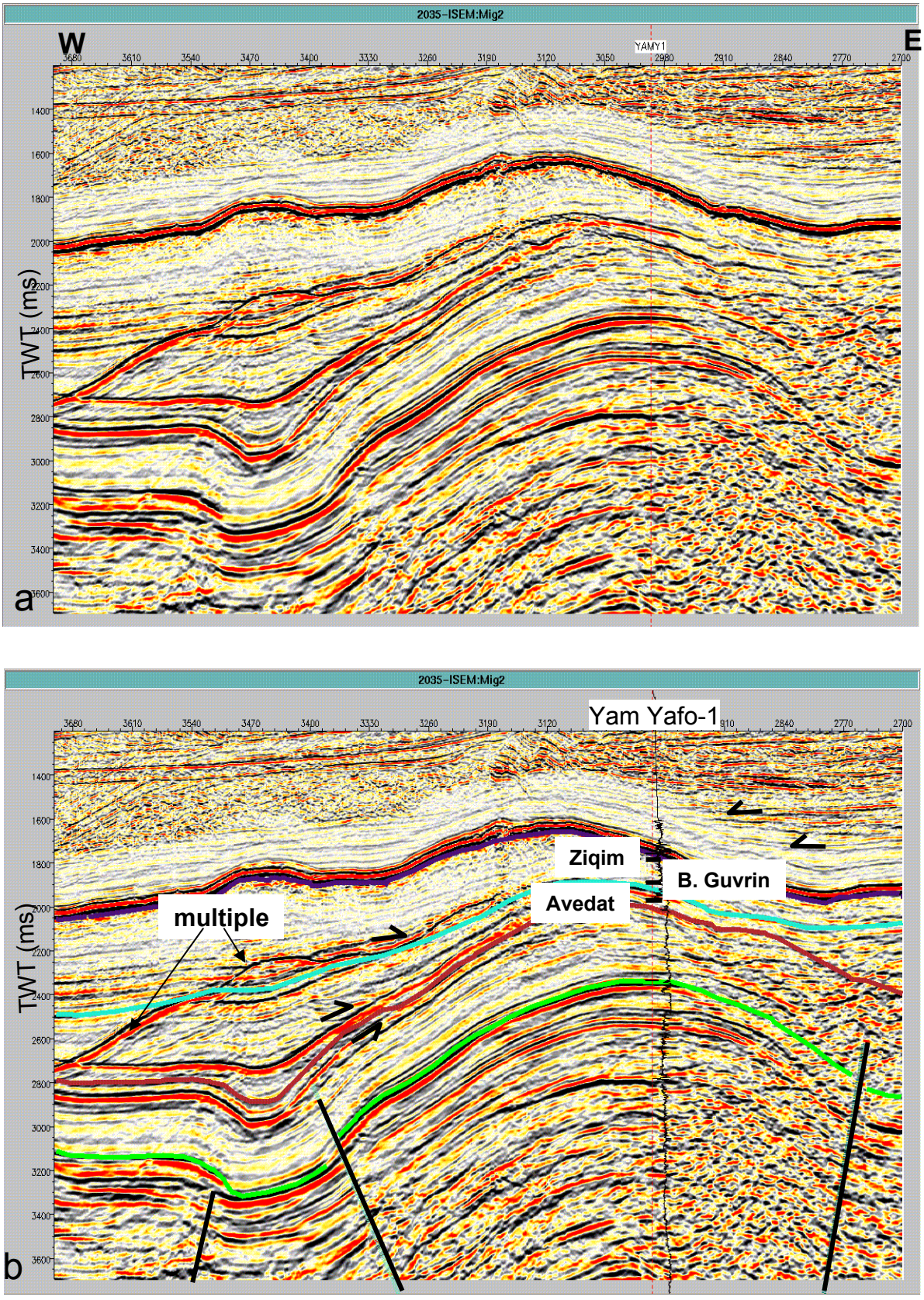

Figure 9: Time migrated 2D seismic profile across the Caesarea Canyon and the Yam Yafo-1 Structure, (a) uninterpreted, (b) interpreted. See location in Figures 13 to 15.

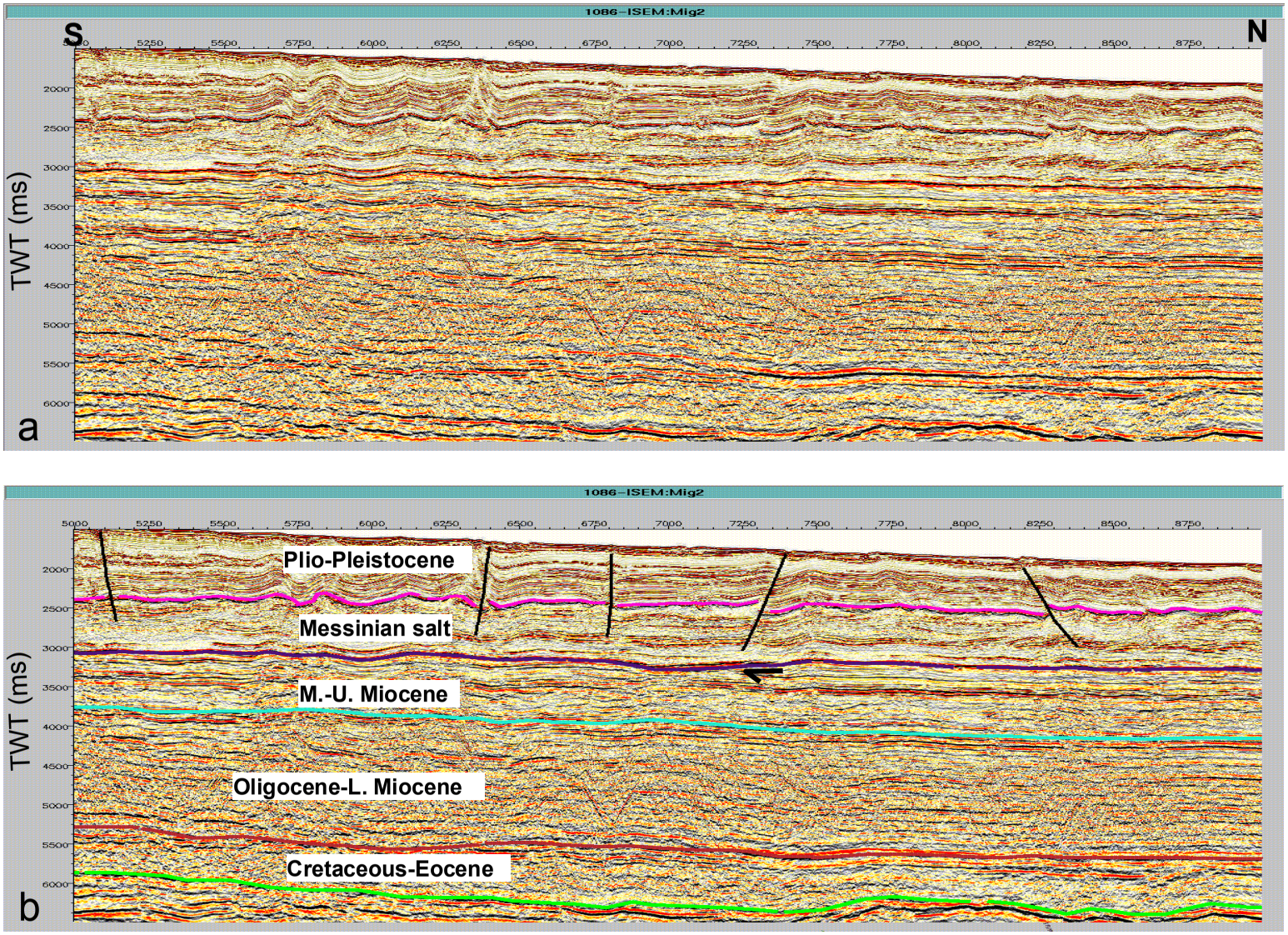

Figure 10: Time migrated 2D seismic profile showing the Tertiary unconformities in the deep part of the basin, (a) uninterpreted, (b) interpreted. See location in Figures 13 to 15.

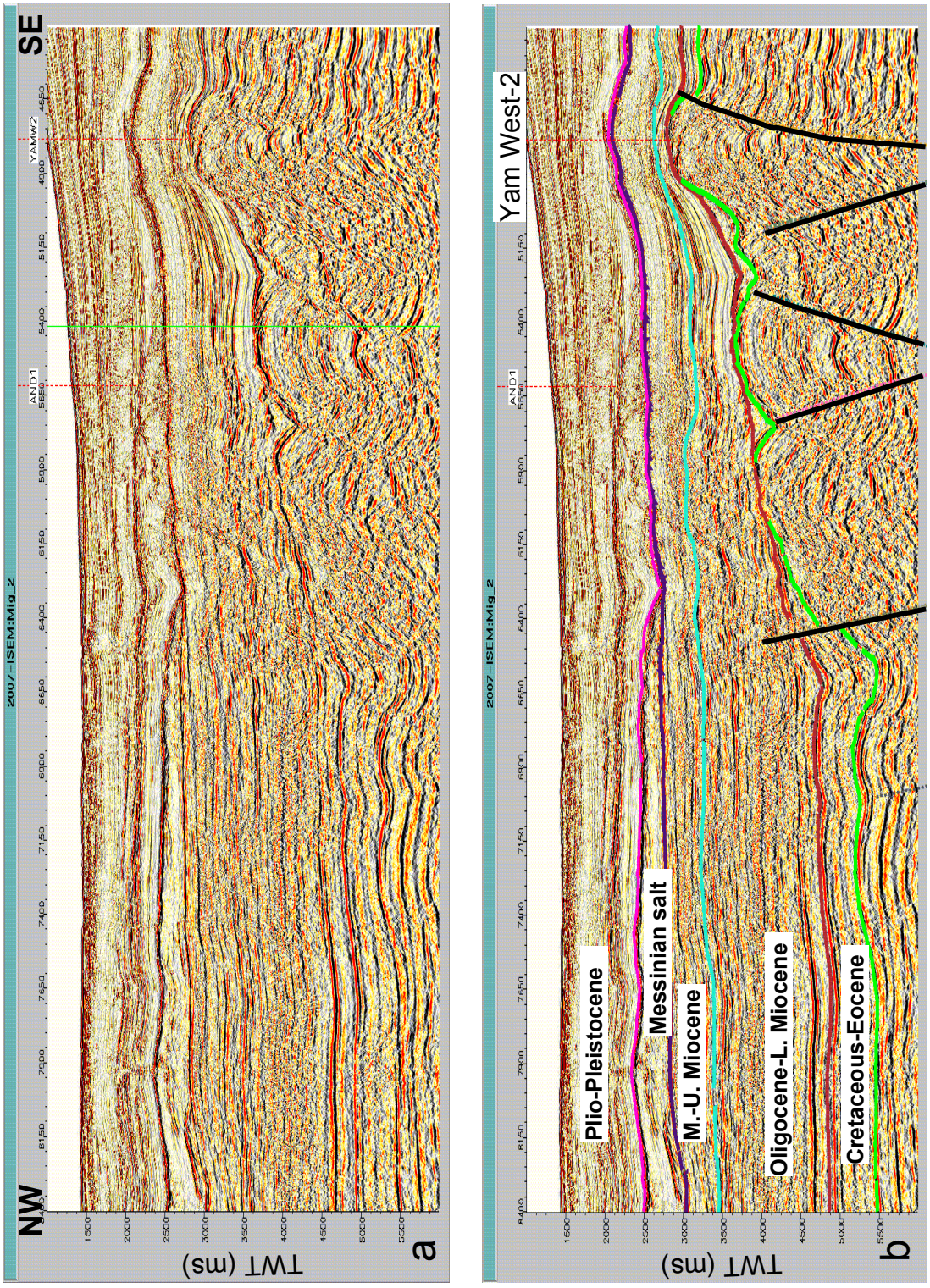

Figure 11: Time migrated 2D seismic profile showing the correlation of the Tertiary unconformities from the shallow to the deep deep part of the basin near the Yam West-2 well, (a) uninterpreted, (b) interpreted. See location in Figures 13 to 15.

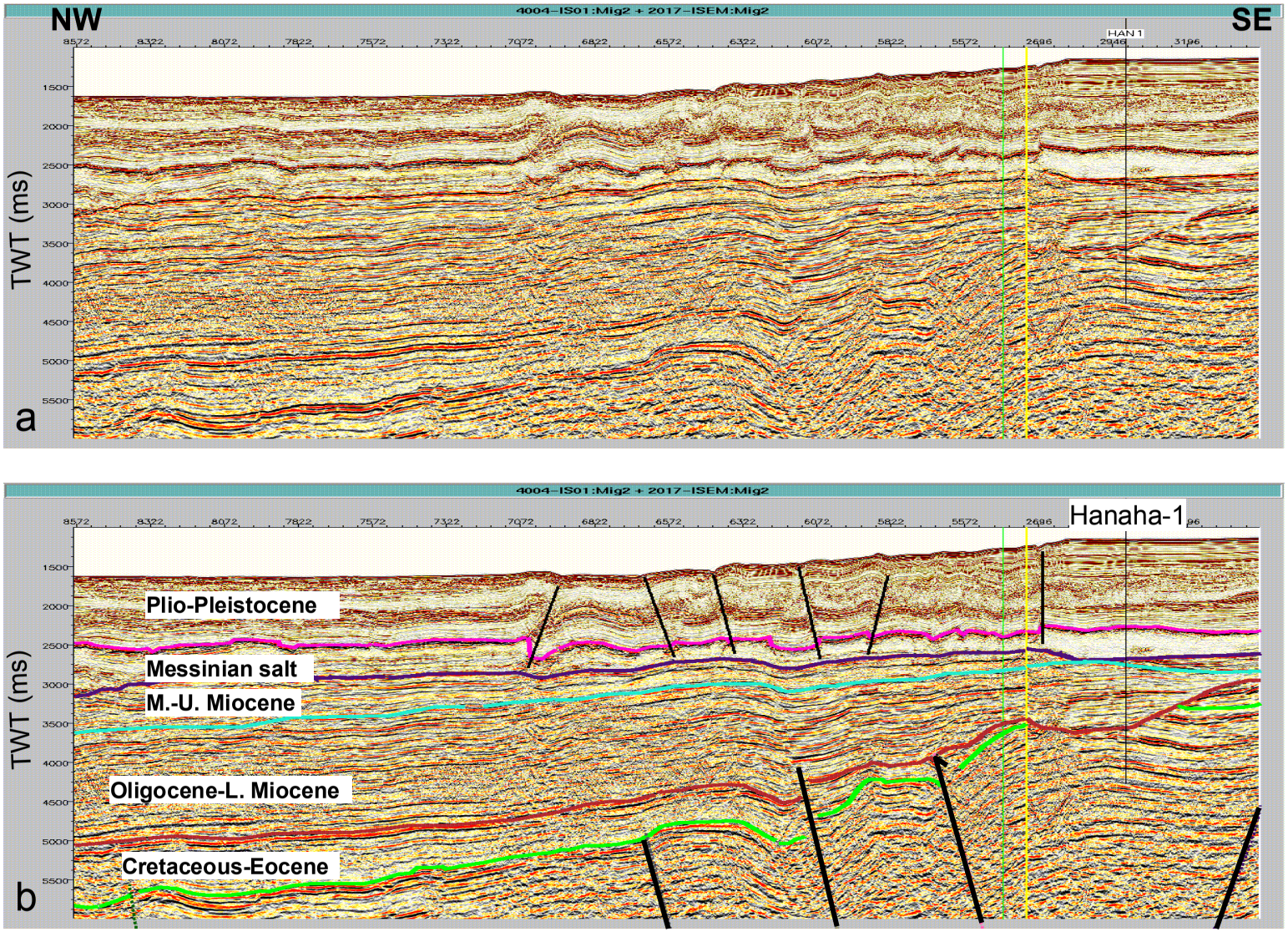

Figure 12: Composite, time migrated 2D seismic profile showing the correlation of the Tertiary unconformities from the shallow to the deep deep part of the basin near the Hanaha-1 well, (a) uninterpreted, (b) interpreted. See location in Figures 13 to 15.

A third incision surface, marked by the purple horizon, is evident on the seismic profile at about 2.6 sec TWT (Fig. 5). Correlation to the Hanaha-1 borehole shows that this surface is overlain by 865 m of Messinian salt (Samedan, Mediterranean Sea, Hannah-1, Composite Log 2003) and it is therefore correlated to the base Messinian regional unconformity.

Another example of Tertiary incision is shown on a seismic profile near the Yam West-2 borehole (Fig. 6). A discontinuous high-amplitude seismic event, marked by the red horizon, is observed east and west of the well. The horizon shows truncation at the top of the Yam West fold structure and within the syncline west of it (Fig. 6). This surface is correlated to an unconformity of Late Eocene to Early Oligocene age (base of Bet Guvrin Formation) found in the Yam West-2 borehole at 2,483 m below MSL (Derin, 1999).

A second shallower incision and onlapping surface, marked by the cyan horizon, is observed at about 2.7-3.1 sec TWT (Fig. 6). In the Yam West-2 borehole this surface is found within the upper part of the Bet Guvrin Formation (of Langhian age) (Derin, 1999) and is therefore correlated to the regional early Middle Miocene unconformity.

The base Messinian unconformity, marked by the purple horizon, is not a significant truncation surface on this profile. It is identified by the high amplitude event at the base of the thin evaporitic section (Mavqiim Formation) found in the Yam West-2 borehole at 1,714 m below MSL (Fig. 6) (Derin, 1999).

On a seismic profile near the Yam West-1 borehole (Fig. 7) the red and cyan horizons show minor truncation. These surfaces are correlated in the well to the base Oligocene (base of Bet Guvrin Formation at 2,395 m below MSL) and to the lower Middle Miocene (top of Bet Guvrin Formation at 2,216 m below MSL) respectively (Gill et al., 1995). The base Messinian (purple horizon) is identified here by the high amplitude event at the base of the thin evaporitic section (Mavqiim Formation) (Fig. 7).

Evidence for significant Tertiary incision is found also near the edge of the marine basin west of the Item-1 borehole (Fig. 2). On a seismic profile taken from the 3D survey C, the red seismic horizon mark a conspicuous truncation surface (Fig. 8). This surface is correlated to an unconformity at the top of the Eocene section found in Item-1 at 777 m below MSL (Fleischer and Varshavsky, 2002). A significant truncation is also evident on the purple horizon (Fig. 8), correlated in the Item-1

borehole to an unconformity at the top of the upper Miocene Ziqim Formation (at 687 m below MSL) (Fleischer and Varshavsky, 2002).

Throughout the elevated margin of the basin, the Tertiary unconformities were interpreted as onlapping surfaces, where either none or only minor incision is observed. An example is shown in a seismic profile near the Yam Yafo-1 borehole where high-amplitude reflections onlap the red, cyan and purple horizons (Fig. 9). In the Yam Yafo-1 borehole the onlapping surfaces are correlated respectively to the base Oligocene unconformity (base of Bet Guvrin Formation at 1,774 m below MSL), lower Middle Miocene unconformity (top of Bet Guvrin Formation at 1,694 m below MSL) and Late Miocene unconformity (top of Ziqim Formation at 1,557 m below MSL) (Druckman et al., 1994).

It is assumed that onlapping and truncation are both related to the same sedimentary process, e.g. the flow of submarine turbidites into the basin. While in some areas these gravity flows resulted with erosion of the sea floor, in others they were associated with accumulation and filling of submarine relief in structural lows.

The seismic profile in Figure 9 shows that the onlapping reflections filled a syncline found west of the Yam Yafo fold. The syncline already existed during the Oligocene, as indicated by the onlapping of reflections on the red horizon. A second phase of folding resulted with further contraction of the structure (note the curvature of the onlapping reflection on the red horizon), followed by onlapping on the Middle Miocene cyan horizon (Fig. 9). These two phases of contraction termed by Gardosh and Druckman (2006) Syrian Arc I and II characterized the Syrian Arc folding activity throughout the Levant area (Walley, 1998).

It should be noted that the correlation of the Tertiary unconformity surfaces in the seismic profiles were based solely on the onlapping criteria; in areas with no well control it is somewhat problematic. It is possible that truncation and incision events that are associated with relative sea-level falls are not contemporaneous with the contractional phases that resulted with the formation of structural lows and their filling by gravity flows. In our view, however, on the Levant margin both relative sea-level falls and folding are related to the contraction and uplifting associated with the Syrian Arc deformation. Therefore, the application of the two different criteria (truncation and onlapping in structural lows) is justified.

4.2.2 Deep, central part of the basin

The identification of the two older Tertiary unconformities in the central part of the basin, west of the elevated margin, is generally difficult due to the lack of well control (Fig. 2). The younger, base evaporites unconformity, is more easily recognized by the marked change in seismic character, from reflection-free, transparent Messinian salt to the underlying, well layered siliciclastic section (Fig. 10). Rarely, some truncation is recognized, as shown in the central part of the seismic profile in Figure 10 (at about 3 sec TWT), where continuous seismic events (terminate on the purple horizon) forming a wide and shallow depression at the base of the salt layer. This phenomenon may indicate a huge sea-level drop prior to the accumulation of the Messinian salt.

The pre-evaporites basin-fill appears on the seismic profiles as a series of parallel, high- and low-amplitude reflections with no indication for incision or onlapping (Fig. 10). Two conspicuous, relatively continuous high-amplitude reflections were identified below the salt in the central part of the basin. An upper reflection between 3.5 and 4 sec TWT, marked by the cyan horizon, separates a more transparent seismic package above from well-layered package below (Fig. 10). A lower high-amplitude reflection between 5 and 5.5 sec TWT, marked by the red horizon, separates the well layered seismic package above from a more transparent, reflection-free package below (Fig. 10). These two seismic events are correlated respectively with the early Middle Miocene and base Oligocene unconformities. We assume that high-amplitude events in the center of the basin are conformable surfaces associated with periods of non-deposition or condensed sections which were formed during early low-stand periods.

The correlation between the base Oligocene and Middle Miocene unconformities in the east and the conformable surfaces in the west is shown in two seismic profiles extending from the elevated fold belt into the deep part of the basin. In Figure 11 the high-amplitude incision surface, marked by the red horizon, near the Yam West-2 borehole extends almost continuously to the high-amplitude event at the deep basin in the west. Minor disruption of this marker in the center of the profile is interpreted as reverse faults at the edge of the elevated fold belt. Similarly, the onlapping surface, marked by the cyan horizon, near the Yam West-2 borehole extends continuously to the high-amplitude event found west of it in the central part of the basin.

The same relations are demonstrated on a composite seismic profile near the Hanaha-1 borehole (Fig. 12). The red and cyan erosive surfaces extend almost continuously from the well area to the

high-amplitude events west of it in the center of the basin. The red horizon appears to be again disrupted by reverse faulting at the western edge of the folded belt (Fig. 12).

It should be emphasized that the correlation of the base Oligocene red horizon shown in Figures 11 and 12 pose a significant constrain on the stratigraphy and age of the Levant basin-fill. It implies that the entire rock section, between about 5 sec TWT and the base of the Messinian salt, is of Oligo-Miocene age (Figs. 11 and 12). Although the amount of offset of the red horizon on the reverse faults can not be determined with precision, this may correspond to an uncertainty in the range of several hundred milliseconds only and does not fundamentally change the overall seismo-stratigraphic interpretation.

4.3 Mapping the Tertiary unconformities in the Levant Basin

Time structure maps of the three Tertiary unconformities that were compiled from the interpreted seismic data set are shown in Figures 13 to 15. Theses maps, which were already presented by Gardosh et al. (2006, 2008), were revised with the inclusion of additional 2D seismic profiles and 3D seismic cubes. The new maps are therefore more accurate, particularly in the eastern part of the basin margin and near the coastline. The time maps were converted to depth maps by using interval velocity maps compiled from well and seismic data (Gardosh et al., 2006; Gardosh et al., 2008). Minor differences between the time and depth maps (Figs. 13 to 15 and 16 to 18) are attributed to the depth conversion process as well as to the calibration of the depth maps with additional well data that was not used in the seismic interpretation (Table 1).

5. Tertiary canyon evolution in the Levant slope

5.1 General

The Oligo-Miocene submarine canyon system is interpreted here, through analyzing the time and depth maps of the three Tertiary unconformity surfaces: base Oligocene, Late Miocene and top Messinian (Figs. 13 to 15 and 16 to 19). The canyon system includes several main conduits; from south to north: the Afiq, Ashdod, Atlit, Haifa and Qishon canyons (Figs. 20 to 21). Most canyons were fed by numerous tributaries that reached considerable length and size in some areas. Three particularly large tributaries of this kind are: the Hadera, Netanya and Caesarea canyons, which are interpreted as tributaries of the Ashdod Canyon (Fig. 20).

The Tertiary canyons vary in their morphology and style. Some of them are deeply incised, while others are associated with filling of preexisting topographic lows or submarine valleys. In either

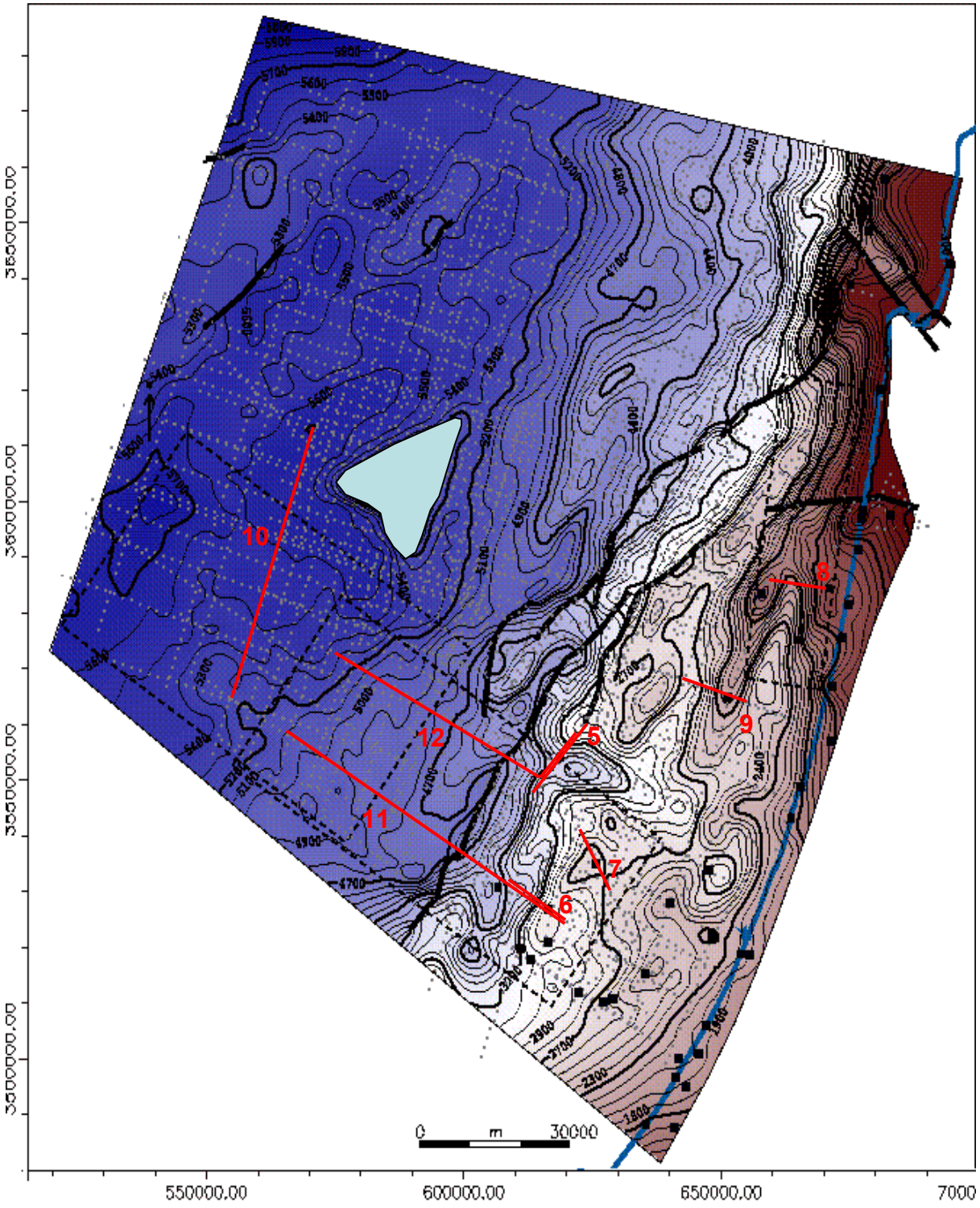

Figure 13: Time structure map (in milliseconds below MSL datum) of the base Oligocene unconformity (red seismic horizon). Contour interval = 100 ms. Red lines mark the location of cross-section of Figures 5 to 12. Light blue polygon shows an area where the horizon is missing on the top of the Jonah volcanic body.

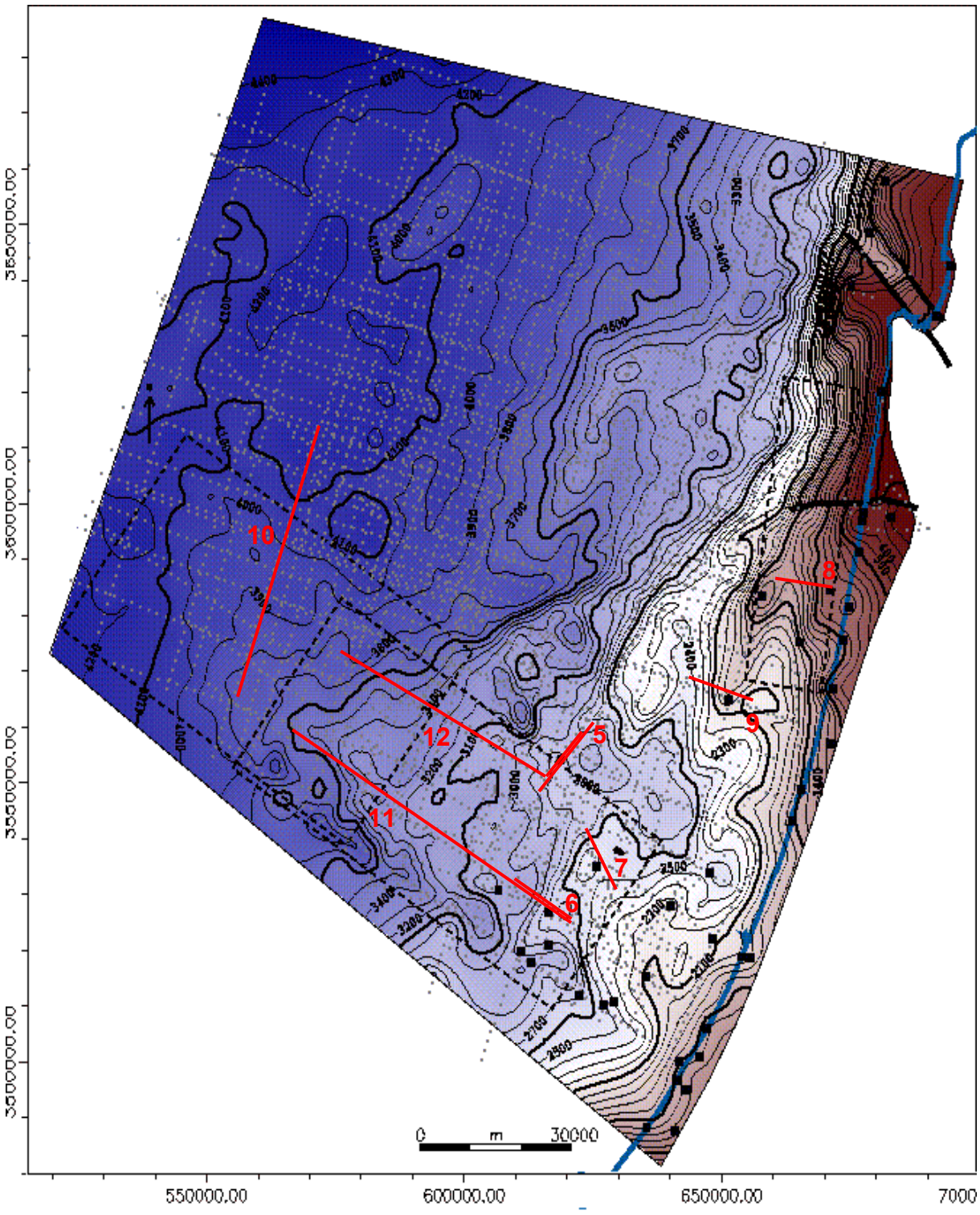

Figure 14: Time structure map (in milliseconds below MSL datum) of the Middle Miocene unconformity (cyan seismic horizon). Contour interval = 100 ms. Red lines mark the location of cross-section of Figures 5 to 12.

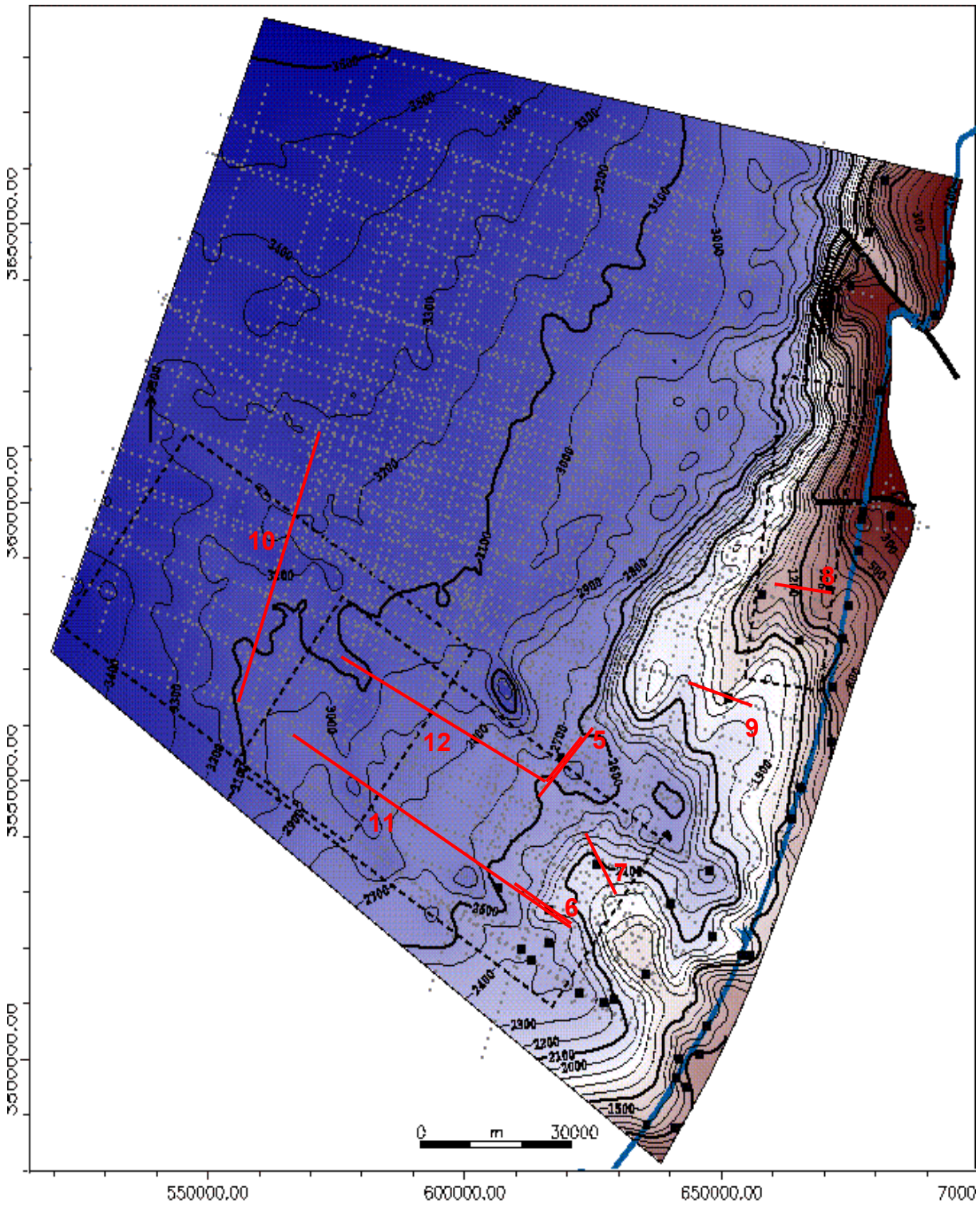

Figure 15: Time structure map (in milliseconds below MSL datum) of the base Messinian unconformity (purple seismic horizon). Contour interval= 100 ms. Red lines mark the location of cross-section of Figures 5 to 12.

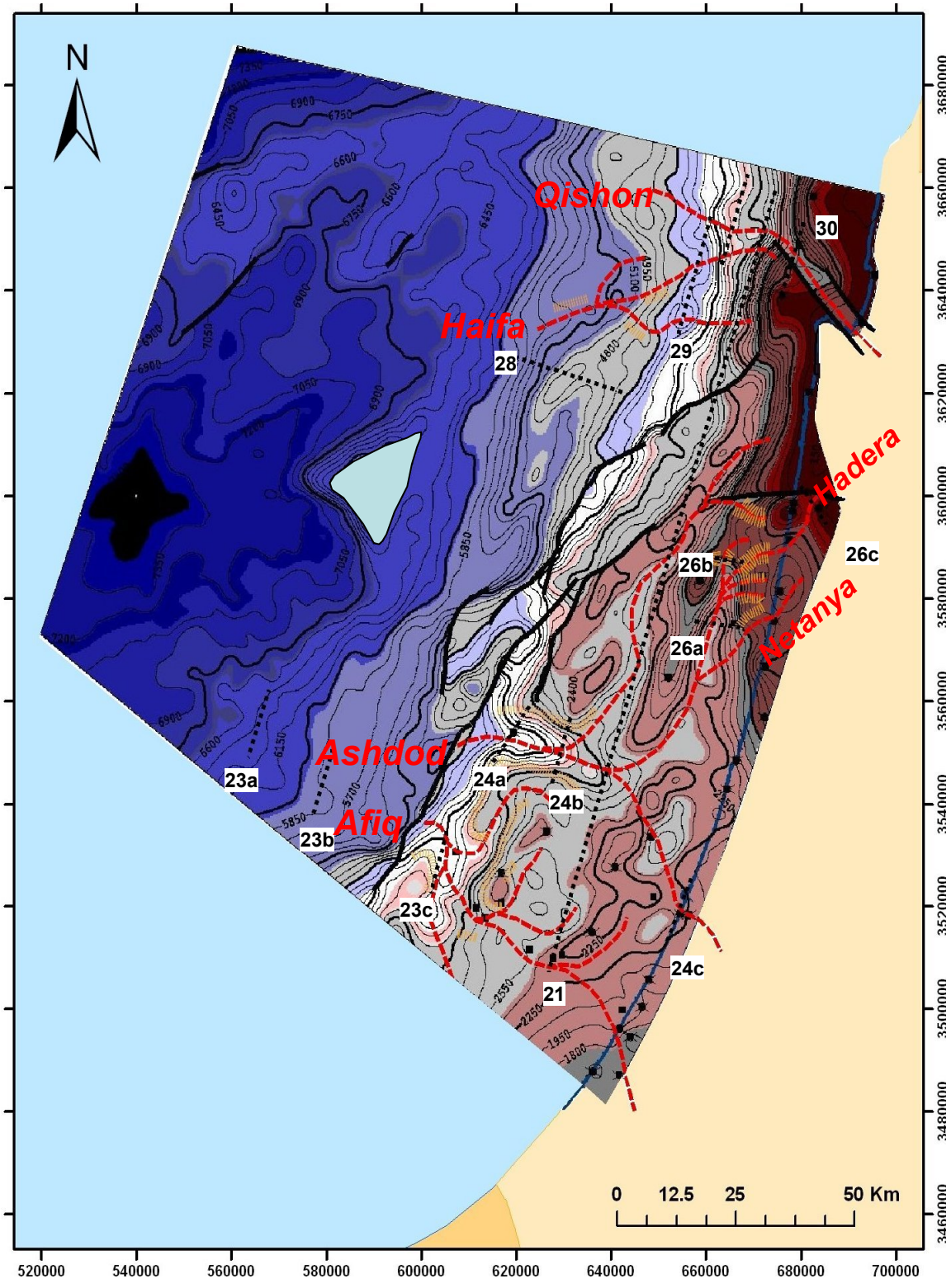

Figure 16: Depth map to the base Oligocene unconformity (meters below MSL). Dashed red lines mark the pathways of the contemporaneous submarine drainage pattern on the Levant slope. Areas of significant incision are marked by hatched orange lines; heavy black lines are faults; light blue polygon marks the Jonah volcanic body where the horizon is missing and dotted black lines mark the location of seismic profiles in Figures 21 to 31.

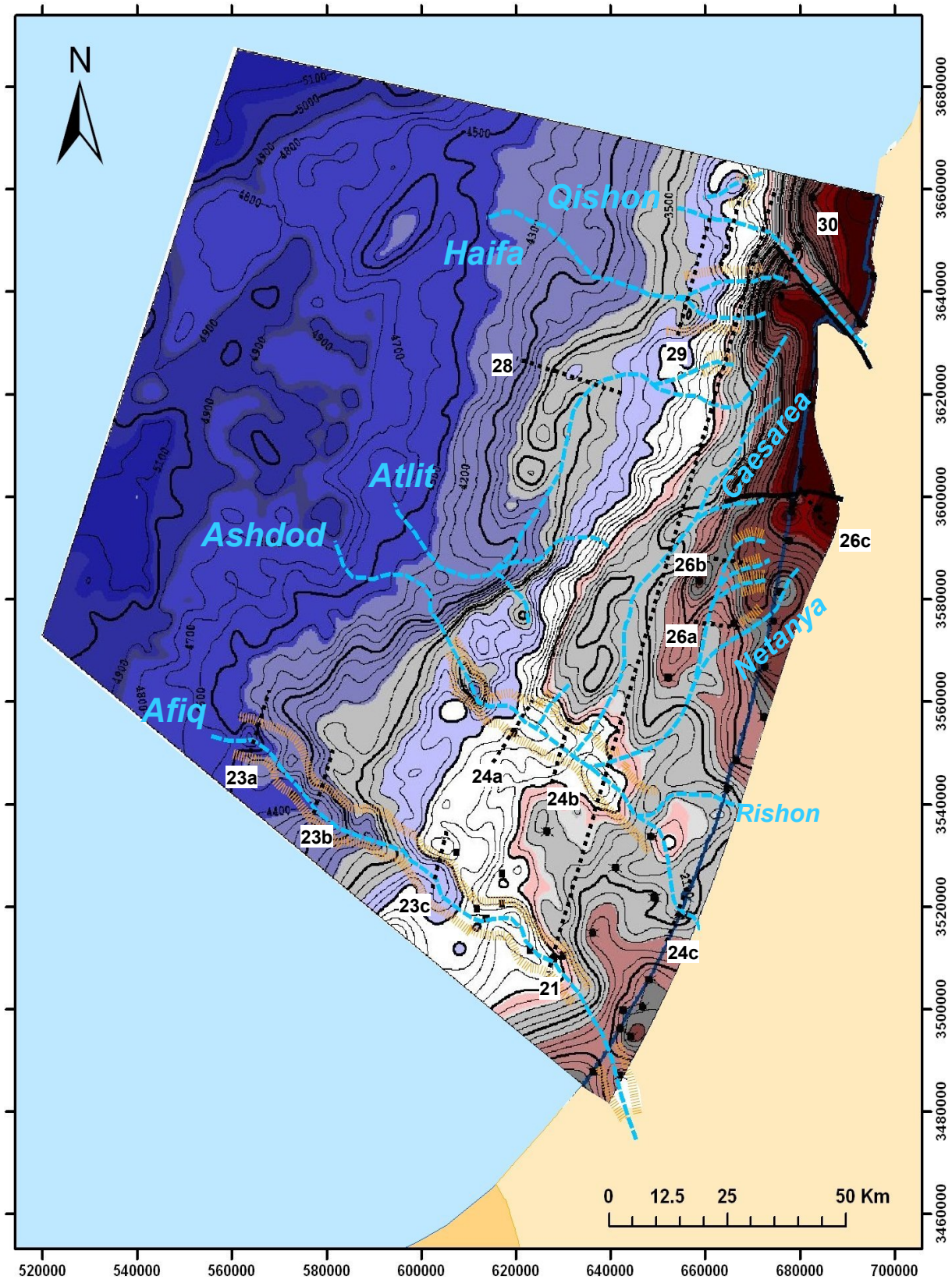

Figure 17: Depth map to the Middle Miocene unconformity (meters below MSL). Dashed cyan lines mark the pathways of the contemporaneous submarine drainage pattern on the Levant slope. Areas of significant incision are marked by hatched orange lines; heavy black lines are faults; dotted black lines mark the location of seismic profiles in Figures 21 to 31.

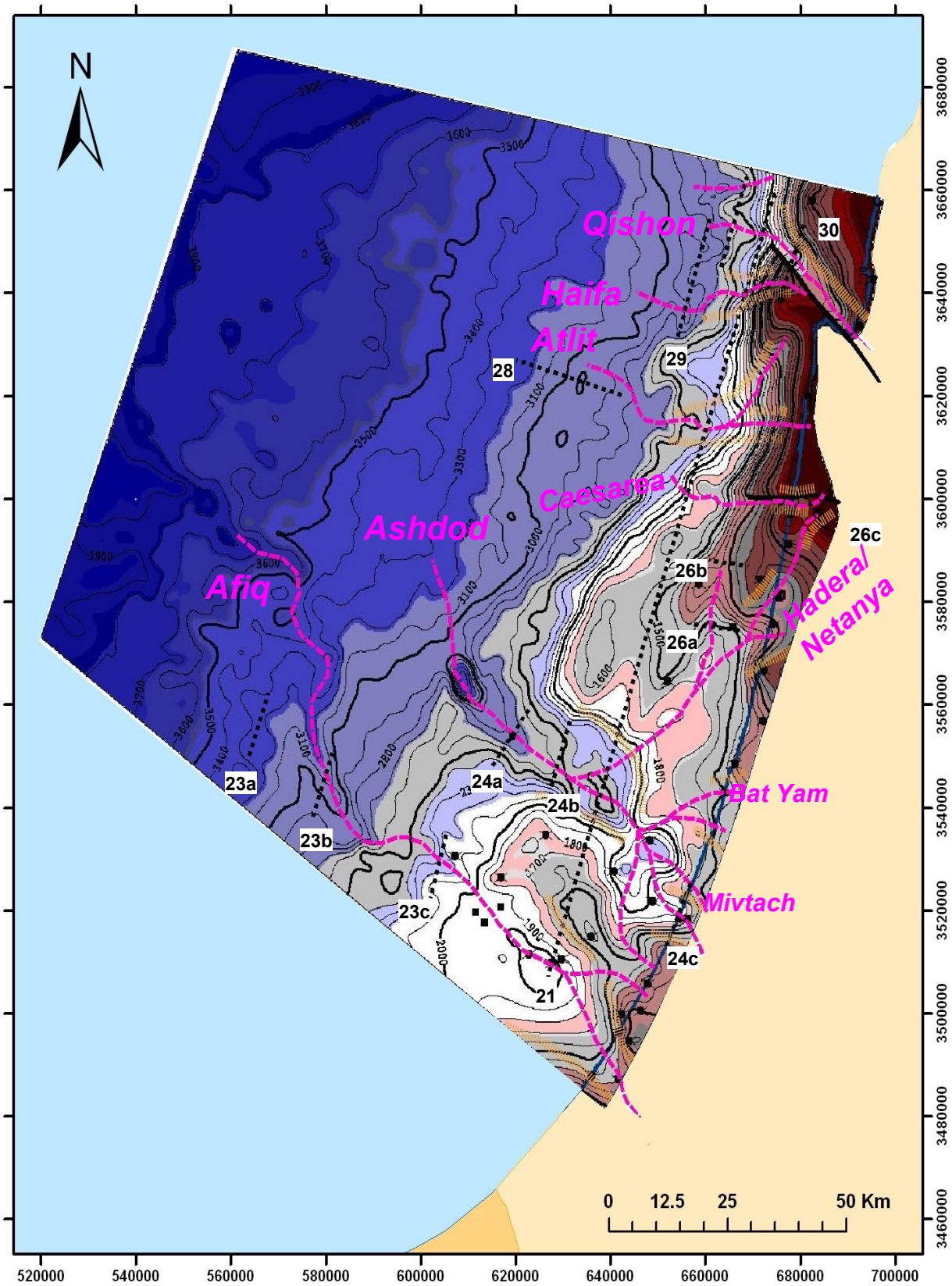

Figure 18: Depth map to the base Messinian (= top Tortonian) unconformity (meters below MSL). Dashed purple lines mark the pathways of the contemporaneous submarine drainage pattern on the Levant slope. Areas of significant incision are marked by hatched orange lines; heavy black lines are faults; dotted black lines mark the location of seismic profiles in Figures 21 to 31. These canyons were carved during the Late Tortonian. The Messinian evaporites filled and leveled this relief.

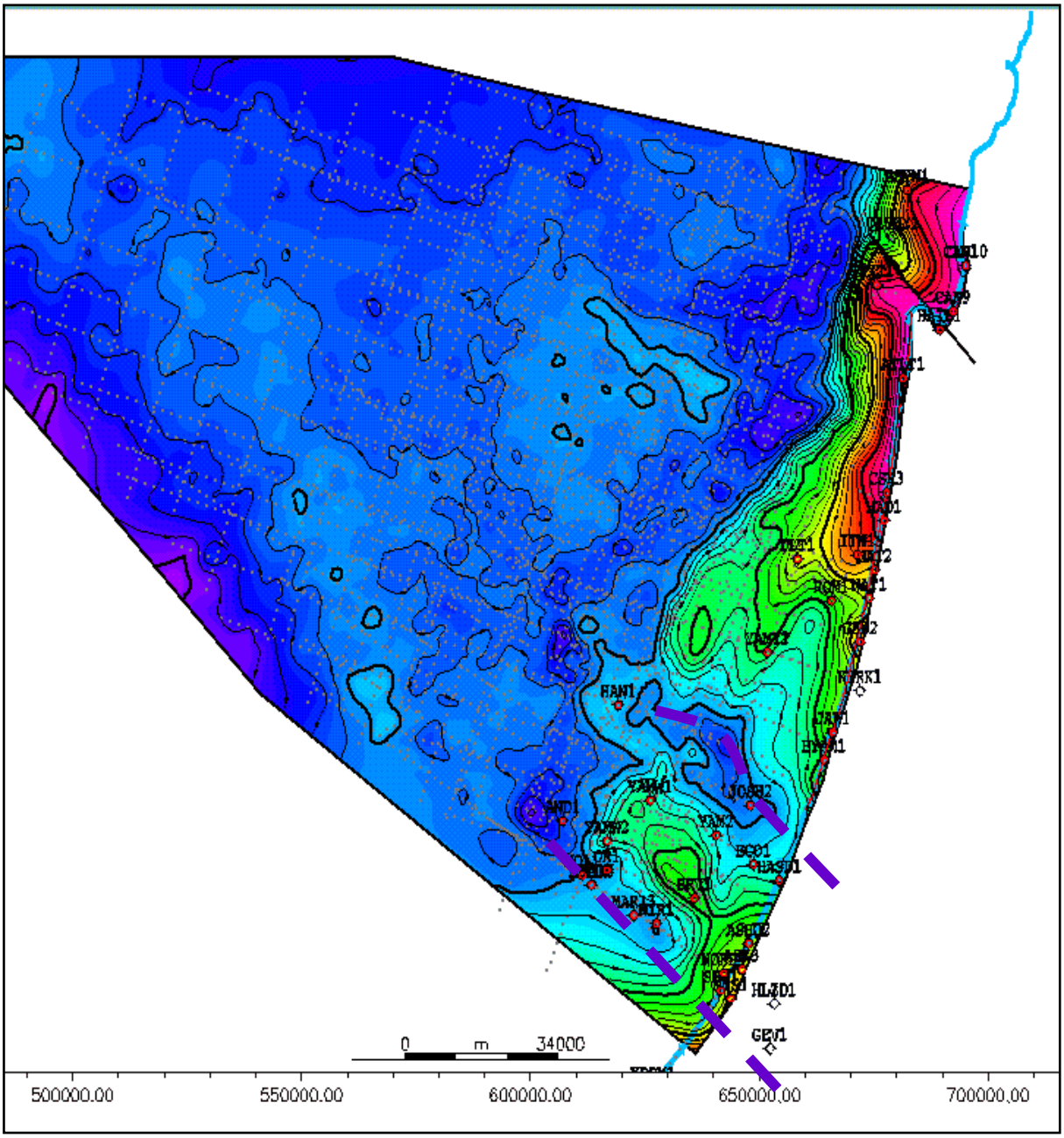

Figure 19: Depth map on the top Messinian unconformity (meters below MSL). Dashed violet lines mark the pathways of the contemporaneous drowned subaereal drainage pattern. These canyons were carved during the latest Messinian, their relief reflects the minimal drawdown of the latest Messinian sea level during the Lago Mare event.

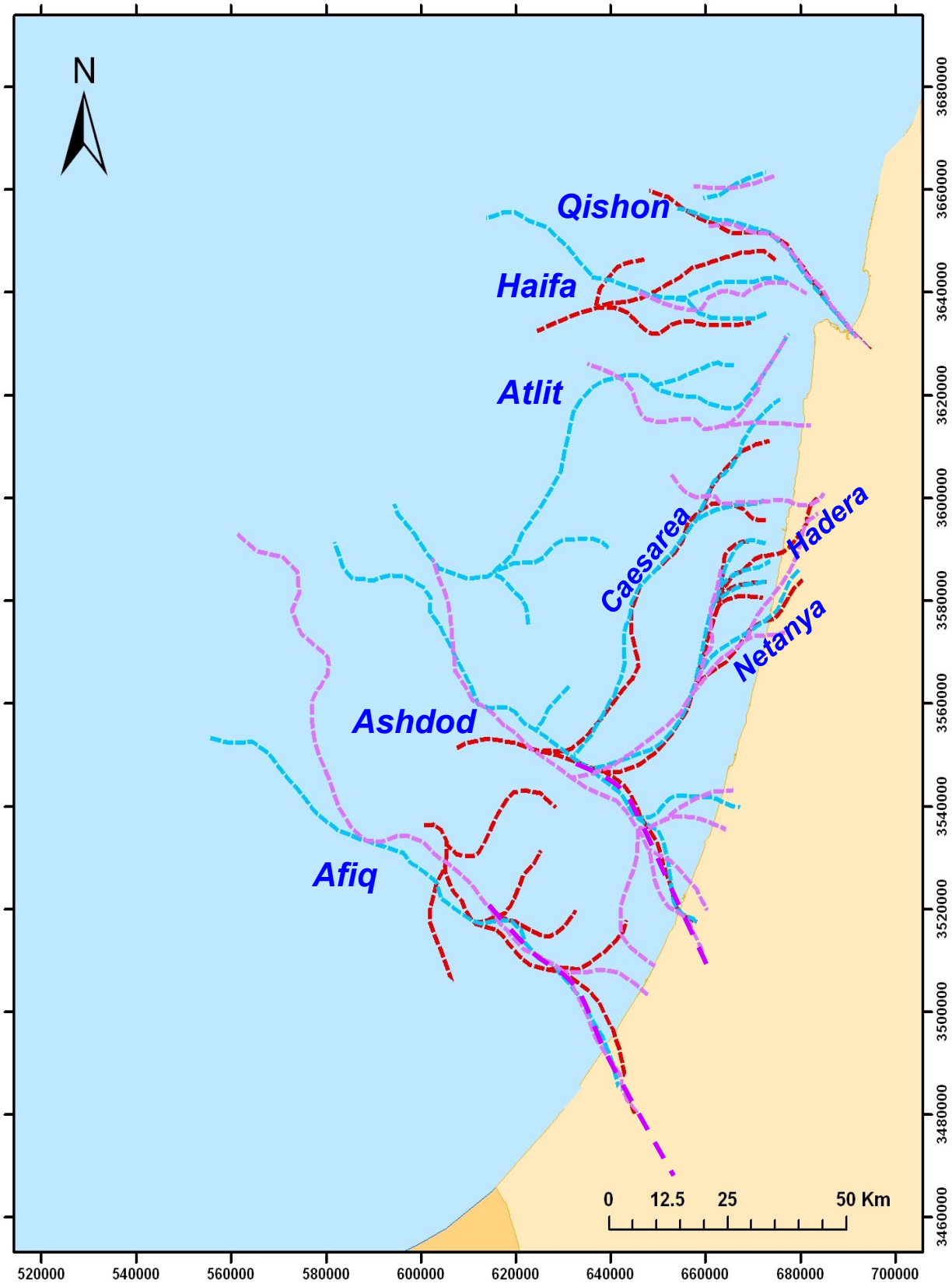

Figure 20: Stacked tracing of the submarine and subaereal drainage pattern during the Oligo-Miocene time on the Levant slope. Dashed red lines mark the Early Oligocene; Dashed cyan lines mark the Middle Miocene; Dashed purple lines mark the top Tortonian; Dashed violet lines mark the latest Messinian.

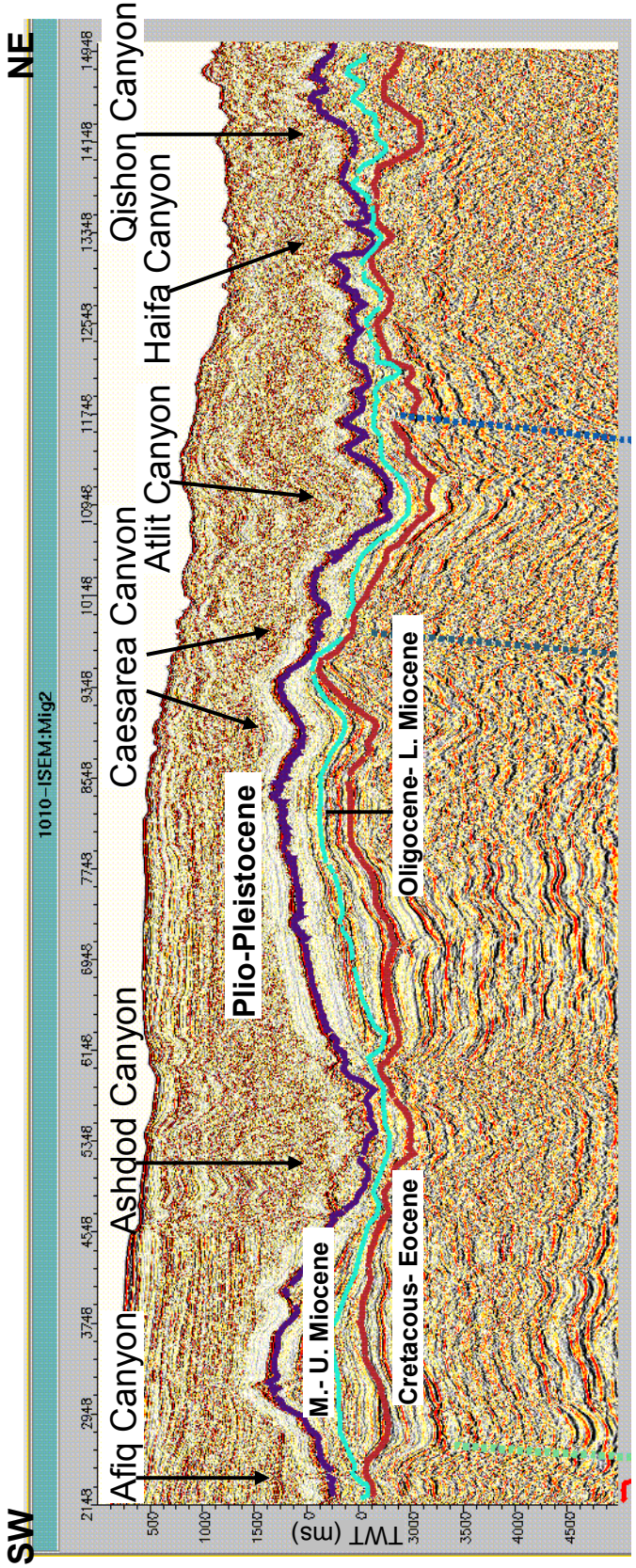

Figure 21: Regional, N-S oriented seismic profile showing the location of Tertiary canyons on the Levant slope. See location in Figures 16 to 18

case, they acted as conduits for submarine mass transport during most of the Tertiary, and their evolution is associated with stages of incision and filling. The two southern canyons, Afiq and Ashdod, appear to have been active intermittently throughout the Oligo-Miocene, and they are essentially vertically stacked (Fig. 20). The northern canyons were active during part of the Oligo-Miocene time span (Fig. 20).

This submarine canyon and channel system evolved during the Early Oligocene and persisted till the Pliocene when it was finally buried under the Nilotic sediments (Figs. 16 to 20).

Tertiary canyons were previously identified in wells at the southern Coastal Plain (Neev, 1960; Gvirtzman and Buchbinder, 1978; Druckman et al., 1995; Buchbinder and Zilberman, 1997). The offshore seismic and well data reveal the extent of this drainage system along the entire eastern part of the Levant Basin, up to 100 km west of the present-day coastline.

5.2 The Afiq Canyon

The Afiq Canyon is the largest erosional feature on the southeastern Levant margin. Its total length exceeds 150 km, extending from the Beer Sheva area in the southeast to about 100 km northwest of the present coastline (Fig. 17 to 20). Druckman et al. (1995) identified Early Oligocene strata (P19/20 biozones) unconformably overlying Cretaceous to Late Eocene rocks; and estimated an Early Oligocene (Rupelian) truncation phase. Based on hiatuses within the canyon-fill, Druckman et al. (1995) suggested three more incision and slumping events during the early Middle Miocene (Langhian), Late Miocene (Tortonian) and latest upper Miocene (Messinian).

The base Oligocene erosional phase of the Afiq Canyon was identified in the offshore seismic data although incision in this area is generally minor (Fig. 16). The most significant submarine erosion took place about 50 km west of the present coastline (Figs. 16), at the edge of an uplifted fold belt that is associated with the Syrian Arc II contractional phase (Gardosh et al., 2006; Gardosh et al., 2008). Incision east of this area is suspected but not yet confirmed. It is possible that the Oligocene canyon was obliterated during subsequent erosional phases.

The Late Miocene erosional phase resulted with extensive incision along the entire length of the Afiq Canyon onshore and offshore. The Afiq erosional scar appears in the offshore seismic lines as a box-shaped, 3-5 km wide and up to about 800 m deep canyon (Fig. 18).

The Beer Sheva-Afiq Canyon located 50 km southeast of the present coastline is filled, in the Beer Sheva area, with the upper Miocene sandy marlstone of the Bet Eshel and Sheva formations, exposed in outcrops in the town of Beer Sheva (Buchbinder and Zilberman, 1997). Near the coastline the canyon is filled with 400 m of conglomerates, sandstones and marls of undetermined age overlying Early Middle Miocene marls. This undefined section is overlain by Messinian evaporites and their replacement products (biochemical limestones) (Fig. 22) (Druckman et al., 1995).

The Gad-1 and Nir-1 boreholes, located about 20 km offshore, penetrated a 500 m thick sections of sandstones interlayered with conglomerate and shale of undetermined age (Fig. 22), overlaying marls and conglomerates of Oligocene to Early Miocene age (Buchbinder et al., 2006).

The age of the incision of this phase, in the Afiq-Beer Sheva Canyon, could not be firmly established because of the nature of the mixed and disordered foraminiferal assemblages. However, the lack of any break in the canyon's fill between the underlying undated section and the Messinian evaporates and the firmly dated upper Tortonian incision event in the Ashdod Canyon, led us to propose a similar age for this incision in the Afiq Canyon.

The latest Miocene (top Messinian evaporites) incision event (Fig. 19) is best evidenced in the Afiq Canyon near the coastline. Over there, a relief of about 800 m is carved below the canyon's rim, into the Messinian evaporites (Beeri gypsum) and the Mavqiim anhydrite. This relief is filled with 90 m of sandstone and conglomerates of the continental Afiq Formation and 600 m of the marine Pliocene Yafo Formation (Druckman et al., 1995). The Afiq Formation yields eurohaline ostracodes which were interpreted to correspond to the Lago Mare deposits, known throughout the Mediterranean (Delrieu, et al., 1993). The reduced evaporitic section and the significantly thicker Pliocene section overlying it (Figs. 21 and 23c) indicate the removal of part of the evaporites due to a ~ 800 m fall of the Messinian sea level by the end of the Messinian salinity crisis (Druckman et al., 1995; Cartwright and Jackson, 2007).

Unlike the two other major incisions discussed above, and which were interpreted to have been carved by submarine mass-flow processes, the latest Miocene (top Messinian evaporates) incision is interpreted to had been taking place under subaerial conditions. A fluvial drainage was thus responsible for the incision and dilution of the terminal Messinian brines to eurohaline degree

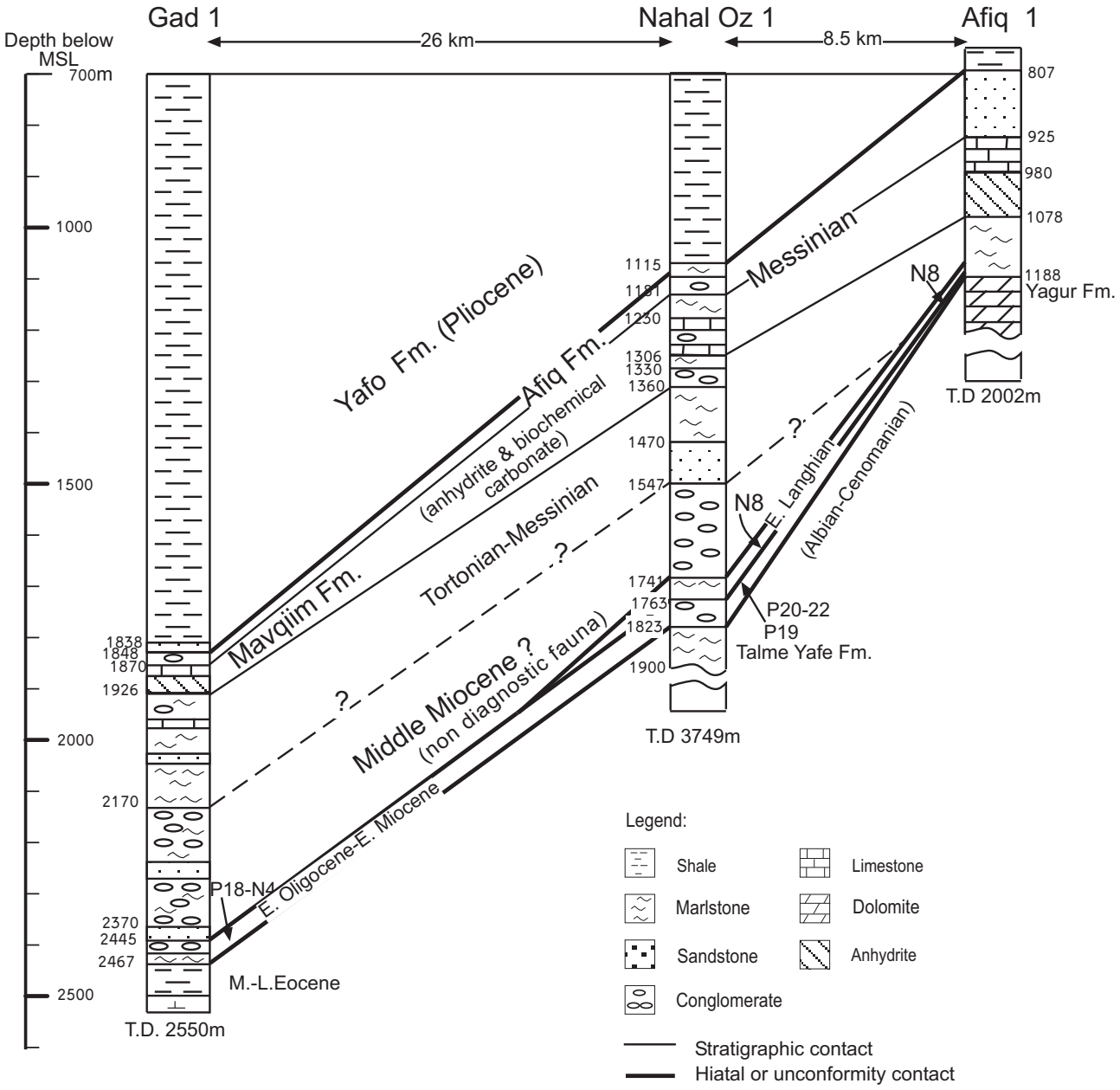

Figure 22: Stratigraphic cross section along the Afiq Canyon. Heavy black lines mark major unconformities. The Messinian anhydrite in the Nahal Oz-1 well was totally replaced by biochemical carbonate. In the Afiq-1 and Gad-1 wells, the anhydrite was partially replaced. Datum: 700 m BSL. (Druckman et al., 1995; Buchbinder et al., 2006).

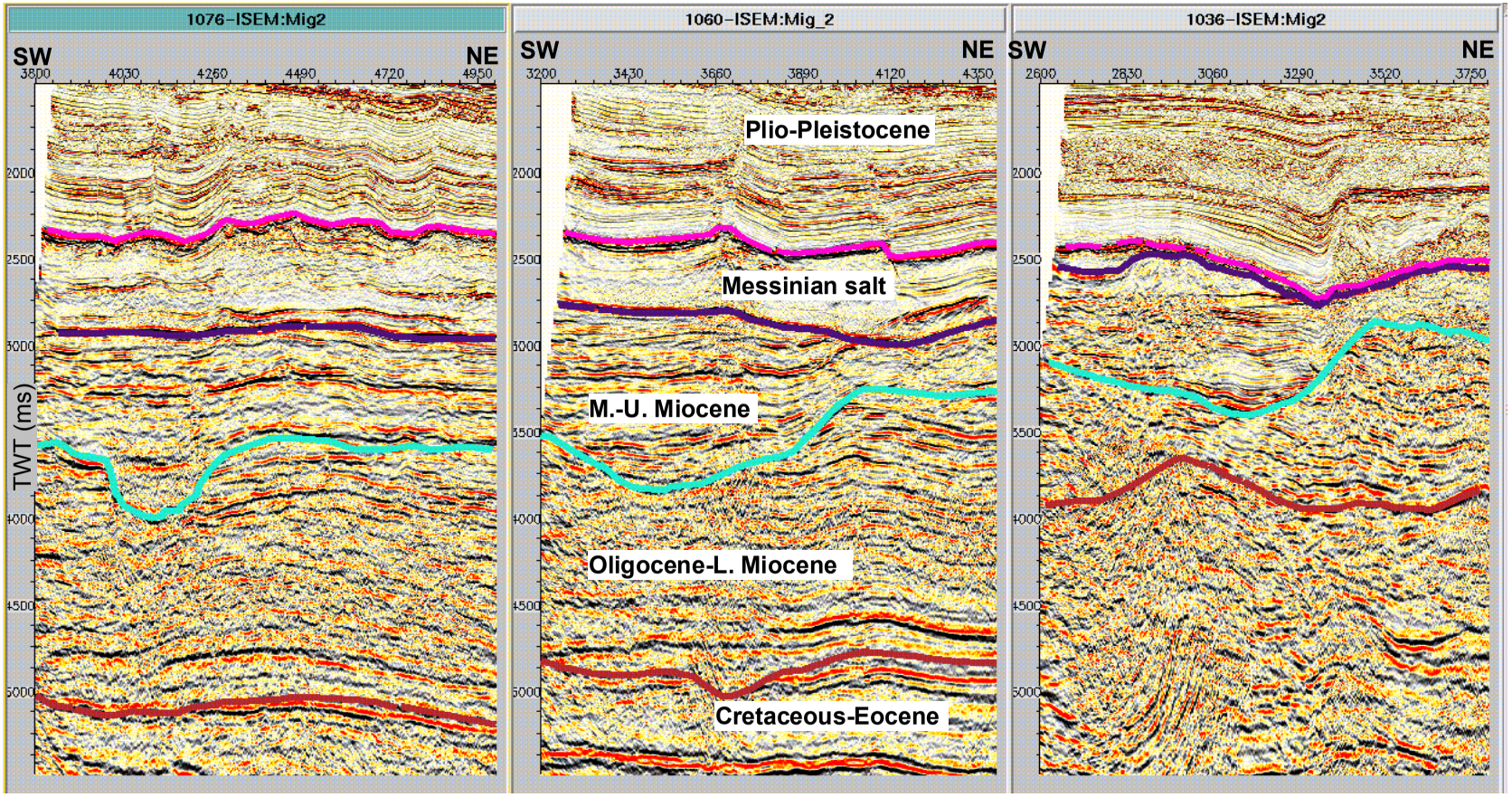

Figure 23: Three seismic profiles (a, b, c) running across the western part of the Afiq Canyon. See location in Figures 16 to 18 . Middle Miocene incision resulted with the formation of several hundred meters deep box-shaped canyon (a, b, c). Base Messinian incision formed a shallower concave canyon cut that was later filled with the Messinian evaporites (b, c). Base Oligocene incision affected the eastern and central part of the canyon (c). Note the lateral shift in the position of the canyon during the three incision episodes.

allowing eurohaline fauna to prevail throughout the Mediterranean (Hsu et al, 1978; Buchbinder et al., 2006).

Bertoni and Cartwright (2007) showed a major erosion event and an unconformity surface at the top of the Messinian evaporates (M marker) in the eastern Mediterranean Levant Basin. They interpreted this unconformity as subaerial in origin. Thus, implying a complete exposure of the Mediterranean at the end of the Messinian.

Our findings together with Bertoni and Cartwright's (2007) findings support the idea of desiccation, erosion and a eurohaline event between the Messinian evaporates and the Pliocene Marine transgression.

Along the coastline, up to a distance of 20 km westward, the seismic cross section shows a 300-500 m deep, box-shaped canyon (Figs. 18 and 21).

5.3 The Ashdod Canyon

The Ashdod Canyon is the most prominent feature in the southeastern Levant margin, extending from the present-day coastal area to a distance of about 100 km westward (Figs. 16 to 20). The existence of an Early Tertiary Ashdod Canyon was suggested by Buchbinder et al. (2005) based on the findings of a few hundred meters of Oligocene sandstones and conglomerate beds in seven wells drilled in the Ashdod area near the coastline. The offshore seismic and well data reveal a spectacular erosional feature (Fig. 24) which, similar to the Afiq Canyon, it is associated with three phases of significant incision events: during the Early Oligocene, Late Tortonian and latest Miocene (top Messinian).

The base Oligocene incision is most pronounced at the edge of the uplifted fold belt about 50 km offshore. The seismic data reveal a 5-10 km wide and up to 1 km deep canyon, incised into the Mesozoic section (Figs, 16 and 24a,b). The Hanaha-1 borehole, drilled near the center of the canyon penetrated a lower Oligocene canyon-fill overlaying the lower Cretaceous Gevar'am Formation. The canyon terminates into the basin, in the west, beyond the Syrian Arc fold belt (Fig. 16).

Relatively minor or no incision was observed in the area east of the Hanaha-1 borehole and the present-day coastline (Fig. 16). Along the coastline the seismic record shows a wide canyon, several

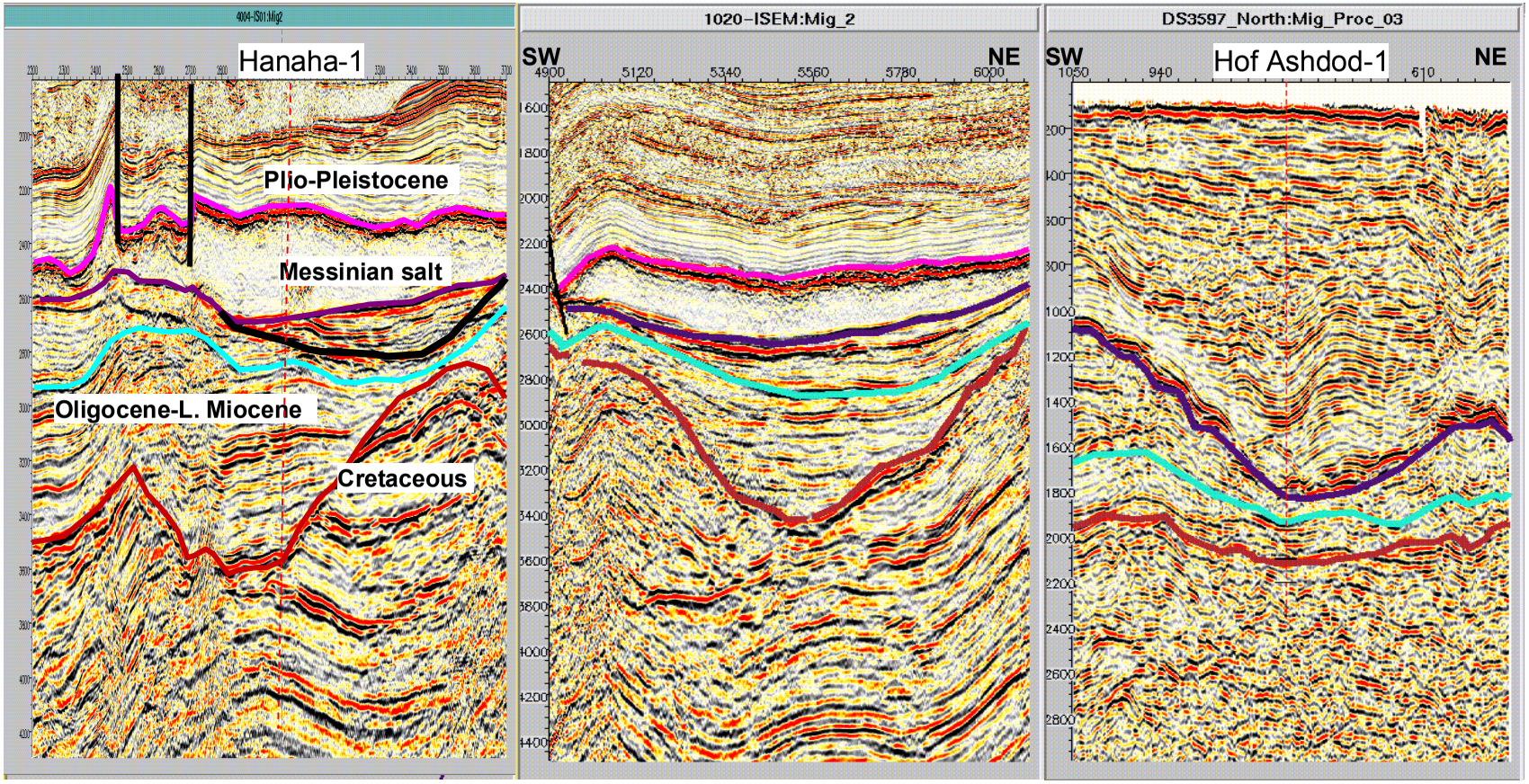

Figure 24: Three seismic profiles (a, b, c) running across the Ashdod Canyon. See location in Figures 16 to 18. Profiles (a) and (b) are located in the western part of the canyon. In this area the base Oligocene incision resulted with the formation of about 1000 m deep canyon, whereas the Middle Miocene and base Messinian canyons are only a few hundred meters deep (a, b). Profile (c) is located at a proximal part of the canyon along the present-day coastline. In this area the base Oligocene canyon is relatively shallow while deep incision is observed on the base Messinian unconformity. Note the lateral shift in the position of the canyon during the three incision episodes.

hundred meters deep, where the Oligocene clastics overlie upper Eocene strata (Fig. 24c and 25 and Buchbinder et al., 2005).

In the Hanaha-1 borehole the Oligocene incision cuts about 968 m (the thickness of the entire Oligocene fill), breaching a NE-SW trending Syrian Arc fold structure (Figs. 5 and 24), thus indicating that the water depth during the Early Oligocene exceeded 1,000 m. In comparison, a range of 1,600 m water depth was estimated for the Afiq Canyon (Druckman et al., 1995) in the Early Oligocene.

A Late Tortonian incision was interpreted in the Hannah-1 borehole, based on the dating of the channel fill underlying the Messinian evaporites (Fig. 24a). No stratigraphic gap was found between the evaporites and the underlying section of the channel fill. Both were assigned the Messinian NN11a nannofossil zone (Micro-Strat, 2003). A major stratigraphic gap was found between the Late Tortonian, at the base of the channel, and the Early Langhian (early Middle Miocene) underlying section (Fig. 25). The Late Tortonian incision carved up to 965 m meters (the cumulative thickness of the Late Tortonian and Messinian canyon fill) (Fig. 24a,b).

Based on the above observation it is concluded that the N marker (base evaporates) is, in fact, merely a velocity contrast between evaporites and low velocity sediments, and does not reflect an unconformity surface. The relief into which the Messinian evaporites were deposited was carved in Late Tortonian time.

Near the coastline, in the Ashdod-1 borehole, the Late Tortonian canyon is about 700 m deep and also overlies unconformably Langhian clastics similarly to the Hannah-1 borehole. It is filled by 50 m of Messinian carbonate reefal debris overlain by a 150 m thick evaporitic section, which in turn is overlain by a thick Pliocene section of ~ 1,740 m (Buchbinder et al., 2005) (Figs. 18, 21, 24 and 25).

The reduced evaporitic section and the significantly thicker Pliocene section overlying it (Fig. 24c) indicate the removal of part of the evaporites due to a ~ 800 m fall of the Messinian sea level (Druckman et al., 1995; Cartwright and Jackson, 2007) and thus signifies the post-evaporite incision event. This event is better pronounced in the Afiq Canyon, where the evaporites are overlain by lacustrine clastic sediment, reflecting the Lago Mare circum Mediterranean event.

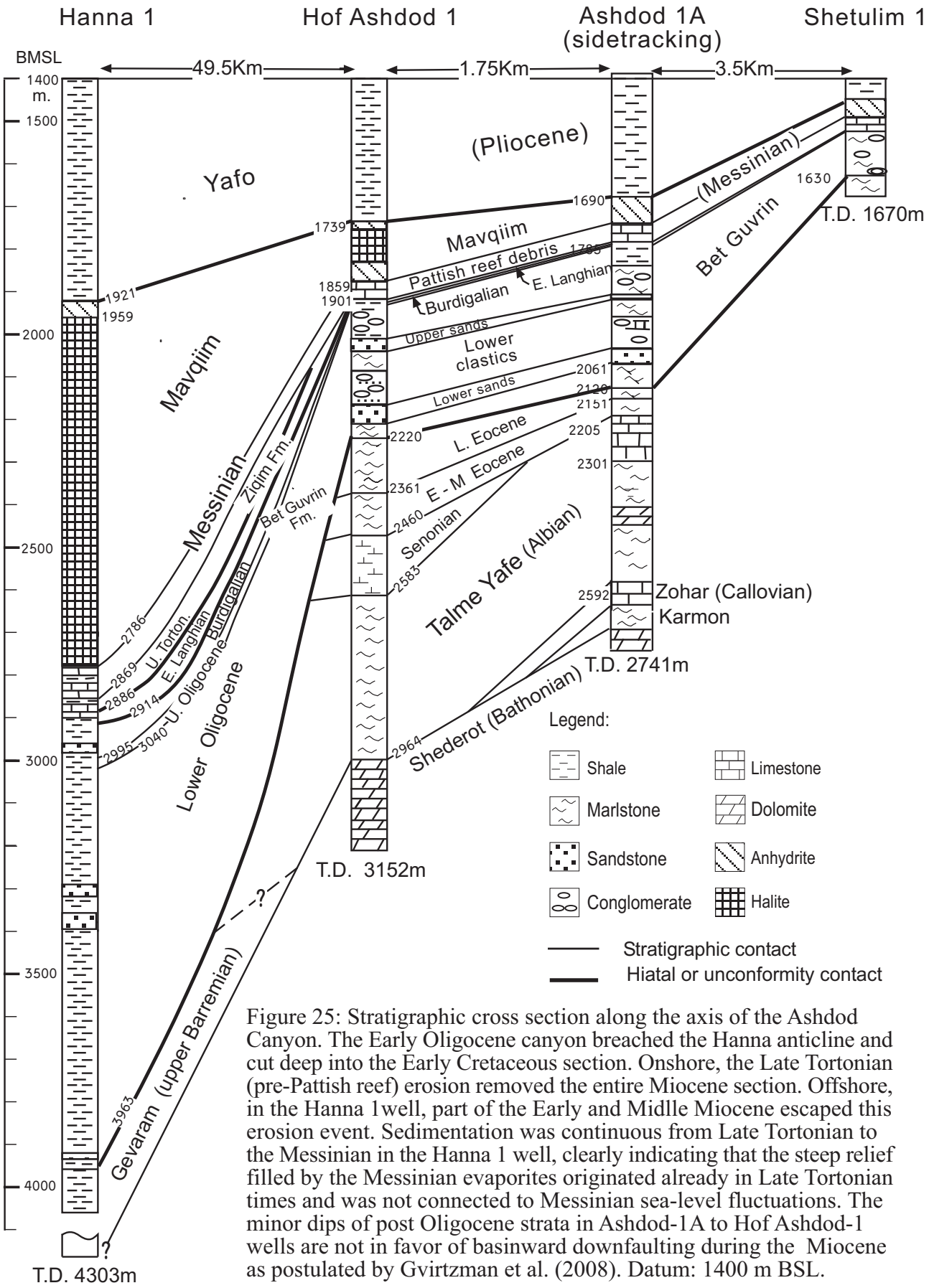

Figure 25: Stratigraphic cross section along the axis of the Ashdod Canyon. The Early Oligocene canyon breached the Hanna anticline and cut deep into the Early Cretaceous section. Onshore, the Late Tortonian (pre-Pattish reef) erosion removed the entire Miocene section. Offshore, in the Hanna 1well, part of the Early and Midlle Miocene escaped this erosion event. Sedimentation was continuous from Late Tortonian to the Messinian in the Hanna 1 well, clearly indicating that the steep relief filled by the Messinian evaporites originated already in Late Tortonian times and was not connected to Messinian sea-level fluctuations. The minor dips of post Oligocene strata in Ashdod-1A to Hof Ashdod-1 wells are not in favor of basinward downfaulting during the Miocene as postulated by Gvirtzman et al. (2008). Datum: 1400 m BSL.

5.4 The Hadera, Netanya and Caesarea canyons

Three, large distributaries: the Hadera, Netanya and Caesarea flow from northeast (Figs. 16 to 18) and converge with the Ashdod Canyon. Their outline was controlled by the preexisting synclines of the Syrian Arc fold belt (Fleischer and Gafsou, 2003). Onlapping reflections, on the base Oligocene and Middle Miocene unconformities (Figs. 8, 9 and 26a), indicate that these were conduits for the transported of mass-flows. The Hadera and Netanya canyons were active during the Tertiary erosional phases, while the Caesarea Canyon was active only during the latest Miocene time, when its course followed the trace of the Or Aqiva (=Binyamina) fault (Fig. 18) (Gelberman, 1990; Steinberg et al., 2008).

Incision at the bottom of these canyons was generally minor and, if existed, was bellow the resolution of the seismic data. However, significant erosion and incision was observed near the coastline at the upper reaches of the Hadera and Netanya canyons. The base Oligocene surface displays a small box-shaped canyon at the upper part of the large syncline located east of the Delta fold (Fig. 26b). Further to the east, the entire slope, west of the Caesarea and Netanya wells, is cut by small canyons that developed on an elevated structural step during the base Oligocene and Middle Miocene times (Figs. 16, 17 and 26b). The Oligocene canyon probably extended eastward within the syncline that developed southeast of the Caesarea High (Fig. 26c). In the Netanya-2 borehole the Middle Miocene erosion is evident by the conglomerate beds that overly the Middle Cretaceous carbonates (Fig. 27). Significant incision in this area was also observed in the seismic record of the upper Tortonian unconformity, probably resulting in the development of two canyons; the Hadera/Netanya Canyon trending to the southwest and the Caesarea Canyon directed to the west (Figs. 18 and 26c).

5.5 The Atlit Canyon

The Middle to Late Miocene Atlit Canyon is indicated by onlapping reflections within a syncline located about 50 km west of the coastline (Figs. 17 and 28). The syncline may have acted as a conduit for southwest directed gravity-flows. Possible incision further to the east is speculated but not clearly observed on the seismic data. Deep incision is observed in the eastern part of the Atlit Canyon at the top Tortonian level (Figs. 18 and 21).

5.6 The Haifa Canyon

Minor incision is observed in some profiles on the base Oligocene level about 50 km west of the coastline (Fig. 16). The development of a Middle Miocene erosional feature is indicated by a

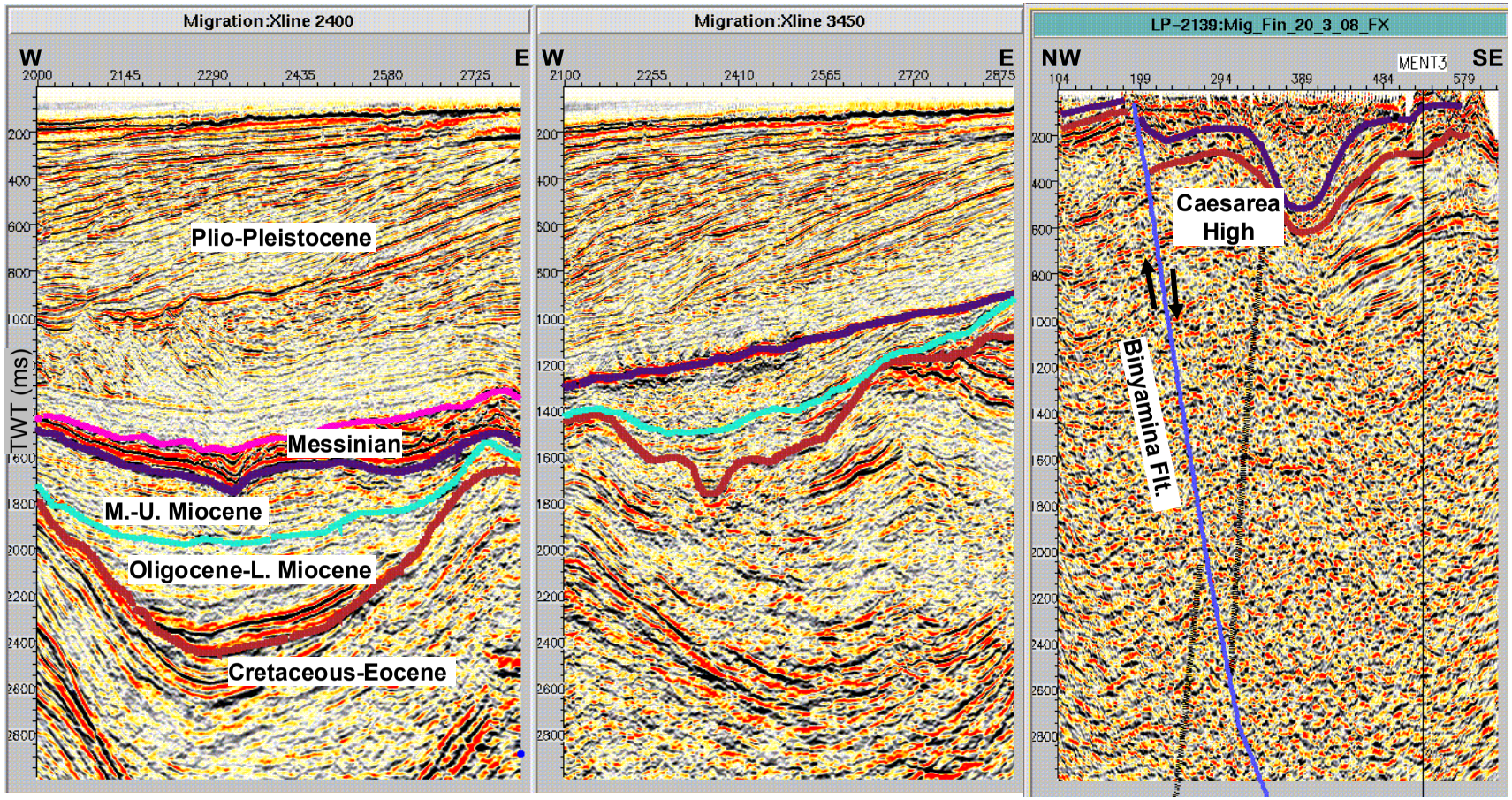

Figure 26: Three seismic profiles (a, b, c) running across the Hadera Canyon. See location in Figures 16 to 18. The canyon is most clearly observed on the base Oligocene unconformity surface. In the southern part (a) it is characterized by high-amplitude onlapping reflections interpreted as channel fill, within a large Syrian Arc type syncline. Incision is observed at the central part of the canyon and on its eastern wall in profile (b), while at the eastern part it is located within a structural low south of the Caesarea High (c). Base Messinian incision is observed on profiles (a) and (c). The base Messinian incision in the Caesarea area may be associated with the activity on the Binyamina Fault (c).

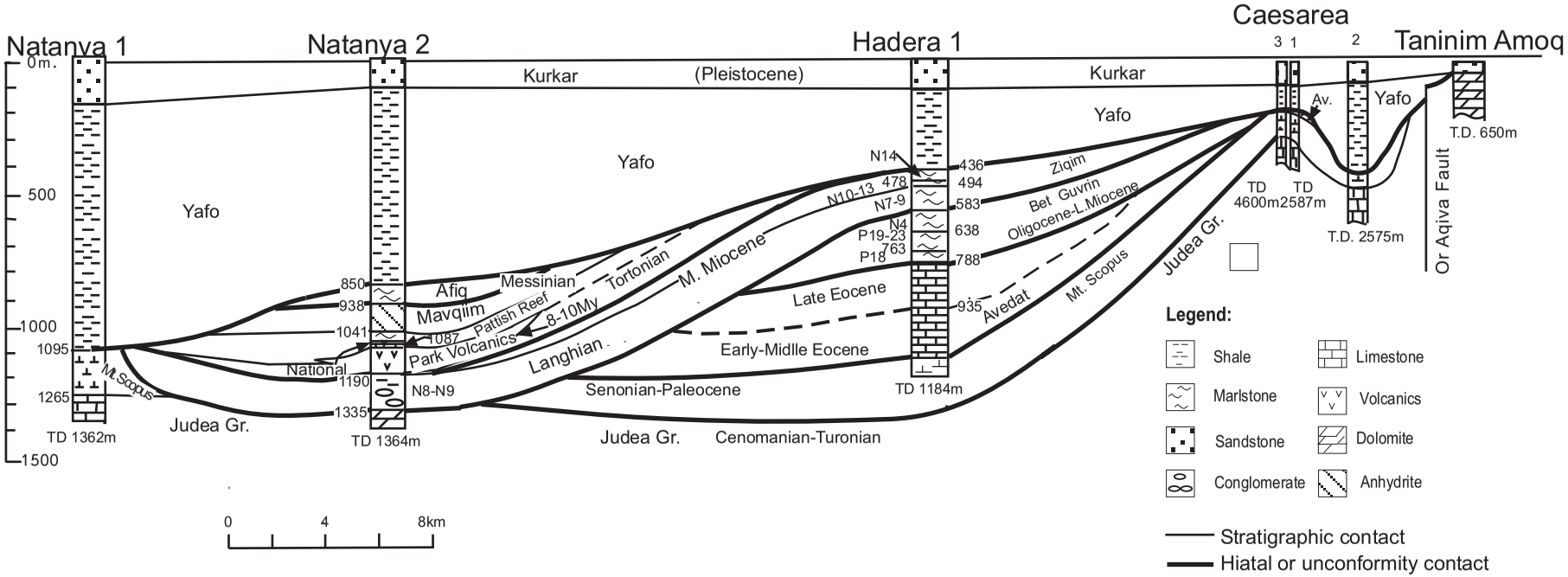

Figure 27: A N-S stratigraphic section across the Natanya Canyon, the Caesarea Canyon and the Hadera syncline . Towards the south-west, the Hadera syncline became an incised canyon at the base Oligocene time (Fig. 26). The earliest incision of the Natanya Canyon is of early Middle Miocene, followed by a repeated incision in Tortonian times. The Tortonian canyon is filled by the National Park Volcanics, Pattish Reef ruble and the Mavqiim evaporites. Finally, in post-Messinian time, both the Natanya and the Ceasaria canyons were incised again. The Or Aqiva fault (Gvirtzman, 1970) at the north end of the section was referred by Gelberman (1990) as the Binyamina fault. Steinberg et al. (2008) extended this fault into the offshore. Datum: MSL.

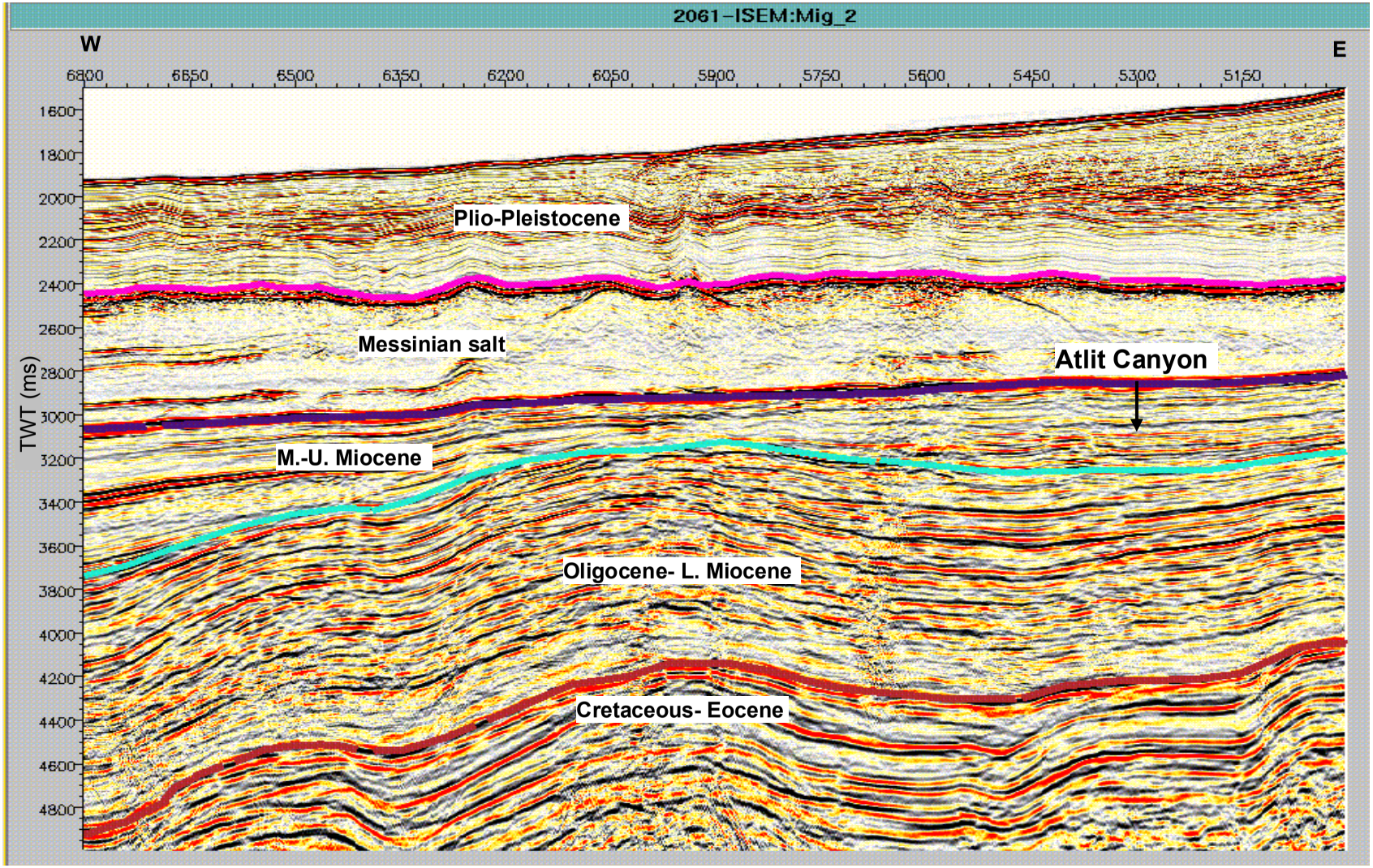

Figure 28: Seismic profile showing the Middle Miocene Atlit Canyon. The existence of a submarine canyon is indicated by the onlapping reflections within a Syrian Arc syncline, interpreted as channel fill. The base Oligocene and base Messinian unconformoty do not show evidence for the existance of a canyon in this area. See location in Figures 16 to 18 .

conspicuous erosional surface identified on seismic profiles west of the Carmel/Foxtrot elevated block (Figs. 17 and 29). A top Tortonian canyon is clearly observed at the upper reach of the Haifa Canyon (Fig. 30).

5.7 The Qishon Canyon

The canyon is located in the Qishon Graben (Neev et al., 1976; Garfunkel and Almagor, 1985; Ben-Gai and Ben-Avraham, 1995) on the hanging-wall of the Yagur fault (Figs. 16 to 18). The graben is a NW-SE trending asymmetric fault block, 5-7 km wide. It is bound by the Yagur fault on the southwest and by a smaller speculated normal fault in the northeast (Figs., 16 and 30). The graben extends from the Zevulun Valley onshore into the Haifa Bay offshore, where the maximal vertical displacement on the Yagur fault exceeds 1,500 m. The Qishon Graben is a tectonic depression that currently forms a conduit for both subaerial (e.g. the Qishon River) and submarine sediment transport on the Levant margin.

The Qishon Yam-1 borehole (Fig. 30) is located within the offshore part of the graben. The age of its sedimentary fill provides important evidence for its geological history. Schattner et al. (2006) studied the stratigraphy of the well, and based on biostratigraphic evidence they concluded that the well penetrated a 400 m thick section of marl and anhydrite dating from Middle Oligocene to early Middle Miocene time. Based on this interpretation Schattner et al. (2006) further suggested that the graben was already active in the Oligocene, and was part of a regional NW-SE rift system termed the Qishon-Sirhan trend.

A reexamination of the biostratigraphy (Siman-Tov, 2008a) revealed the following results: (1) no Early Pliocene section was found in the well; (2) Late Pliocene section overlies an alternating section of anhydrite and marl, containing a mixed (not in sequence) assemblage of Oligocene to Messinian fauna. Based on these findings it is suggested that the mixed marl and anhydrite interval penetrated in the Qishon Yam-1 borehole, between 1,200 and 1,663 m, is a mass transported pile of Messinian evaporates with reworked older faunal elements. Likewise, the absence of the lower Pliocene part of the Yafo Formation is similarly explained (Fig. 31).

Further onshore, the Messinian evaporites correlate with the 60 m thick section of gypsum penetrated in the Canusa-9 borehole, and further eastward in the Qishon Valley with the gypsum beds penetrated at the very bottom of the Shefa Yamim wells. Due to their elevation (250-360 m BSL) it is inferred that these gypsum layers are coeval with the Beeri gypsum encountered in the

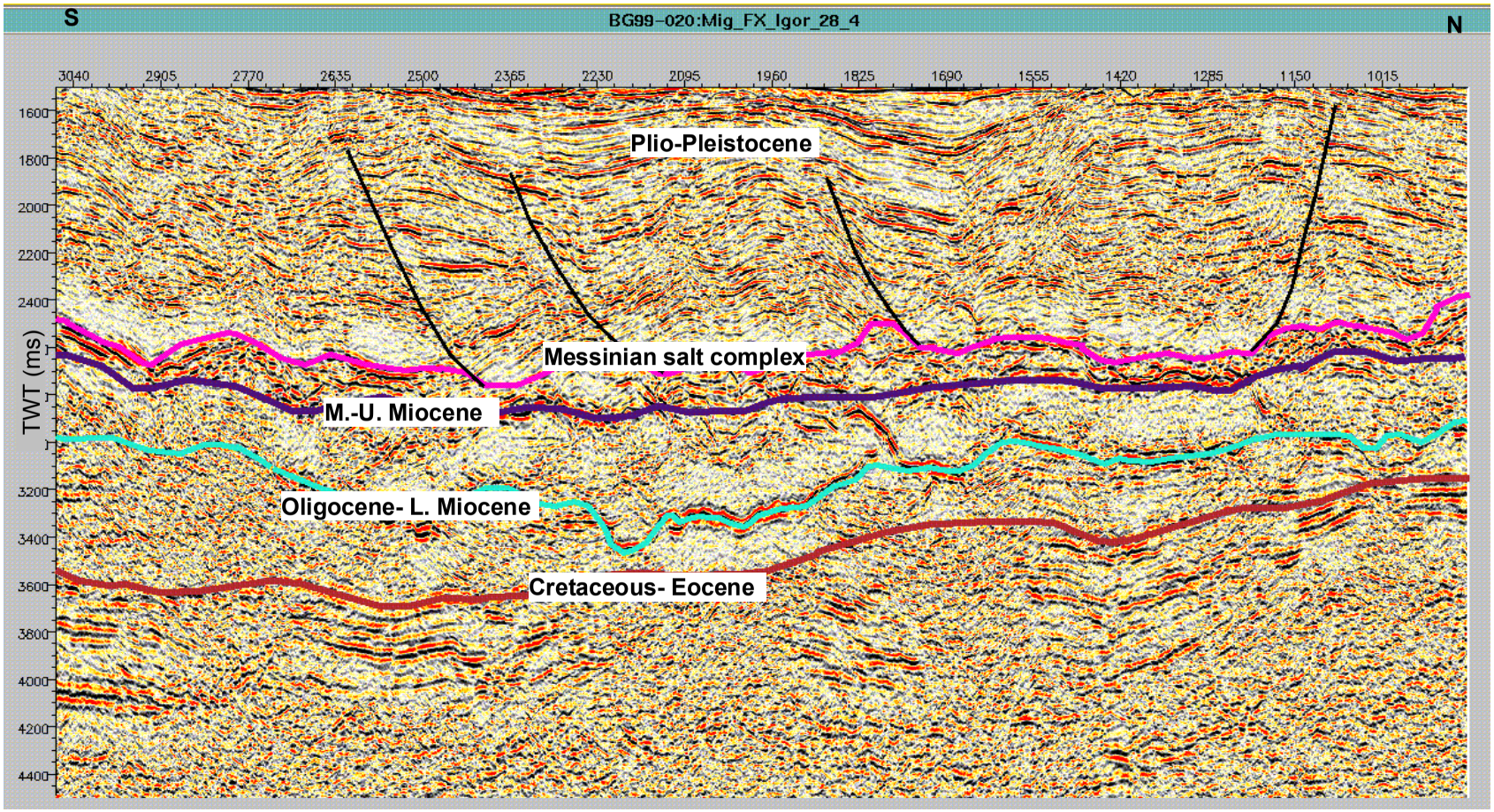

Figure 29: Seismic profile showing the Middle Miocene Haifa Canyon. Pronounced incision, associated with the early Middle Miocene unconformity is observed below the Messinian salt, forming about 10 km wide canyon cut. Similar although less pronounced incision is associated with the base Messinian and possibly also with the base Oligocene unconformities. See location in Figures 16 to 18 .

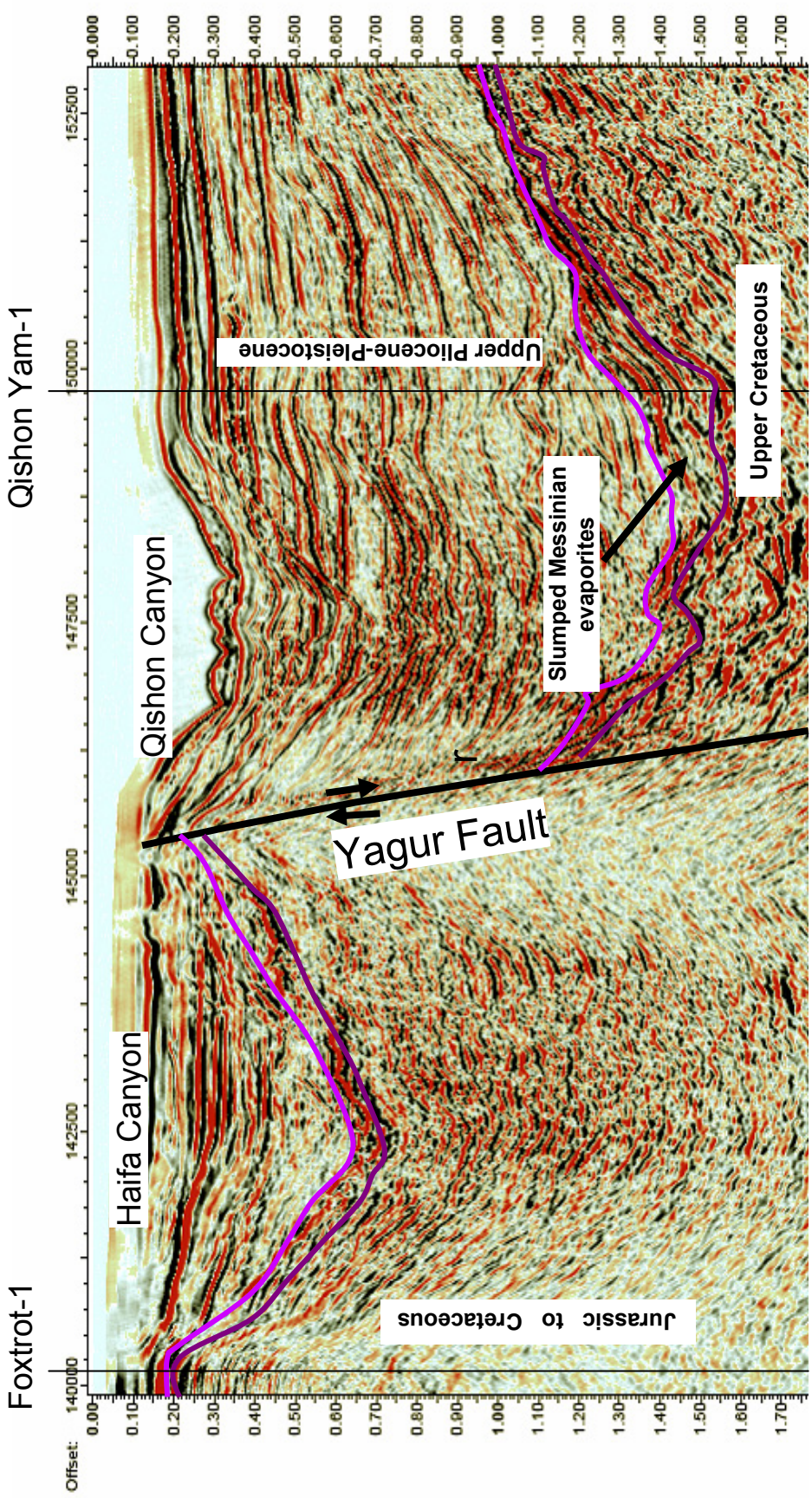

Figure 30: Seismic profile showing the Qishon and Haifa canyons. Base Messinian incision is observed on both sides of the Yagur fault. The chaotic, high-amplitude reflections below the Late Pliocene-Pleistocene fill is interpreted as a mass transported pile of Messinian evaporates with reworked older faunal elements. See location in Figures 16 to 18 .

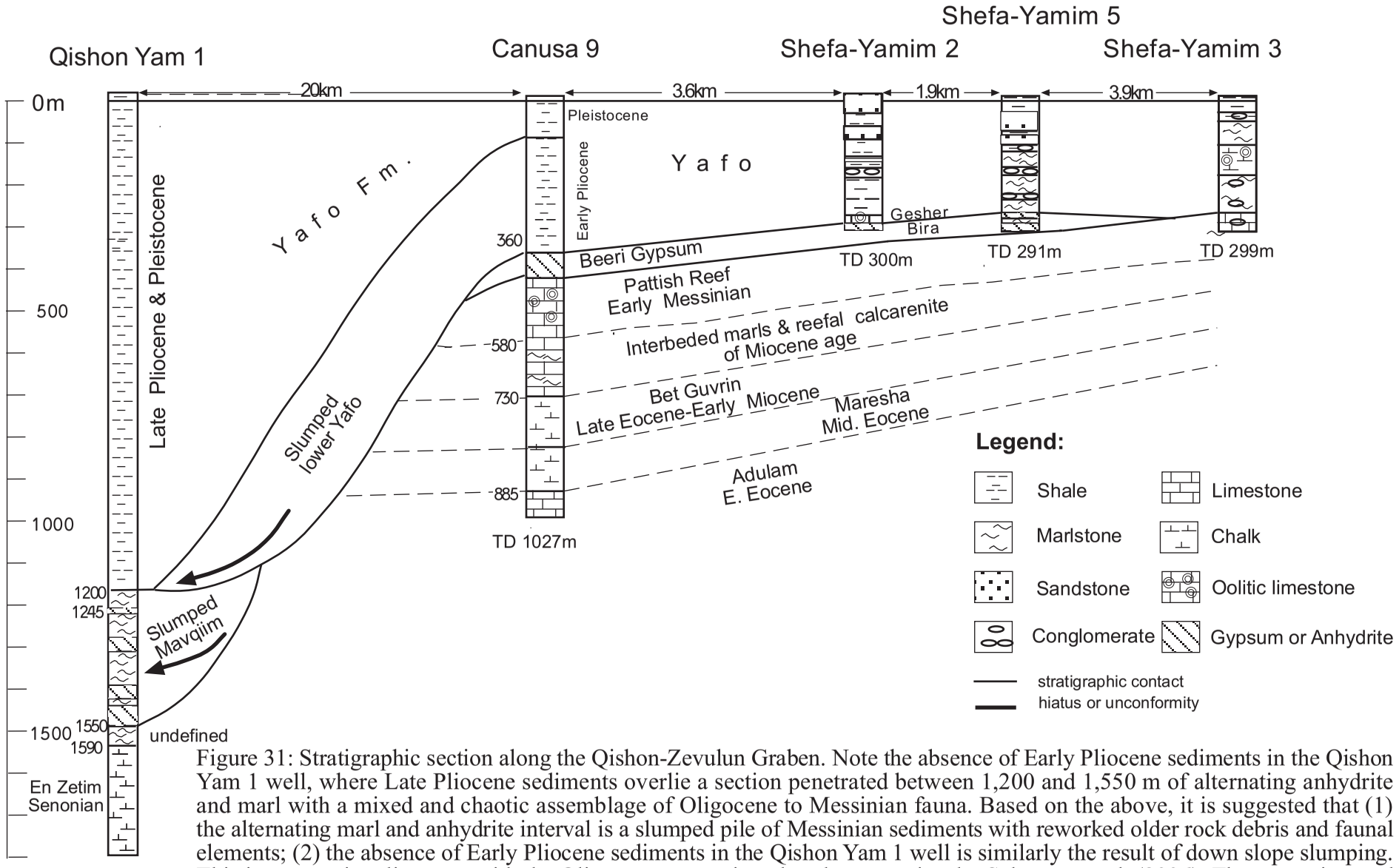

Figure 31: Stratigraphic section along the Qishon-Zevulun Graben. Note the absence of Early Pliocene sediments in the Qishon Yam 1 well, where Late Pliocene sediments overlie a section penetrated between 1,200 and 1,550 m of alternating anhydrite and marl with a mixed and chaotic assemblage of Oligocene to Messinian fauna. Based on the above, it is suggested that (1) the alternating marl and anhydrite interval is a slumped pile of Messinian sediments with reworked older rock debris and faunal elements; (2) the absence of Early Pliocene sediments in the Qishon Yam 1 well is similarly the result of down slope slumping. This interpretation disagrees with the Oligocene age assigned to the evaporites by Schattner et al. (2006). The evaporites and oolitic limestones penetrated in the Shefa Yamim boreholes are correlated with the Gesher and Bira evaporites and oolitic limestones of the northern Jordan Valley, thus providing an evidence for the coeval deposition of the Dead Sea Rift evaporates with the Messinian salinity crisis. Datum: MSL.

Afiq Canyon (Druckman et al., 1995), and thus represent the upper evaporites of the Messinian event.

These evaporite beds separate the overlying Pliocene section from the Miocene underlying section in the Canusa-9 borehole. In the Shefa Yamim wells, east of Canusa-9 borehole, these evaporites and the overlying oolitic limestones may be correlated with the Gesher and Bira evaporites and oolitic limestones in the northern Jordan Valley (Shulman, 1962; Cohen 1997). Moreover, this correlation may imply that the Dead Sea Rift evaporates may have originated from the Mediterranean Messinian brines during the upper evaporites highstand (Fig. 31).

6. Depositional pattern and reservoir elements

6.1 General

The canyon systems acted as conduits for submarine gravity flows that transported coarse-grained siliciclastic into the basin. These sediments were either deposited in the upper, intra-slope area, where they were confined by topographic lows and the incised canyon, or in the middle to lower slope area, where they accumulated in an unconfined setting on the basin floor (Fig. 32). It is assumed that in the confined setting the Oligo-Miocene strata contain various types of channel fills and in the unconfined setting it includes sheet sands and lobes (Weimer and Slatt, 2006; Fig. 32).

Although this generalized depositional model may be applied, in our view, to the Oligo-Miocene section, its details can not be identified in all parallel sections. For example, Oligocene coarse-grained deposits are found on the slope, but their inland source is generally missing due to later erosion. Similarly, continental deposits of uppermost Miocene age (latest Messinian) are found in the southern part of Israel, but are not identified above the Messinian salt in the offshore wells. In the following chapter we will describe the occurrences of Oligo-Miocene clastic deposits and their reservoir potential in onshore and offshore settings. We will attempt to contemplate on their origin and distribution in the basin based on the available well and seismic data.

Long distance clastic transport across the Rift Valley was possible since Early Oligocene times, through most of the Miocene but was obstructed since Pliocene times because of excess subsidence in the Rift Valley floor and the uplifting of its flanks.

6.2 Oligocene to lower Miocene succession

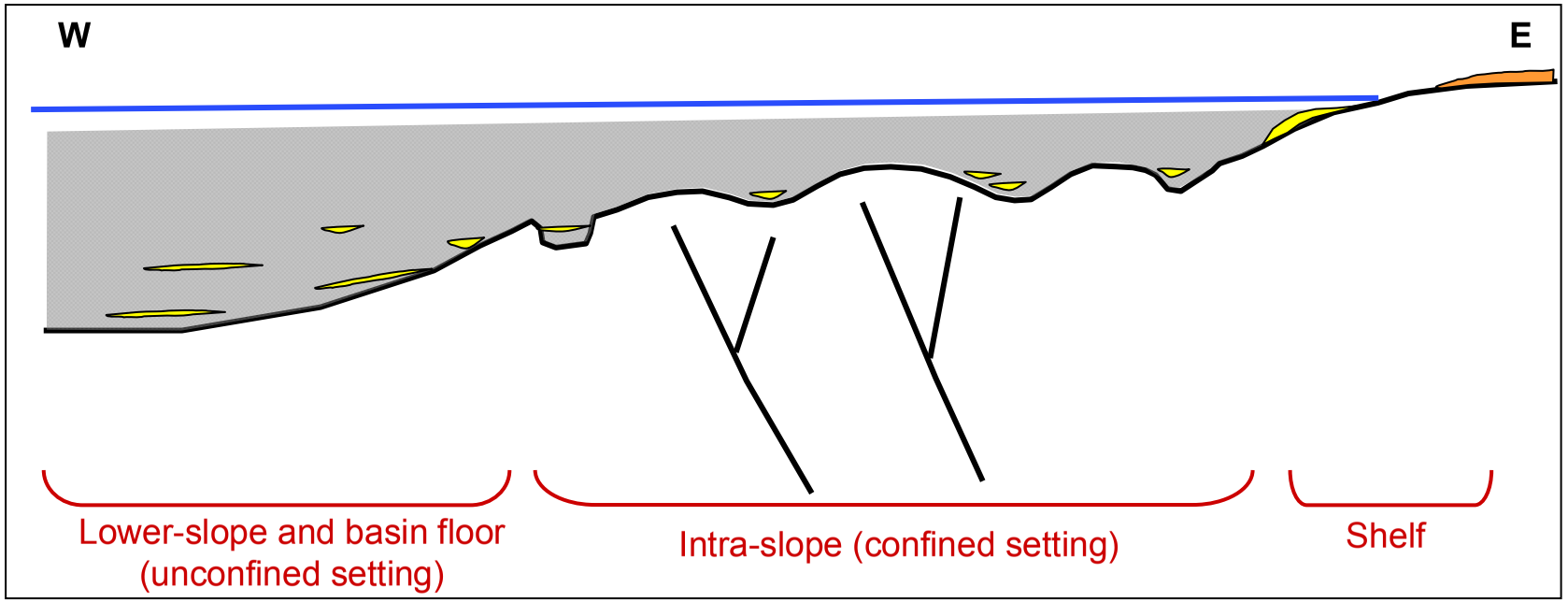

Figure 32: Schematic model of Oligo-Miocene depositional patterns on the Levant slope.

The Oligocene to Early Miocene succession was interpreted and mapped in the seismic records as a single seismic unit encompassing a few high order depositional cycles of Oligocene and lower Miocene age (Fig. 3).

A considerable shedding of clastic material into the Levant Basin occurred during the early part the Oligocene, resulting in the exposure of Nubian sandstone terrain in proximal areas (Fig. 33). Oligocene continental deposits are absent in Israel. Apparently, clastic material was either not stored inland, or was deposited and later eroded following the uplift of central Israel during the Miocene and Pliocene.

Approximately 250 m of Oligocene coarse-grained clastics (sandstones and conglomerates, named "Ashdod Clastics") were penetrated in the Ashdod wells, located in the southern Coastal Plain, where the Ashdod Canyon meets the present-day shoreline (Fig. 25) (Buchbinder and Siman-Tov, 2000; Buchbinder et al., 2005). The age of the Ashdod Clastics is not strictly defined. It may range from upper Rupelian to lower Chattian (zones P19 to P21 in Figure 8; Buchbinder et al., 2005). Core #2 from the Ashdod-2 borehole reveals a conglomerate consisting of boulders, imbricated pebbles (mostly of Cretaceous limestones and dolostones) and bioclastic sandstones of turbidite origin. Two intervals of highly porous sandstones, 20 m to 50 m thick, were detected in the Ashdod Clastics section. Their SP (Spontaneous Potential) and GR (Gamma-Ray) logs response exhibit blocky to fining-upward patterns. Other parts of the section show a serrated log motif, reflecting interbedded conglomerates, sandstones and marls (Buchbinder et al., 2005). The Oligocene clastic succession is interpreted as a proximal slope fan, deposited within the upper part of the submarine Ashdod Canyon (Fig. 33).

Further offshore, at the intra-slope part of the Ashdod Canyon, the Hanaha-1 borehole encountered several sand-rich beds at the upper part of the Oligocene canyon fill (Fig. 34). The section includes about 30 m of net sands with average porosity of 20-27%. These may be interpreted as channel fill sands that were derived from the slope fan at the upper part of the canyon.

In the Afiq Canyon, Martinotti (1981) reported a Cretaceous boulder within hemi-pelagic Middle Oligocene sediments in the Gaza-1 borehole. Apparently, sands either bypassed the present-day onshore part of the Afiq Canyon and were deposited offshore, or were eroded during the repeated canyon entrenchments in the Miocene.

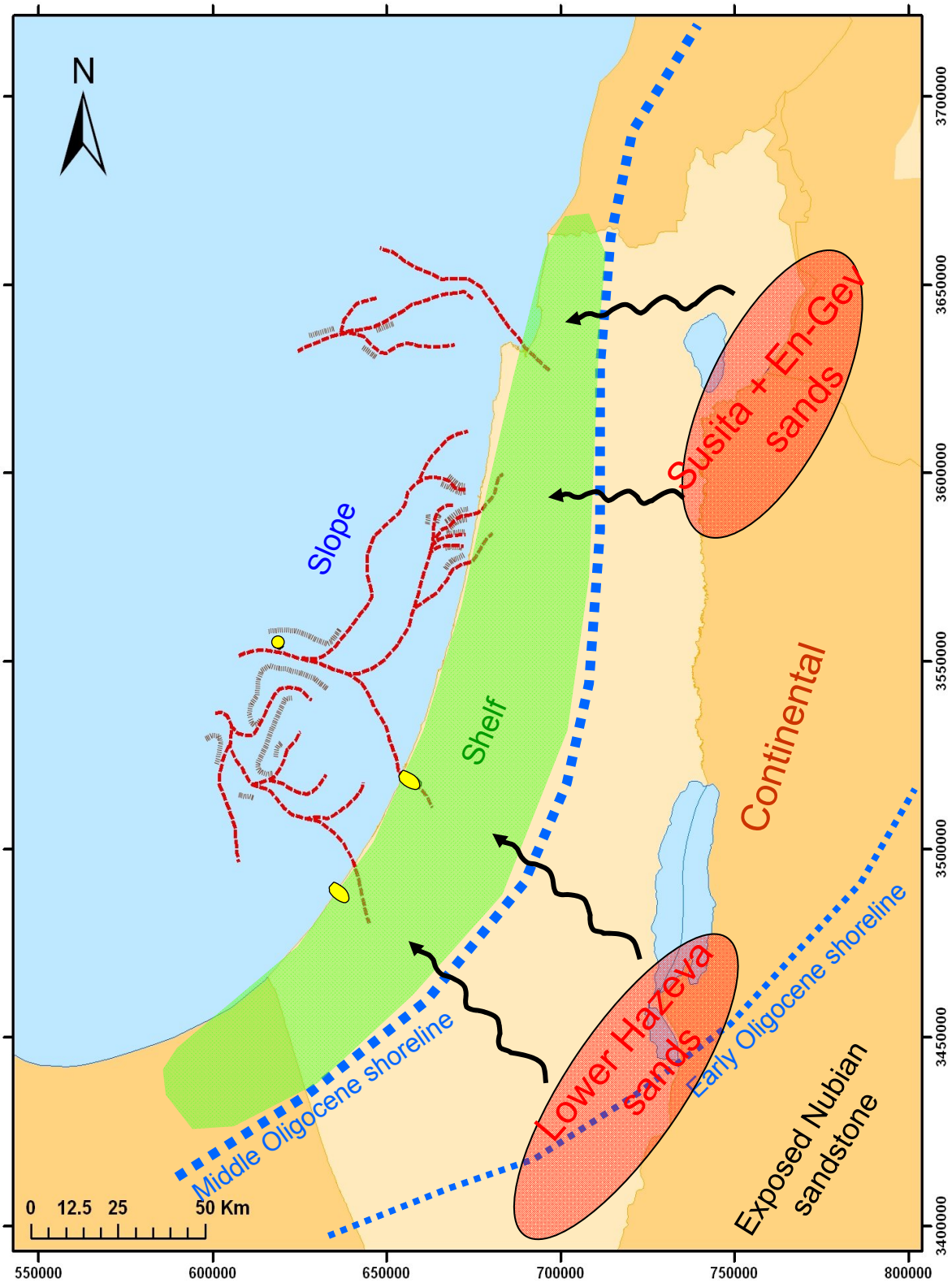

Figure 33: The paleogeography of the Levant margin during the Oligocene - Early Miocene time. Continental drainage system (marked by black arrows) carried siliciclastic sediments from the east to the Levant shelf, from where it was further transported into the basin through submarine canyons (marked by red dashed lines). The source of siliciclastics was redeposited Nubian sandstone found in outcrops at southern and northern Israel. Occurrences of shelf and deep-water sands in wells are marked by yellow polygones.

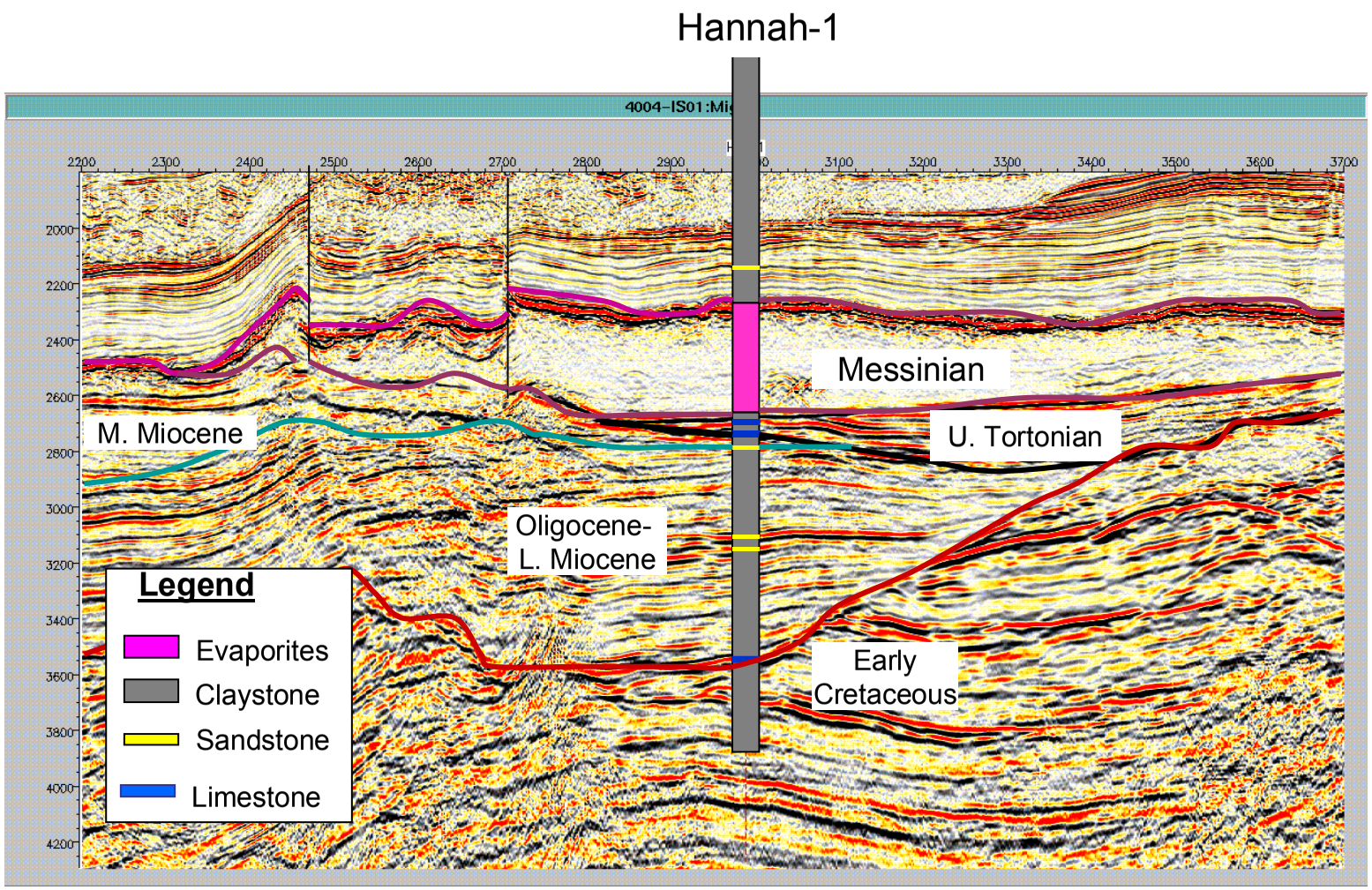

Figure 34: Oligo-Miocene reservoir elements in the Hannah-1 well at the western part of the Ashdod Canyon. High-amplitude events on the seismic profile correlate to thin sandstone and carbonate interval, interpreted as channel fill within the Oligocene and Middle to Late Miocene canyons. Location is as in Figure 24 (after Samedan, 2003).

In the Hadera Canyon the seismic data show several positive, high-amplitude reflections that onlap the canyon walls (Fig. 35). Amplitude extraction map of one of these events reveal linear features with maximum amplitude values (70-80) along the canyon. The high-amplitude event may represent a channel-levee complex where the maximum amplitudes are the coarser-grained, sandy portion of the channel fill.

No confined settings were observed in the seismic records in the deep part of the basin, west of the elevated incised fold belt. Nonetheless, high-amplitude seismic events, which are observed at the lower part of the section near the distal outlets of the main canyons (Fig. 11, left side at about 4.7 sec), may be associated with unconfined setting of sheet sands and basin floor fans.

A 17 m thick sand interval of lower Miocene age was encountered in the Gaza-1 borehole, in the Afiq Canyon, where it crosses the present coast line (Fig. 33). It was interpreted as a channel fill deposits and may represent the proximal tail of much more extensive accumulation further downstream the Afiq Canyon. In the unconfined setting, west of the outlet of the Afiq Canyon into the Levant deep basin, the seismic records show high-amplitude events below the cyan horizon, (Fig. 11, central part at about 3.7 sec). These seismic events may represent sheet sands generated by basin floor fans.

Notably, continental clastic sediments started to accumulate in proximal inland areas in Early Oligocene times. The Hazeva Group, several hundred meters thick in the Negev, started to accumulate before 20 m.y. (Calvo and Bartov, 2001). In the northern part of Israel, the mixed carbonates-clastic deposites of Hao'n and Nukev Formations and the continental sand deposits of the En-Gev Member (Susita Formation) were deposited during the Early Oligocene and Early Miocene (Buchbinder et al., 2005). The deposition of the Hordos sands in the Galilee and the Golan Heights was initiated before 17 m.y. (Shaliv, 1991).

Shaliv (1991) suggested that the similarities between the En-Gev sands and the continental deposits of the Damascus basin show that the two sites are, in fact, parts of the same basin. All these clastic occurrences strongly suggest the existence of a widespread source for siliciclastics both in the southern and the northern parts of the country (Fig. 33). Clastic deposits could have been transported into the basin through the Afiq and Ashdod canyons, in south and central Israel, and through yet undefined conduits in northern Israel during the Oligocene to Early Miocene time span (Figs. 3 and 33).

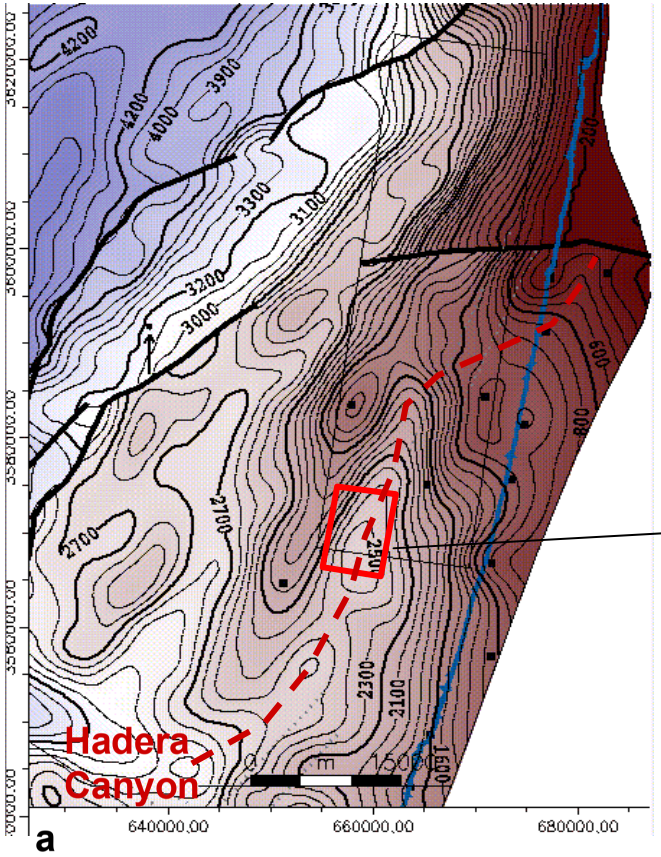

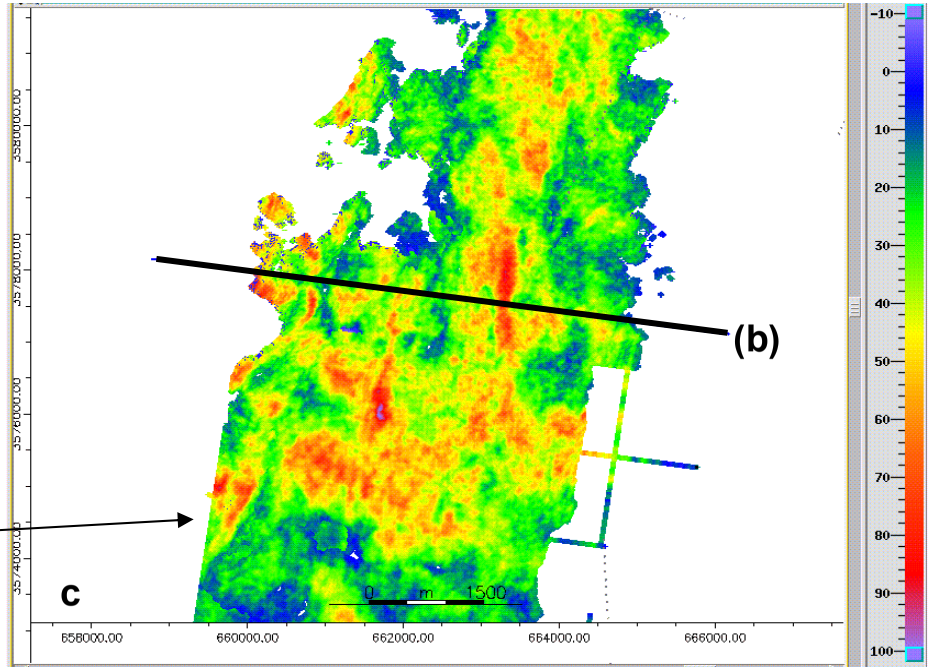

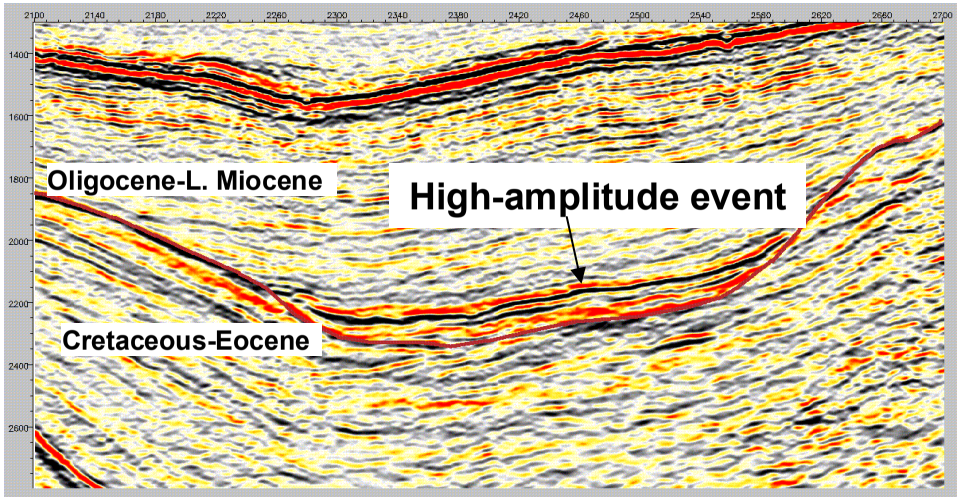

Figure 35: Oligocene reservoir elements in the Hadera Canyon (a). The seismic profile (b) show high-amplitude reflection onlapping the canyon walls. An amplitude map (c) extracted from this reflection show linear shaped amplitude maximum that is interpreted as a sand rich channel fill.

Additional mechanisms for transporting siliciclastics from nearshore areas in Egypt into the deep basin could have been: (1) Oligocene coarse clastics deposits in northern Egypt could have been a source for potential basin floor sheet sands, transported by canyons and channels running northwards across the Egyptian slope; (2) Longshore currents that interact with tidal currents diverting the drifting load of sand down the slope (Boyd et al, 2008). Study of these two suggested mechanisms is beyond the scope of the present report.

In summary, the Oligocene to Late Miocene periods are characterized by widespread transport of clastic sediment into the deep basin via submarine canyon and channel systems along the Levant margin. The provenance of these siliciclastic sediments were both continental and near-shore Oligo-Miocene deposits, recycled from Nubian sandstone (Fig. 33).

6.3 The Middle to Late Miocene succession

The upper Tortonian is associated with submarine incision on the Levant slope, depicted by the Late Miocene unconformity (Fig. 17). The canyon pattern closely followed the older, base Oligocene system, although the incision appears to have been more widespread.

Coarse clastic material was transported basinward through the Late Miocene canyon system. Evidence for clastic deposition is found along the Afiq Canyon. A 250 m thick conglomerate interpreted as channel fill of debris flow was found in the Nahal Oz-1 borehole, located in a proximal part of the canyon, at the southern Coastal Plain (Fig. 22). Further downdip, the Gad-1 borehole penetrated a 477 m thick clastic section composed of alternation of sandstone, conglomerate and clay of ?Middle Miocene to Messinian age (Figs. 22 and 36) (Buchbinder et al., 2006). The section includes 200 m of sand with average porosity of 16-19%. On the seismic records, it appears as a series of high-amplitude events onlapping the Afiq Canyon wall (Fig. 36). These are interpreted as stacked channels and channel-levee complexes.

Additional channel fill deposits, of apparent Langhian age (Siman-Tov, 2008b), were encountered in the Netanya-2 borehole, and located in the Netanya tributary of the Ashdod Canyon. These deposits consist of a conglomerate (100 m thick), of limestone and chert pebbles, and quartz sand grains (Fig. 27).

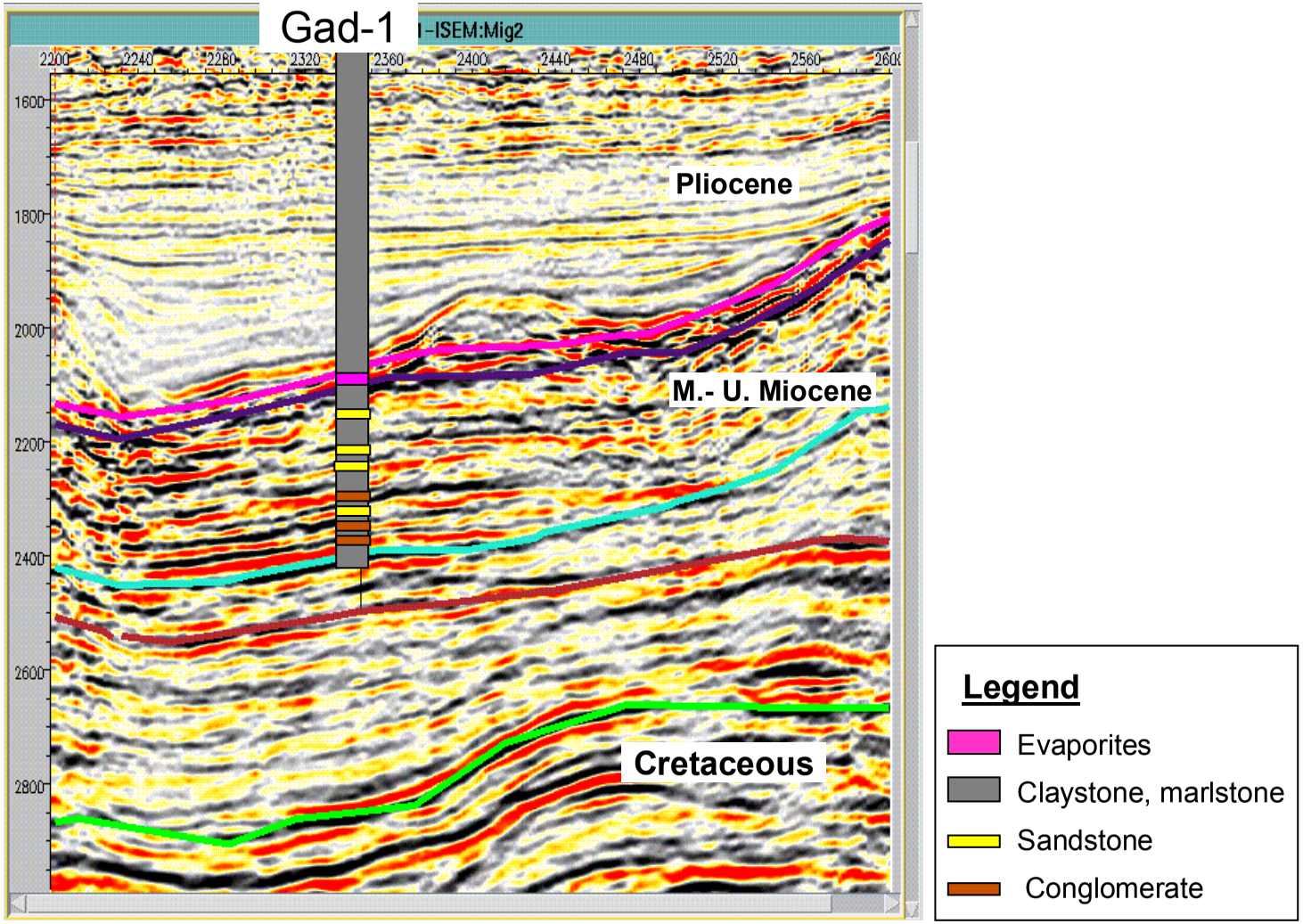

Figure 36: Middle-Late Miocene reservoir elements in the Hanha-1 well at the eastern part of the Afiq Canyon. High-amplitude events on the seismic profile correlate to sandstone and conglomerate beds, interpreted as channel fill within the canyon. See location in Figures 2 and 17

The existence of channel fill deposits in the confined upstream part of the Afiq and Ashdod (Netanya tributary) canyons may suggests further transport to the unconfined setting within the basin. Support for this transport is found at the western part of the Afiq Canyon. In this area a high-amplitude event appears on a time slice taken from the 3D survey E as an elongated feature oriented in a NW-SE direction that may be interpreted as channel fill near the outlet of the canyon (Fig. 37).

Continental clastic sediments of the Hazeva Group and Hordos Formation continued to accumulate in proximal inland areas during Late Miocene times (Figs. 3 and 38). This indicates the existence of an extensive source for siliciclastics. Sands could have been remobilized and transported from the shelf area basinward through the entire upper Miocene canyon system.

Due to the lack of information on Miocene and older sediments in the Qishon Graben in northern Israel, except for the Canusa-9 borehole and a few wells that barely penetrated the Messinian gypsum, no statement can be made as to the age and geometry of any pre-Messinian incisions or confined deposition in the Qishon Graben. The Miocene reefal carbonates below the Messinian evaporites in the Canusa-9 borehole have the characteristics of carbonate platform sedimentation, unlike transported carbonate debris found in channels. It may therefore indicate the existing of widely spread Miocene carbonate platform which was later largely removed leaving sparse relicts like the platform carbonates in the Canusa-9 borehole. The seismic data do not provide unequivocal information for any pre-base-Messinian incision event. It is therefore suggested that the Qishon Graben was not formed prior to Messinian and not later than Early Pliocene.

6.4 The Latest Miocene (post-evaporite) succession

Substantial subaerial incision and denudation of the circum Mediterranean took place during the latest Messinian, following the drawdown of the Mediterranean Sea by some 800 m due to its partial desiccation (Hsu et al., 1978; Delrieu et al., 1993; Druckman et al., 1995). The reduced evaporitic section, and the significantly thicker Pliocene section overlying it (Figs. 21 and 24c), indicate the removal of part of the evaporites due to a ~ 800 m fall of the Messinian sea level (Druckman et al., 1995; Cartwright and Jackson, 2007) and signifies the post-evaporite incision event. This event is better pronounced in the Afiq Canyon, where the evaporites are overlain by a succession of 90 m of lacustrine clastic sediment, reflecting the Lago Mare circum Mediterranean event.

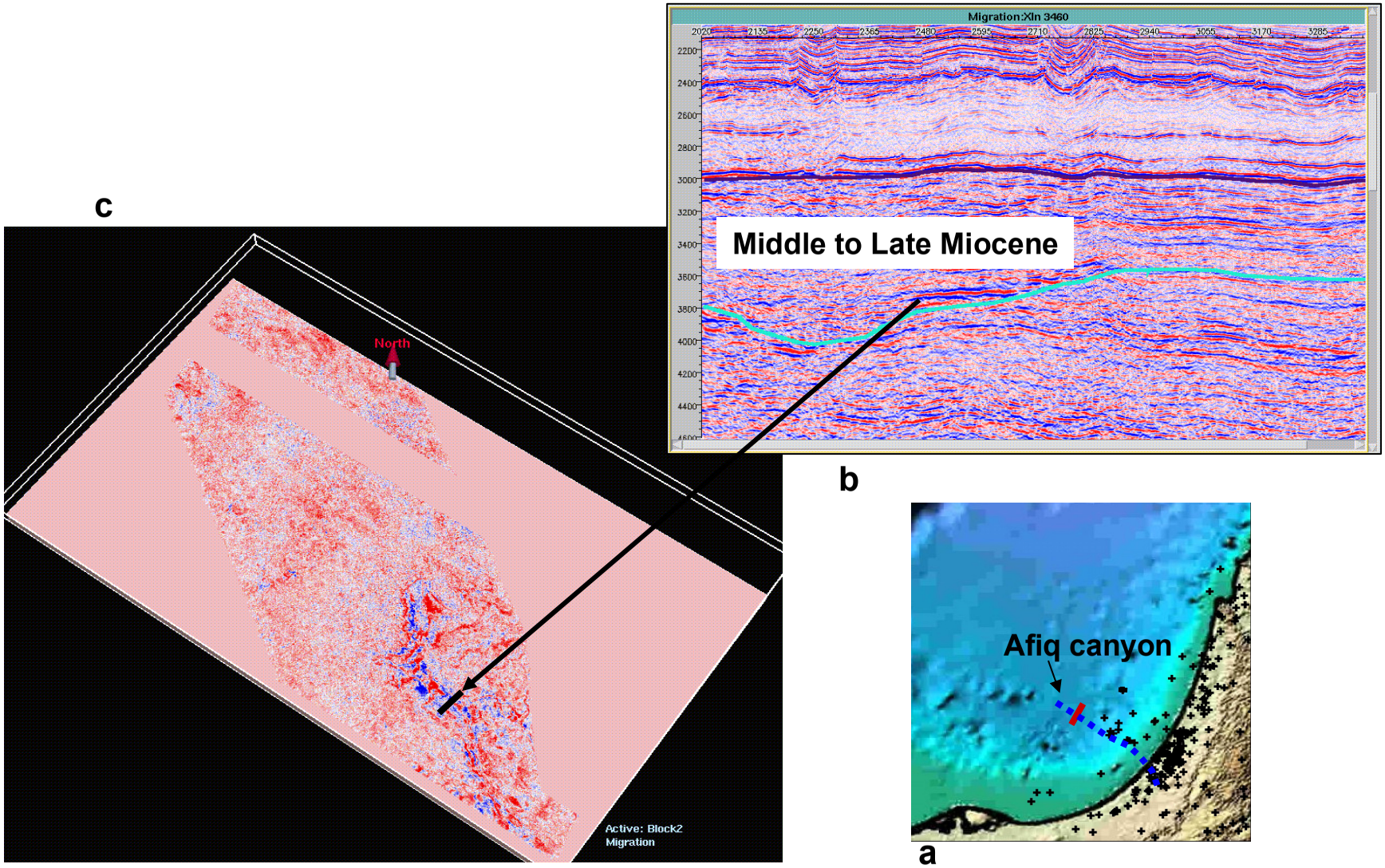

Figure 37: Upper Miocene reservoir elements in the western part of the Afiq Canyon (a). The seismic profile (b) show a high-amplitude reflection within the canyon. On a time slice (c) from 3D seismic survey C this reflection is part of a linear feature that is interpreted as a channel fill.

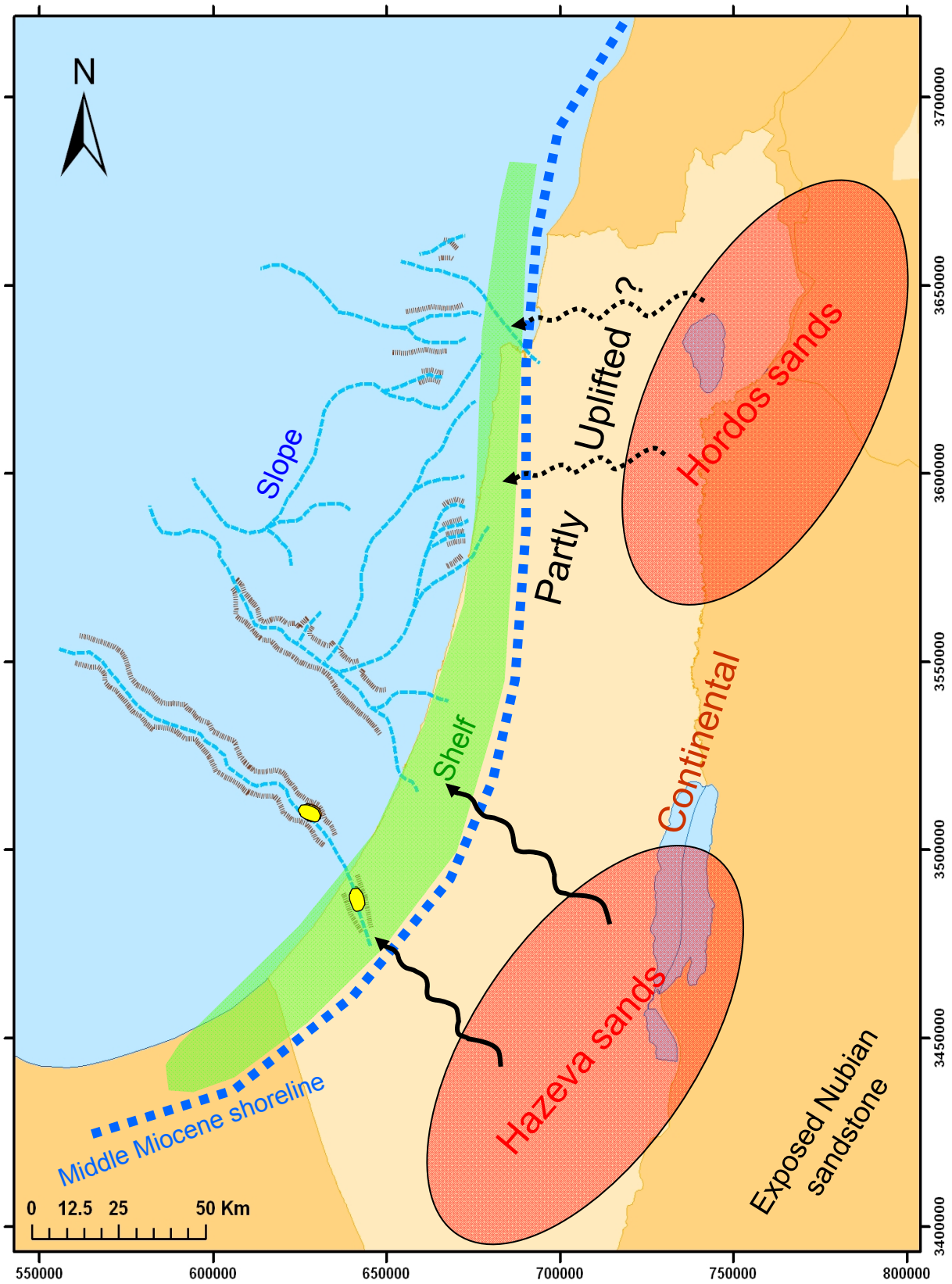

Figure 38: The paleogeography of the Levant margin during the Middle to upper Miocene. Continental drainage systems are marked by black arrows, submarine canyons are marked by red dashed lines, and occurrences of shelf and deep-water sands in wells are marked by yellow polygones. Hazeva and Hordos sands where the source of siliciclastics. The transport fron the NE may have been restricted by uplifting, associated with Syrian Arc deformation.

Clastic channel-fill deposits, other than the Afiq Formation, were not found in wells. However, their existence in the offshore may be speculated. It can be assumed that sediments of the Hazeva Group, which were widely exposed in southern Israel during this time, were transported to the shelf area and further into the basin through the Afiq-Beer Sheva Canyon.

7. Summary and Conclusion

The study of the Oligo-Miocene section through modern seismic data and well information reveals the detailed stratigraphy and structure of an extensive, siliciclastic deep-water system in the Levant Basin and margin.

The onset of clastic deposition, in the Oligocene, reflects a major change in the regional setting. The accumulation of a few thousand meters of Oligo-Miocene sediments in the deeper parts of the basin was caused by a regional uplift and denudation onshore and transportation of the eroded product into the basin. Only the distal marine deeper parts are preserved today, while the coeval proximal non-marine parts have been eroded. The latest Messinian short-lived lacusrine and fluvial sediments are the only non marine exceptions.

The factors that controlled the depositional settings are: (1) updoming and break apart of the Arabian Massif, (2) folding on both local and regional scale due to the collision between the Afro-Arabian and Eurasian plates, and (3) relative sea-level fluctuations.

Four regional unconformity surfaces were detected in the seismic records within the Oligo-Miocene succession: (1) Early Oligocene; (2) Middle Miocene; (3) Late Miocene (upper Tortonian); and (4) latest Miocene (post-evaporites) age. The Early Oligocene, Late Miocene (upper Tortonian) and latest Miocene (post-evaporites) surfaces reveal a series of stacked submarine canyons on the Levant slope.

Some of the canyons are deeply incised, others show minor incision and are developed within topographic lows. Both types acted as conduits for gravity flows. Mass flow into the basin is associated with complex and repeated processes of erosion, transportation and deposition.

Transport of sands from the East was quite effective during the Oligocene to Miocene section. In contrast, the transport of sands during the Pliocene was more restricted, because of increased subsidence within the Dead Sea Rift which became a major trap for coarse clastics.

Oligo-Miocene sands were deposited in two settings: (1) as channel fill within the canyons, in a confined, intra-slope setting, or (2) as sheets and lobes in an unconfined setting at the lower slope and basin floor. Channel fill sands were penetrated by several wells in the Afiq and Ashdod canyons. The existence of other sand-rich channels in these and other canyons is indicated by the seismic data. Basin floor sands were not yet tested by drilling and their existence is only inferred based on the seismic data. Both types of reservoirs are considered as attractive, potential hydrocarbons traps.

The Oligo-Miocene deep-water system of the Levant Basin is stratigraphicly located between potential Mesozoic source rocks and the Messinian evaporite seal. The combination of this setting and the evidence for transport and deposition of reservoir elements strongly suggest a significant potential for major hydrocarbon discoveries in the Levant Basin.

References

Ball, M. W., and Ball, D., 1953, Oil prospects of Israel. Am. Assoc. Petrol. Geol. Bull., 37:1-113.

Bar, O., Zilberman, E., Gvirtzman, Z., and Feinstein, S., 2006, Reconstruction of the uplift stages of the mountain backbone in central Israel. Geol. Surv. Report GSI/28/2006, 73 p. (in Hebrew, English abstract).

Bar, O., Gvirtzman, Z., Zilberman, E., and Feinstein, S., 2008, The development of the continental margin of central and southern Israel from Early Mesozoic formation to Late Tertiary reshaping: the role of tectonic and sedimentary processes in structural and morphological evolution of a continental shelf. GSI report GSI/31/2008, 68 p. (in Hebrew, English abstract).

Bein, A., and Gvirtzman, G., 1977, A Mesozoic fossil edge of the Arabian plate along the Levant coastline and its bearing on the evolution of the eastern Mediterranean, In: Biju-Duval B. and Montadert, L. (eds.) Structural History of the Mediterranean Basins: Editions Technip, Paris, 95-110.

Ben-Gai, Y., and Ben-Avraham, Z., 1995, Tectonic processes in the offshore northern Israel and the evolution of the Carmel structure. Marine Petrol. Geol., 12:553-548.

Benjamini, C., 1979, Facies relationships of the Avdat Group (Eocene) in northern Negev, Israel. Isr. J. Earth Sci., 28:47-69.

Benjamini, C., 1980, Stratigraphy and Foraminifera of the Qezi'ot and Har-Aqrav formations (latest Middle to Late Eocene) of the Western Negev, Israel. Isr. J. Earth Sci., 29:227-244.

Benjamini, C., 1984, Stratigraphy of the Eocene of the Arava valley (eastern and southern Negev, southern Israel). Isr. J. Earth Sci., 33:167-177.

Benjamini, C., 1993, Paleobathymetry of the Eocene of Israel. Isr. Geol. Soc., Annu. Meet., Arad, Abstr. p. 17.

Bertoni, C., and Cartwright J. A., 2006, Controls on the basinwide architecture of Late Miocene (Messinian) evaporates on the Levant margin (Eastern Mediterranean). Sedimentary Geology, 188-189:93-114.

Bertoni, C., and Cartwright J. A., 2007, Major erosion at the end of the Messinian Salinity Crisis: evidence from the Levant Basin, Eastern Mediterranean. Basin Research., 19:1-18.

Boyd, R., Ruming, K., Goodwin, I., Sandstrom, M., and Schroeder-Adams, C., 2008, Highstand transport of coastal sand to the deep ocean: A case study from Fraser Island, southeast Australia. Geology, 36:15-18.

Buchbinder, B., Sneh, A., and Dimant, E., 1986, The Neogene Bet Nir Formation, a study of alluvial aggradation along the toe of the Judean monoclines. Isr. J. Earth Sci., 35:183-191.

Buchbinder, B., Benjamini, C., Mimran, Y., and Gvirtzman, G., 1988, Mass transport in Eocene pelagic chalk on the northwestern edge of the Arabian platform, Shefela area, Israel. Sedimentology, 35:257-274.

Buchbinder, B., Martinotti, G. M., Siman-Tov, R. and Zilberman, E., 1993, Temporal and spatial relationships in Miocene reef carbonates in Israel. Paleogeog. Paleoclim. Paleoecol., 101:97-116.

Buchbinder, B., and Zilberman, E., 1997, Sequence stratigraphy of Miocene-Pliocene carbonate-siliciclastic shelf deposits in the eastern Mediterranean margin (Israel): effects of eustasy and tectonics. Sedimentary Geol., 112:7-32.

Buchbinder, B. and Siman-Tov, R., 2000, Oligocene clastics in the Ashdod area: mass flow and turbidite deposits in a sub-marine fan setting. Isr. Geol. Soc. Annual meeting p. 25, (Abstract).

Buchbinder, B., Calvo, R., and Siman-Tov, R., 2005, The Oligocene in Israel: A marine realm with intermittent denudation accompanied by mass-flow deposition. Isr. J. Earth Sci., 54:63-85.

Buchbinder, B., Siman-Tov, R., Grossowicz, L., Calvo, R., and Almogi-Labin, A., 2006, Stratigraphic and Environmental Analysis of the Gad-1 Borehole, Offshore Israel. Geological Survey of Israel, Rep. GSI/1/2006, 22 p.

Calvo, R., and Bartov, Y., 2001, Hazeva Group, southern Israel: New observations and their implications for its stratigraphy, paleogeography and tectono-sedimentary regime. Isr. J. Earth Sci., 50:71-99.

Cartwright, J. A., and Jackson, M. P. A., 2007, Initiation of gravitational collapse of an evaporate basin margin: The Messinian saline giant, Levant Basin, eastern Mediterranean. GSA Bull., 120:399-413.

Cohen, A., 1988, Stratification of the Messinian evaporites in Israel. Isr. Jour. Earth Sci., 37:193-203.

Cohen, A., 1997, The Menahemya Gypsum in the Jordan Valley: The Messinian Mavqiim Formation exposed. GSI Report GSI/2/97, 17 p.

Delrieu, B., Rouchy, J. M., and Foucault, A., 1993, La Surface d'erosion finimemessininne en Crete centrale (Grece) et sur le pourtour méditerranéen: rapports avec la crise de salinité méditerranéen. C.R. Acad. Sci. Paris, 316(II):527-533.

Derin, B., 1999, Stratigraphy and Environments of Deposition of Yam West-2. Isramco Inc, Rep. 1/99, 19 p.

Druckman, Y., 2001, The hydrocarbon potential of Israel. Isr. Geol. Soc. Meet. Elat, Abstr., p. 28.

Druckman, Y., Conway, B.H., Eshet, Y., Gill, D., Perelis-Grossowicz, L., Lipson, S., Moshkowitz, S., Rosenfeld, A., and Siman-Tov, R., 1994, The Stratigraphy of the Yam-Yafo ! borehole. Report GSI/28/94, p.27.

Druckman, Y., Buchbinder, B., Martinotti, G. M., Siman-Tov, R., and Aharon, P., 1995, The buried Afiq Canyon (eastern Mediterranean, Israel): a case study of a Tertiary submarine canyon exposed in Late Messinian times. Marine Geol., 123:167-185.

Esteban, M., Braga, J. C., Martin, J. C., and Santisteban, C., 1996, An overview of Miocene reefs from the Mediterranean areas: general trends and facies models. In: Models for Carbonate Stratigraphy from Miocene Reef Complexesof Mediterranean. (Eds E.K. Franseen, M. Esteban, W. Ward, and J.M. Rouchy) SEPM Concepts Sedimentol. Paleontol., 5:3-53.

Flexer, A., Rosenfeld, A., Lipson-Benitah, S., and Honigstein, A., 1986, Relative sea level changes during the Cretaceous in Israel. Am. Assoc. Petrol. Geol. Bull., 70:1685-1699.

Fleischer, L., and Gafsou, R., 2003, Top Judea Group- digital structural map of Israel (1:200.000). Geophys. Inst. Isr. Rep. 753/312/03.

Fleischer, L., and Varshavsky, A., 2002, A lithostratigraphic data base of oil and gas wells drilled in Israel. Ministry of National Infrastructure, Oil and Gas Unit, Rep. OG/9/02, 280 p.

Freund, R., Goldberg, M., Weissbrod, T., Druckman, Y., and Derin, B., 1975, The Triassic-Jurassic structure of Israel and its relation to the origin of the eastern Mediterranean. Isr. Geol. Surv. Bull. 65, 26 p.

Gardosh, M., 2002, The sequence stratigraphy and petroleum systems of the Mesozoic, southeastern Mediterranean continental margin. Ph.D. thesis, Tel Aviv Univ. 159 p.

Gardosh, M., and Druckman, Y., 2006, Seismic stratigraphy, structure and tectonic evolution of the Levantine Basin, offshore Israel. In: Robertson, A. H. F. and Mountrakis, D. (eds.) Tectonic Development of the Eastern Mediterranean Region. Geol. Soc., London, Spec. Publ., 260:201-227.

Gardosh, M., Druckman, Y., Buchbinder, B., and Rybakov, M., 2006, The Levant Basin Offshore Israel: Stratigraphy, Structure, Tectonic Evolution and Implications for Hydrocarbon Exploration. GII Rep. 429/218/06, GSI Rep. GSI/14/2006, 119 p.

Gardosh, M., Druckman, Y., Buchbinder, B., and Rybakov, M., 2008, The Levant Basin Offshore Israel: Stratigraphy, Structure, Tectonic Evolution and Implications for Hydrocarbon Exploration, Revised Edition. GII Rep. 429/328/08, GSI Rep. GSI/4/2008, 119 p.

Garfunkel, Z., 1988, The pre-Quaternary geology of Israel. In: Yom-Tov Y. and Tchernov, E. (eds.), The Zoogeography of Israel, Jung Publishers, Dordrecht, 7-34.

Garfunkel, Z., 1998, Constraints on the origin and history of the eastern Mediterranean basin. Tectonophysics, 298:5-35.

Garfunkel, Z., and Horowitz, A., 1966, The upper Tertiary and Quaternary morphology of the Negev, Israel. Isr. J. Earth Sci., 15:101-117.

Garfunkel, Z., and Derin, B., 1984, Permian-Early Mesozoic tectonism and continental margin formation in Israel and its implications to the history of the eastern Mediterranean. In: Dixon, J., E. and Robertson, A.H.F. (eds.) The Geological Evolution of the Eastern Mediterranean. Geol. Soc. London, Spec. Publ., 17:18-201.

Garfunkel, Z., and Almagor, G., 1985, Geology and structure of the continental margin of northern Israel and adjacent part of the Levantine basin. Marine Geology, 62:105-131.

Gelberman, E., 1990, Seismic interpretation based on a high resolution seismic survey, Ceasarea area. Geophysical Institute, Report 879/275/90.

Gill, D., Conway, B. H., Eshet, Y., Lipson, S., Perelis-Grossowicz, L., Rosenfeld, A., and Siman-Tov, R., 1995, The stratigraphy of the Yam West 1 borehole, Isr. Geol. Surv., Rep. GSI/13/95, 43 p.

Gvirtzman, G., 1970, The Saqiye Group (Late Eocene to Early Pleistocene) in the Coastal Plain and Hashephela regions, Israel. Isr. Geol. Surv. Rep. OD/5/67.

Gvirtzman, G., and Buchbinder, B., 1978, The Tertiary history of the coastal plain and continental shelf of Israel and its bearing on the history of the Eastern Mediterranean. Initial Report Deep Sea Drilling Project, 42B:1195-1222.

Gvirtzman,, Z., Zilberman, E., and Folkman, Y., 2008, Reactivation of the Levant passive margin during the Late Tertiary and formation of the Jaffa basin offshore central Israel. Jour. Geol. Soci. London, 2008:563-578.

Haq, B. U., Hardenbol, J., and Vail, P. R., 1988, Mesozoic and Cenozoic chronostratigraphy and cycles of sea-level changes. In: Wilgus, C.K., Hastings, B.S., Kendall, C. G. St. C., Posamentier, H.W., Ross, C.A. and Van Wagoner, J.C. (eds.), Sea-level Changes: an Integrated Approach, SEPM - Soc. Sediment. Geol. Spec. Publ. 42:71-108.

Hardenbol, J. et al, 1998, Cenozoic sequence chronostratigraphy (Chart 2). In: de Graciansky, P-C., Hardenbol, J., Jacquin T. and Vail, P. (eds.), Mesozoic and Cenozoic Sequence Stratigraphy of European Basins. SEPM - Soc. Sediment. Geol. Spec. Publ. 60.

Hsu, K.J., Cita, M.B., and Ryan, W. B. F., 1973a, The origin of the Mediterranean evaporites. Initial Reports of the Deep Sea Drilling Project, 42:1203-1232.

Hsu, K.J., Ryan, W. B. F., and Cita, M. B.,1973b, Late Miocene desiccation of the Mediterranean. Nature, 242:240-244.

Hsu, K.J., Montadert, L., Bernoulli, D., Cita, M. B., Erickson, A., Garrison, R. G., Kid, R. B., Melieres, F., Muller, C., and Wright, R., 1978, History of the Mediterranean salinity crisis. Initial Reports of the Deep Sea Drilling Project, 42A:1053-1078.

Krenkel, E., 1924, Der Syrische Bogen. Zentralblatt Mineralogie, 9:274-281 and 10:301-313.

Martinotti, G. M., 1973, *Miogypsina* in the Gaza-1 well, coastal plain, Israel. Isr. Geol. Surv. Bull., 57:1-6.

Martinotti, G. M., 1981, An Oligocene unconformity and its interregional interest. Isr. Geol. Surv. Current Research, 1981:30-35.

Martinotti, G. M., 1990, The stratigraphic significance of *Globigerinoides ruber* and *Globigerinoides obliquus obliquus* in the Mediterranean Middle Miocene. Micropaleontol., 36:96-101.

Michelson, Ch., and Lipson-Benitah, S., 1986, The litho and biostratigraphy of the southern Golan Heights. Isr. J. Earth Sci., 35:221-240.

Micro-Strat Inc., 2003, High resolution biostratigraphy of the Samedan Mediterranean sea Hannah 1 well, offshore Israel. Report prepared for Samedan Mediterranean Sea, 40 p.

Miller, K. J., Kominz, M. A., Browning, J. V., Wright, J. D., Mountain, G. S., Katz, M. E., Sugarman, P. J., Cramer, B. S., Christie-Blick, N., and Pekar, S.F., 2005, The Phanerozoic record of global sea-level change. Science, 310:1293-1298.

Neev, D., 1960, A pre-Neogene erosion channel in the southern coastal plain. Isr. Geol. Surv. Bull. 25, 20 p.

Neev, D., Almagor, G., Arad, A., Ginzburg, A., and Hall, J. K., 1976, The geology of the southeastern Mediterranean. Isr. Geol. Surv. Bull. 68, 52 p.

Oats, M., 2001, Origin and genesis of lower Oligocene sand mounds, Afiq Canyon, Israel. Isr. Geol. Soc.Annu. Meet., Elat, Abstr. p. 89.

Picard, L., 1951, Geomorphology of Israel, Part I- The Negev. Isr. Geol. Surv. Bull. 1, 28 p.

Picard, L. 1959, Geology and oil exploration of Israel. Bull. Res. Council Isr., G8:1-30.

Robertson, A. H. F., 1998, Mesozoic-Tertiary tectonic evolution of the easternmost Mediterranean area: integration of marine and land evidence. In: Robertson, A.H.F., Eneis, K.C., Richter, C. and Camerlenghi, A. (eds.), Proceed. Ocean Drilling Prog., Scientific Results, 160:723-782.

Ryan, W. B. F., 1978, Messinian badlands on the southeastern margins of the Mediterranean Sea. Mar. Geol., 27:349-363.

Samedan, Mediterranean Sea Corp., 2003, Hannah-1, Composite Log, scale 1:500.

Schattner, U., Ben-Avraham, Z., Reshef, M., Bar-Am, G., and Lazar, M., 2006, Oligocene–Miocene formation of the Haifa basin: Qishon-Sirhan rifting coeval with the Red Sea-Suez rift System. Tectonophysics, 419:1-12.

Shaliv, G., 1991, Stages in the tectonic and volcanic history of the Neogene basin in the Lower Galilee and the valleys. Isr. Geol. Surv. Rep. GSI/11/91,94 p. (In Hebrew).

Shulman, N., 1962, The geology of the central Jordan Valley, Ph.D. thesis, The Hebrew University of Jerusalem (in Hebrew).

Siman-Tov, R., 1984, Notes on the Saqiye Group as determined from foraminifera. Isr. Geol. Surv. Rep., GSI/61/84, 14 p.

Siman-Tov, R., 1991. The *Turborotalia cerroazulensis* Zone at Tel Nagila, southeastern Hashefela. Isr. Geol. Surv. Rep. GSI/38/91, 15 p.

Siman-Tov, R., 2008a, Summary of the foraminiferal examination of the Qishon Yam 1 well (1190-1742m.) written communication.

Siman-Tov, R., 2008b, Summary of the foraminiferal examination of the Netanya 2 well (1199-1334m.) written communication.

Steinberg, J., Gvirtzman, Z., Folkman, Y., and Gvirtzman, Z., 2008, The Or Akiva fault: E-W Miocene faulting of the continental margin and its relation to the Carmel block. Israel Geological Survey annual meeting, Nazareth, Abstract. p. 107.

Tibor, G., Ben-Avraham, Z., Steckler, M., and Fligelman, H., 1992, Late Tertiary subsidence history of the southern Levant margin, eastern Mediterranean Sea, and its implications to the understanding of the Messinian event, J. Geophys. Res. 97(B12):17593-17614.

Walley, C. D., 1998, Some outstanding issues in the geology of Lebanon and their importance in the tectonic evolution of the Levantine region. Tectonophysics, 298:37-62.

Walley, C. D., 2001, The Lebanon passive margin and the evolution of the Levantine Neo-Tethys. In: Ziegler, P.A., Cavazza, W., Robertson, A. H. F. and Crasquin-Soleau (eds.), Peri-Tethys Memoir 6: Peri-Tethyan Rift/Wrench Basins and Passive Margins. Mem. Mus. natn. Hist. Nat., 186:407-439.

Weimer, P., and Slatt, R., 2006, Petroleum Geology of Deepwater Settings. AAPG studies in Geology, 57.

Zilberman, E., 1992, Remnants of Miocene landscape in the central and northern Negev and their paleogeographical implications. Isr. Geol. Surv. Bull. 83, 54 p.

Zilberman, E., 1993, The Mahmal graben and Nahal Hawwa: an introduction to the paleogeography of central Negev in the Miocene. Isr. J. Earth Sci. 42:197-209.